Result of the survey of Hashima Coal Mine buildings, etc.

Survey of accommodation facilities deterioration level

The current deterioration condition, etc. (as of fiscal 2014) were surveyed to understand the present situation of deteriorated concrete constructions including Building No.70 (Former Hashima Elementary School and Hashima Junior High School), the foundation of which has considerably been scoured out.

(1) Survey of the current condition of Building No.70

Building No.70 used to be used as the school building of Takashima Municipal Hashima Elementary School and Hashima Junior High School. The existing school building was built as a six-story reinforced concrete structure in 1958, to which a seventh story was added in 1961 to form the current structure. Before the construction of Building No.70, there used to be a two-story wooden school building, which had been built in 1934, on the north side of the current location, but it was destroyed by a fire in 1957. The remains that appear to be the foundation of the destroyed school building was confirmed in the archaeological excavation of fiscal 2015 (see Chapter 2, Section 3, 3. Archaeological excavation).

Since its construction 60 years ago, Building No.70 has been deteriorating: collapses and cracks are confirmed in some external walls; and the foundation, which has been eroded by sea water, exposes the pile head and has been partially lost. Moreover, many cracks have been confirmed in columns and beams inside the building (Photo 2-4-111). To understand the deformed state of Building No.70, the foundation of which has been considerably scoured out, we measured the altitude twice by using the eastern corner of the building as a reference point and recorded the progress of subsidence, while marking the measurement points so that we can find them in the future. For the slant (north-south and east-west directions) of the building too, we measured the gradient twice and recorded the current state and the progress, while marking the measurement points so that we can find them in the future. After completing the survey, we created a deformed state drawing on the basis of the survey results. For the scoured part, a drawing was created in fiscal 2014 (see Chapter 2, Section 3, 2. (4)).

It was estimated that several concrete pile foundations supporting the structure of Building No.70 have been lost or broken after having been scoured by sea water, losing their proper function. Therefore, a survey was conducted to understand the deterioration levels of the building and the foundation. To the deterioration level of the building, we applied the methods of deterioration survey and durable year prediction based on the category of damage degree of structures, which was calculated in the “Deterioration survey of concrete structures in Gunkanjima” conducted by the working group for the Deterioration survey of concrete structures in Gunkanjima in March 2013.

Meanwhile, the deterioration level of the foundation was calculated using the three-dimensional elastic analysis by FEM, in which foundation piles and the undermost layer of the structure were turned into a model, and the results obtained were summarized as the current deterioration level. In considering the deterioration level of the foundation, the “Foundation status drawing” created in fiscal 2014 was used as a reference (see Chapter 2, Section 3, 2. (4)).

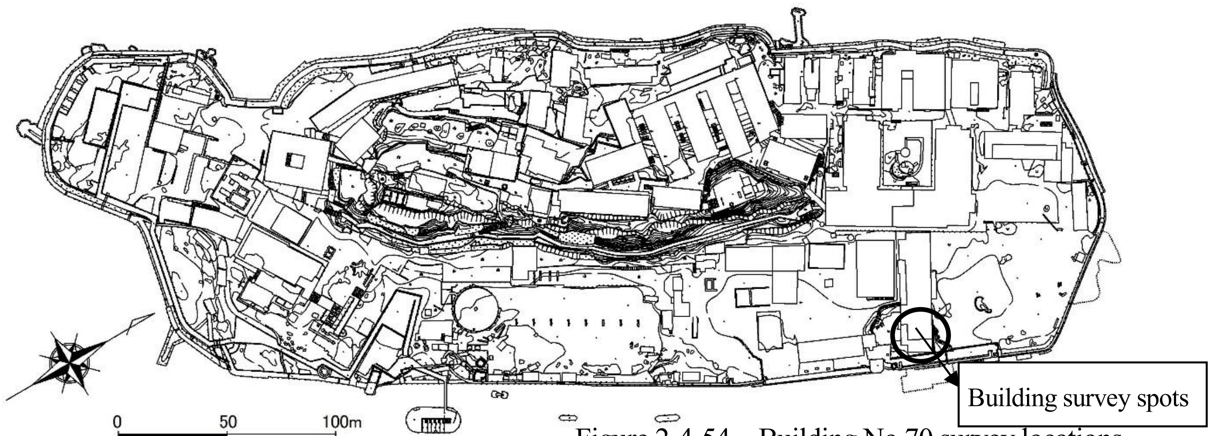

Figure 2-4-54　Building No.70 survey locations

Appendix 1

Building No.70 appearance

Building No.70 foundation

North side front view

From the southeast side

Foundation on the north side of the building

Enlarged foundation

Photo 2-4-111 Current condition of Building No.70

1) Slant estimation and deformed state drawing (damage drawing) creation for Building No.70

① Measurement plan

The altitude was measured twice by using the eastern corner of the building as a reference point, and the progress of subsidence was recorded; the gradient (north-south and east-west directions) was also measured twice, and the current state and progress were recorded. The two measurements were conducted on the dates below.

・The first measurement: October 3, 2014

・The second measurement: February 27, 2015

② Setting of measurement points

②-1Basic policy

Before measurement, we set two points to measure altitude and slant on each of the east and north faces of Building No.70. In setting them, we selected the points at which there was no floating of concrete and a decoration mortar wall had peeled off. For the continual measurement of altitude and slant, there were the two possible methods for setting measurement points: using survey rivets and marking with a paint marker. Because the measurement surfaces were severely deteriorated (Photo 2-4-112) and mortar on the surfaces might peel off during the drilling of rivets, and there was no stable footing on the lower part of the eastern end of Building No.70 due to scouring, we adopted marking with a paint marker. Nevertheless, we adopted survey rivets only for the north end on the east face of Building No.70 to use it as the general standard.

②-2 Measurement point observation

The point without the danger of surface peeling-off, etc. was selected from among the four points selected, and rivets were placed at 70-2 (see Figure 2-4-55), which served as a reference. As a result of leveling using the near third-order control point (NO. 2 H=5.171) (Photo 2-4-113), the altitude of 70-2 was H = 6.550 m. Then, we set all of the four points at the same altitude (H = 6.550 m) so that we can promptly calculate displacement at the time of next measurement.

Photo 2-4-112 Building No.70 east face

Photo 2-4-113 Third-order control point (No. 2)

Photo 2-4-114 Leveling

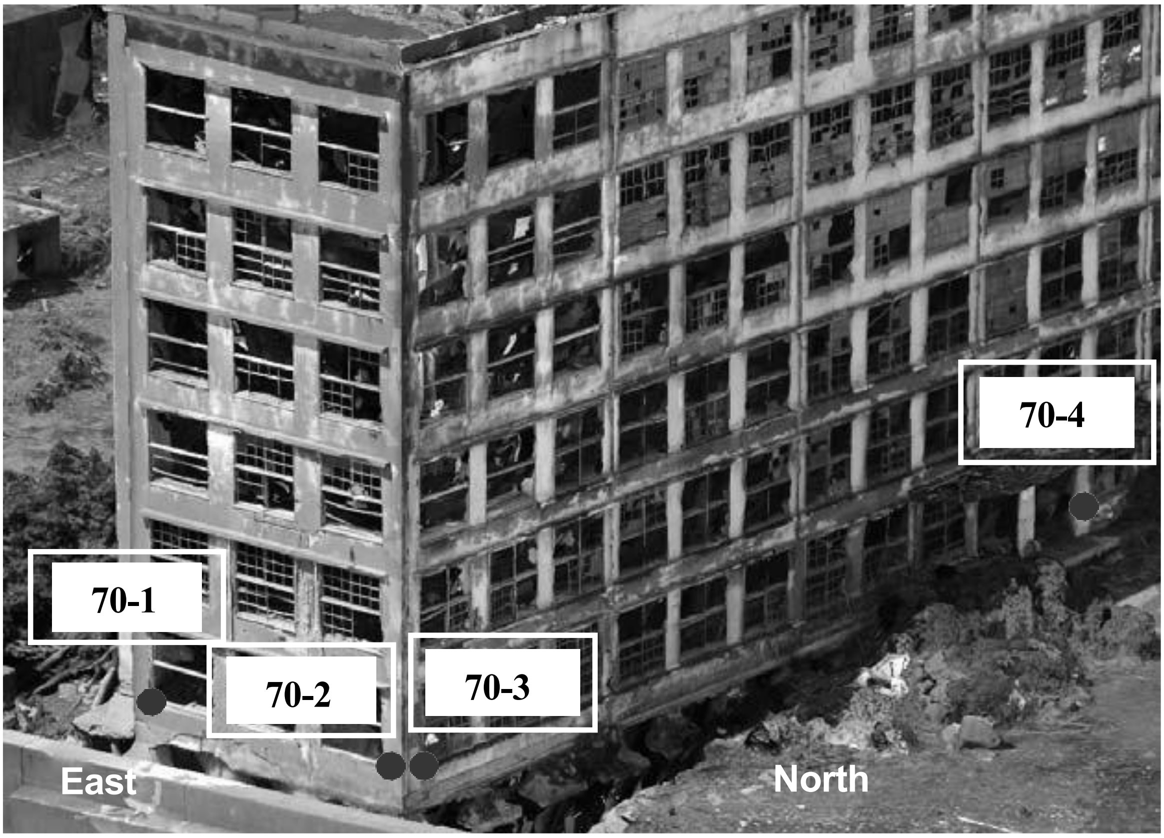

Figure 2-4-55 Locations where measurement points were set

②-3 Measurement for confirmation

After setting the measurement points with an automatic level, we calculated distances between the points 70-1 and 70-2 and between the points 70-2 and 70-3 with a total station and confirmed the altitudes of the points at the same time. As a result, the difference in altitude among all points was confirmed to be within 3 mm (Table 2-4-47).

Table 2-4-47 Result of measurement for conformation

Point	Altitude	Difference from "70-2"
70-1	6.549 m	-0.001 m
70-2	6.550 m	0
70-3	6.551 m	+0.001 m
70-4	6.552 m	+0.002 m

③ Altitude measurement

The results of altitude measurement were shown in Table 2-4-48. The difference between first and second measurements reading was 1 mm at all measurement points.

Table 2-4-48 Altitude measurement results

Measurement timing	Measurement date	Measurement result (altitude)			
		70-1	70-2	70-3	70-4
First measurement	Oct. 3, 2014	6.550 m	6.550 m	6.550 m	6.550 m
Second measurement	Feb. 27, 2015	6.551 m	6.551 m	6.551 m	6.551 m

④ Slant measurement

For the slant, the initial values, or the gradients, obtained from the altitude of each point measured on October 3, 2014 was set as "0" and the values measured on February 27, 2015 were compared with those.

The slant and the horizontal distance that were measured twice were compared, and as a result, the difference was within 2 mm for the both. Since the results include measurement errors, it is unlikely that there were changes in the gradient. Conducting measurements at the four points regularly in the future will make continual monitoring of the gradient possible, which is considered to contribute to the collection of basic data for maintenance. (The gradient was calculated by using the initial value of horizontal distance as a reference.)

Table 2-4-49 List of slant measurement results

	Oct. 3, 2014		Feb. 27, 2015	
Point	Altitude [m]	Displacement [m]	Altitude [m]	Displacement [m]
70-1	6.550	0.000	6.551	0.001
70-2	6.550	0.000	6.551	0.001
70-3	6.550	0.000	6.551	0.001
70-4	6.550	0.000	6.551	0.001
Between points	Distance [m]	Displacement [m]	Distance [m]	Displacement [m]
70-1 and 70-2	9.892	0.000	9.89	-0.002
70-3 and 70-4	33.290	0.000	33.288	-0.002
Between points	Difference in altitude [m]	Gradient [deg]	Difference in altitude [m]	Gradient [deg]
70-1 and 70-2	0.000	0.000	0.000	0.000
70-3 and 70-4	0.000	0.000	0.000	0.000

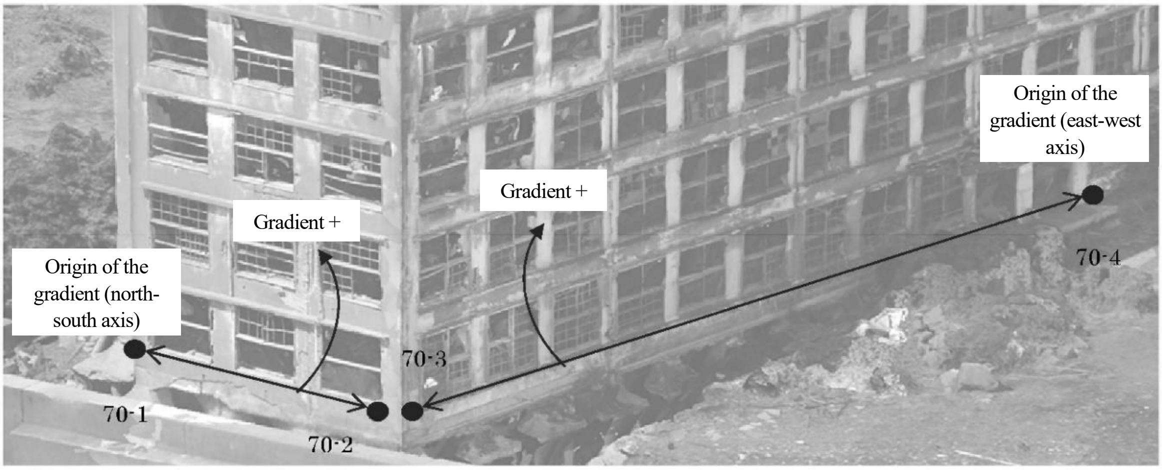

Figure 2-4-55 Direction of the gradient

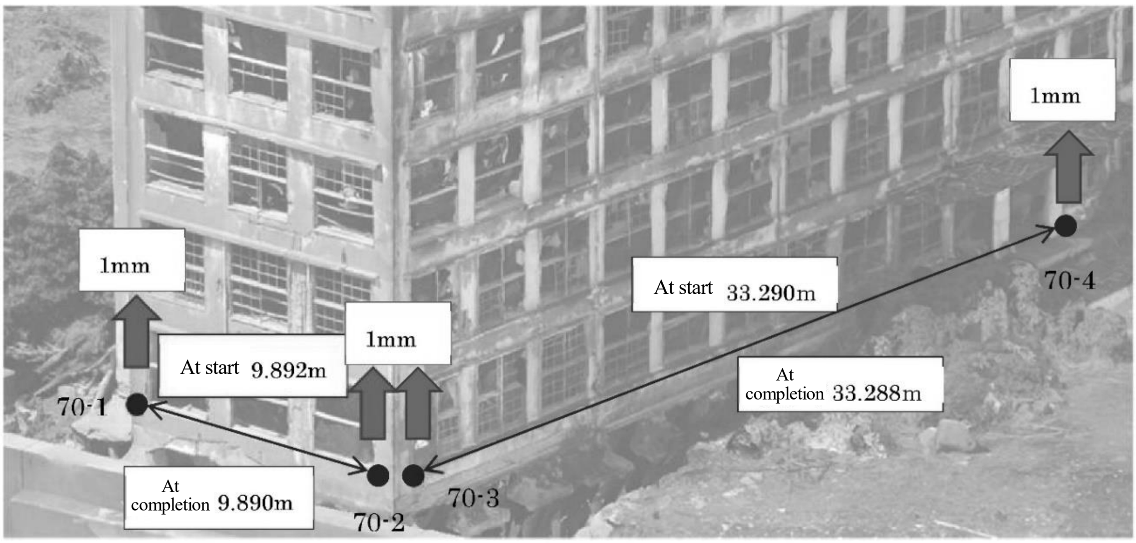

Figure 2-4-56 Measurement results of altitude/distance between two points

④-1 Three-dimensional laser measurement

In calculating the gradient of Building No.70, a three-dimensional laser measurement was performed supplementarily. Shown below is the result obtained by combining a total of 10 cuts measured around Building No.70 as well as in the east end room within Building No.70. All the data are expressed as points with three-dimensional coordinates. Extracting an arbitrary section is also possible; the thickness of wall/slab can be calculated by measuring the inside and outside of the building.

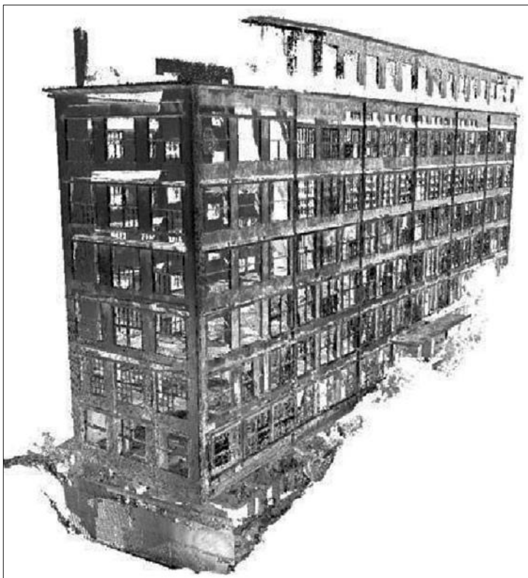

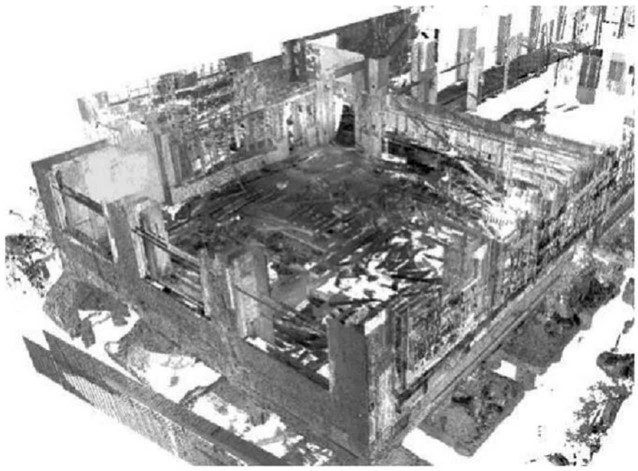

An area below waist height on Level 1 of Building No.70

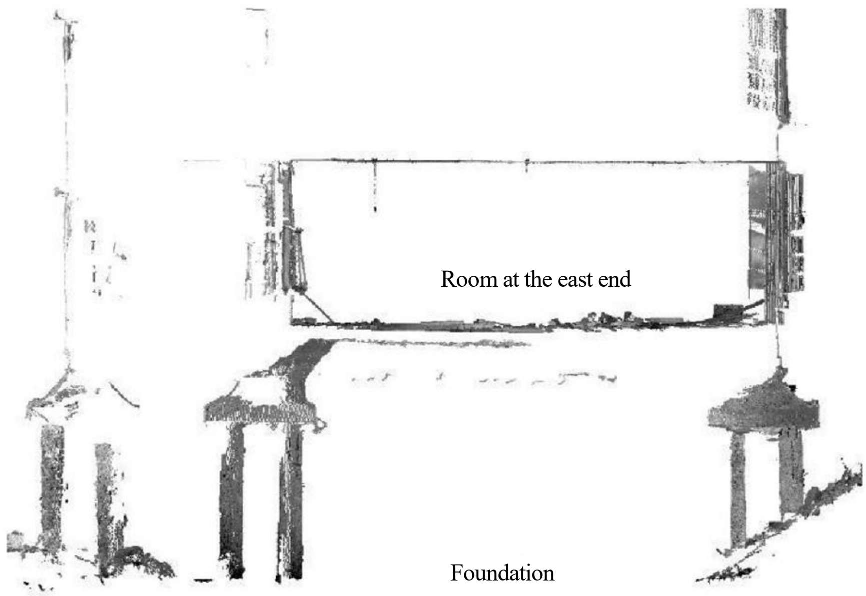

Cross section of Building No.70

Figure 2-4-57 Building No.70 data of a group of three-dimensional points

⑤ Deformed state drawing

The deformed state drawing (damage drawing) that reflects the two measurements and the three-dimensional laser measurement is shown in Figure 2-4-58.

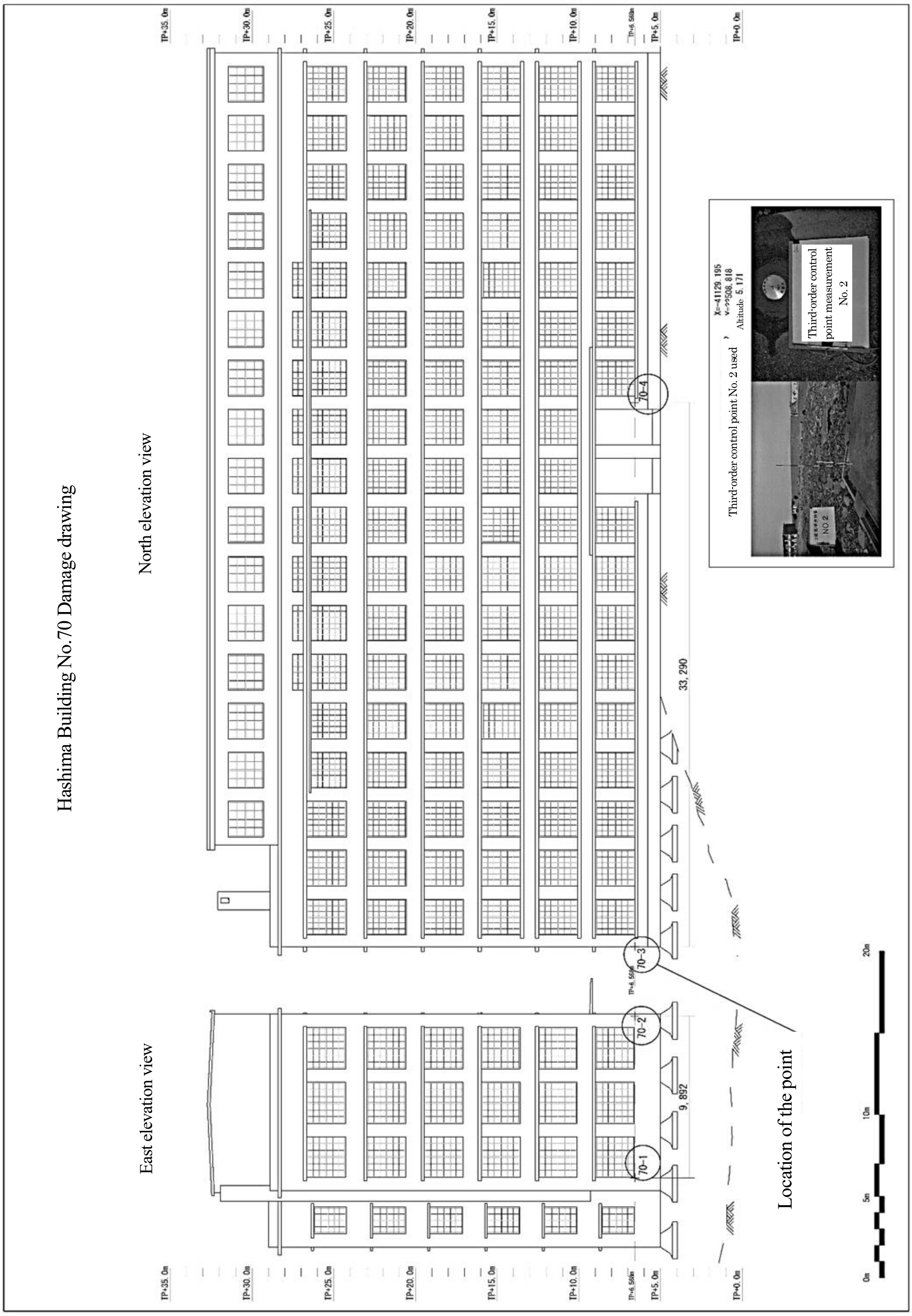

Figure 2-4-58 Building No.70 Deformed state drawing

⑥ Slant estimation

Figure 2-4-59 shows the displacement of a wall surface from a plane vertical to a reference line, which is set below the window on Level 1 of the east face of Building No.70, using colors. As the legends show, the green color is used as a reference, while the red and blue colors indicate the groups of points measured on the wall surfaces 30 mm front and 30 mm back of the reference plane, respectively. It should be noted that measurements were conducted only from the ground this time, and accordingly, the point density is low in the upper areas. Observation of measurement results show the upper areas exhibit colors closer to blue, suggesting that wall surfaces are at the back of the reference plane. However, because only Level 1 strongly shows a green to red color, Level 1 appears to project to the east side by 15–20 mm compared with Level 2 and upper floors.

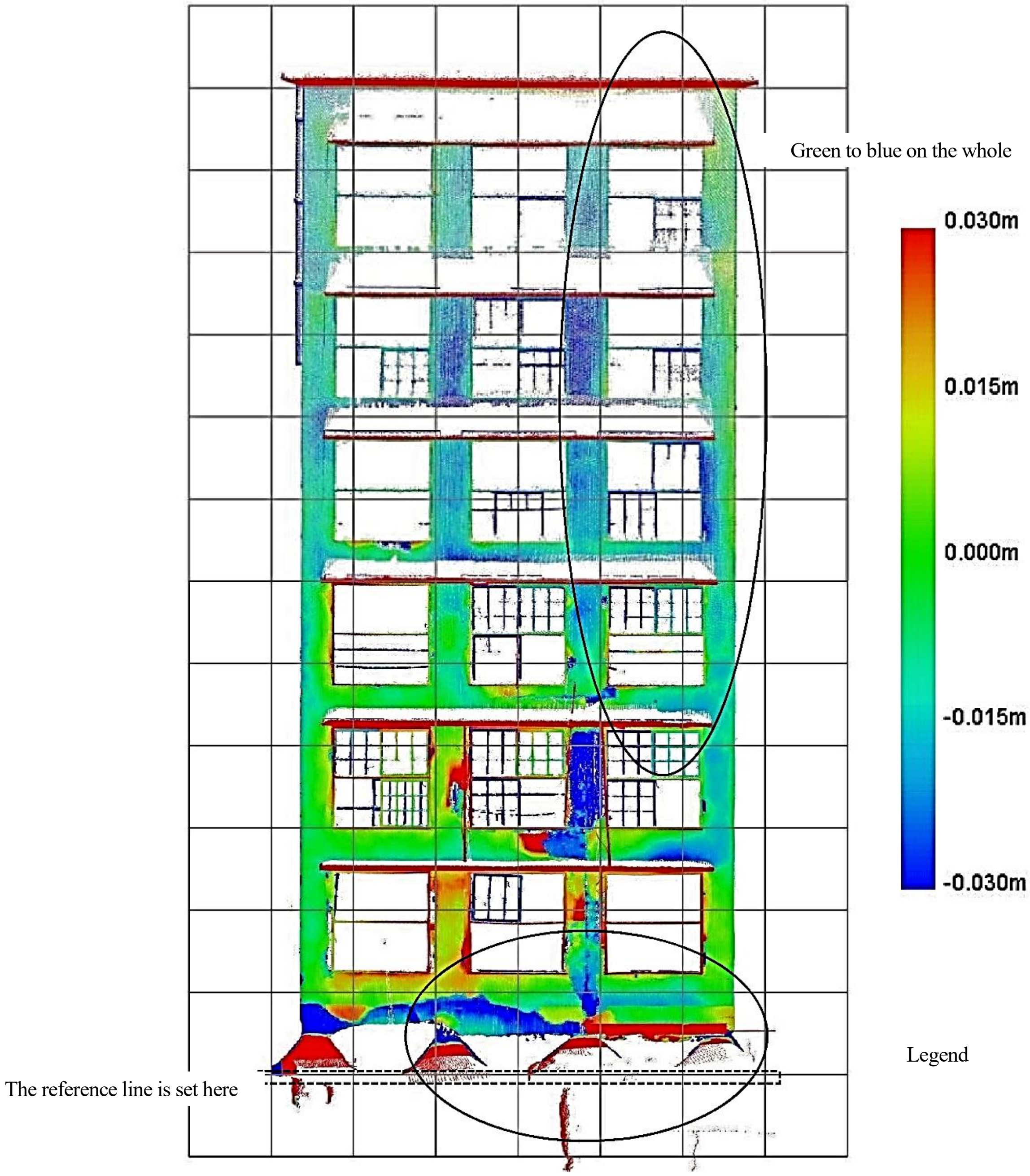

Figure 2-4-59 Building No.70 east face color contour drawing (± 30 mm)

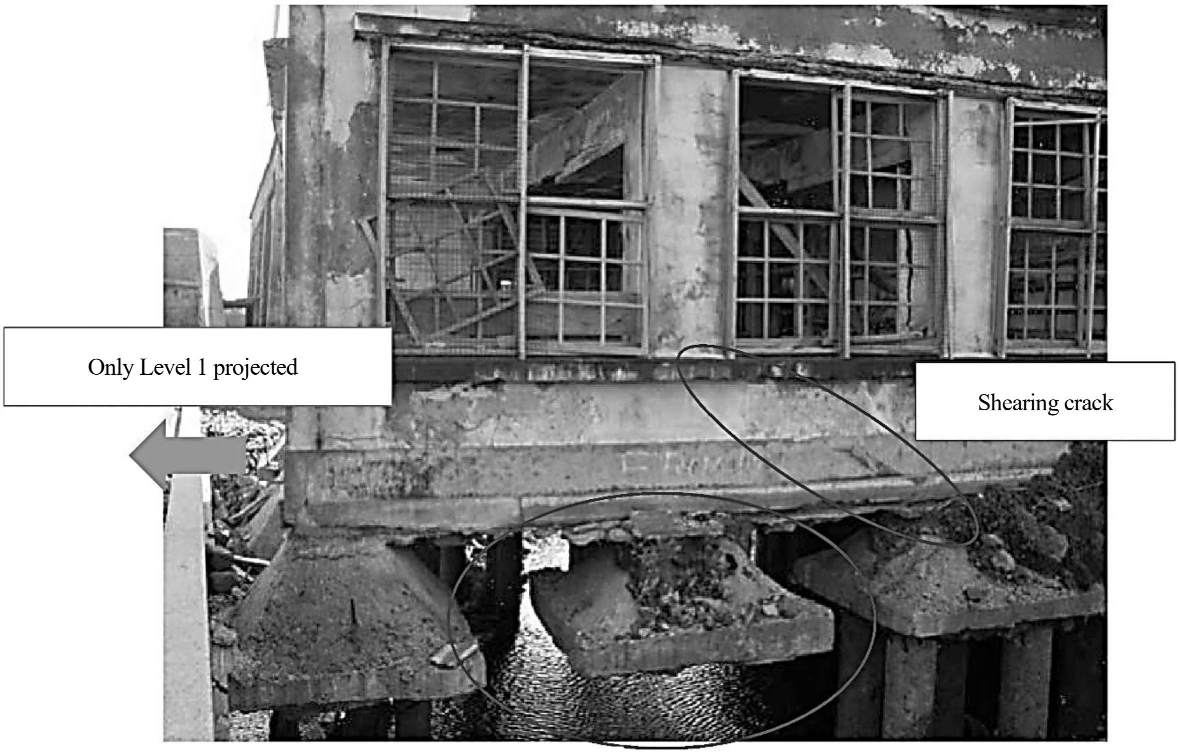

Photo 2-4-115　Building No.70 north face east end

2) Survey of the current deterioration level of Building No.70

① Outline of the survey

To determine the current deterioration level of Building No.70 structures, "Corrosion grading," which focuses on the corrosion of rebars, and "Structural performance grading," which focuses on structural performance, were used. For each grading, the methods based on those described in the "Report of deterioration survey of concrete structures in Gunkanjima (Architectural Institute of Japan, 2013)" were used.

② Corrosion grading evaluation

Visual inspection of columns and beam members is made, and the damage degree is determined on the basis of the condition of cracks, rust fluid, and rebar exposure on the surface. Described below are criteria tables and reference examples (Photo 2-4-116), as well as the results of corrosion grading visual inspection for Level 1 to Level 6 of Building No.70 (Figure 2-4-60 / 61). Table 2-4-50 shows the ordinary classification of damage degrees, and Table 2-4-51 indicates evaluation criteria that reflect the current circumstances of Hashima, which were established by the Architectural Institute of Japan. In this visual inspection, Table 2-4-51 was used for evaluation.

Through the observation of the evaluation results, we can find marked deteriorations on the east side on many Levels. In addition, deteriorations are more serious on the north side than on the south side. This is presumably because there are no structures that block wind and rain as well as sea breezes on the east side and the north side.

Table 2-4-50 Ordinary classification of damage degrees

Damage degrees	Damaged condition
No damage	No damage is found
I	Only minor cracks and rust fluid are found
II	Cracks , rust fluid, or peeling is found in some parts
III	Cracks , rust fluid, peeling, or falling is found successively
IV	Exposure or rupture of steel materials, or a loss of cross-sectional area in concrete is found

Table 2-4-51 Evaluation criteria tailored to the current circumstances of Hashima

Damage degree	Damaged condition	Legend
Grade I	Cracks + rust fluid on the surface	■
Grade II		■
Grade III	Corroded rebar is exposed	■
Grade IV		■
Grade V	Rebar leaves its trace but has decayed (does not exist)	■

Grade I

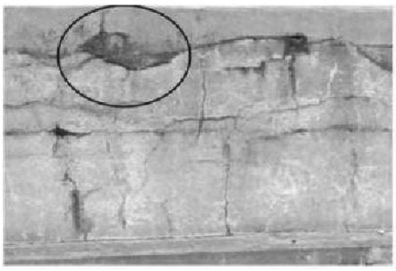

Grade II

Grade III

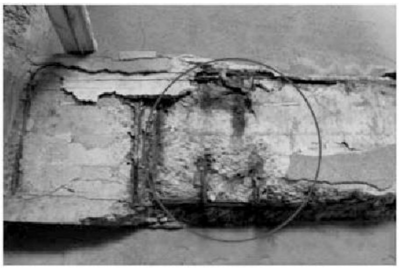

Grade Ⅳ

Grade Ⅴ

Source: Report of the Architectural Institute of Japan

Photo 2-4-116 Examples of deterioration grades tailored to the current state of Hashima

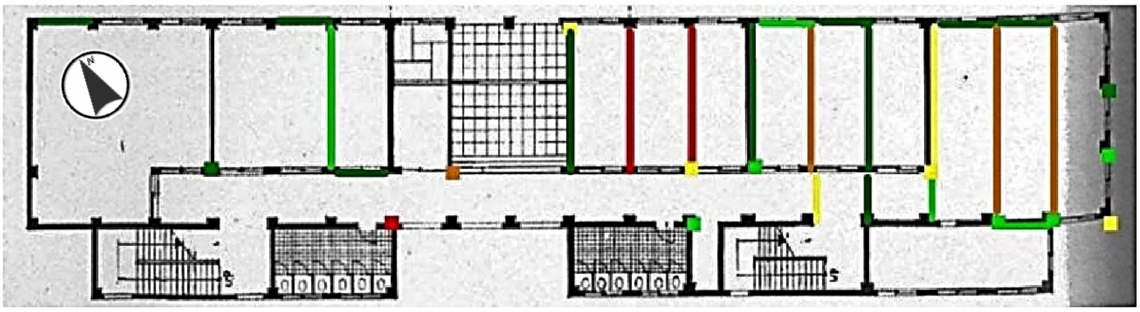

Building No.70 deterioration level distribution map (Level 1)

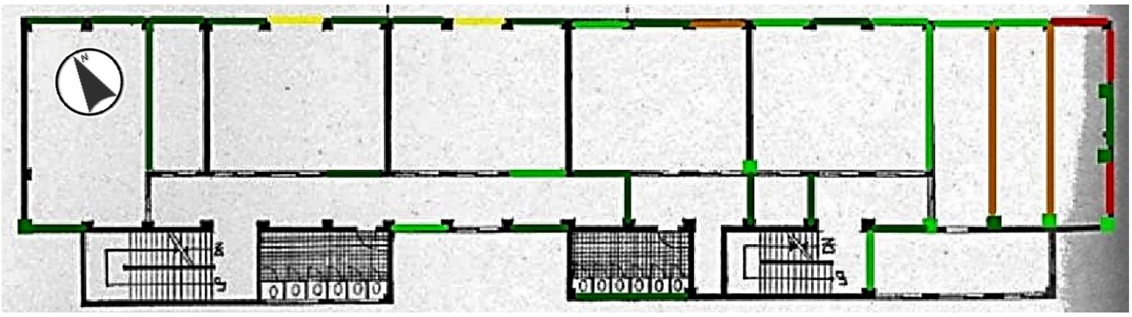

Building No.70 deterioration level distribution map (Level 2)

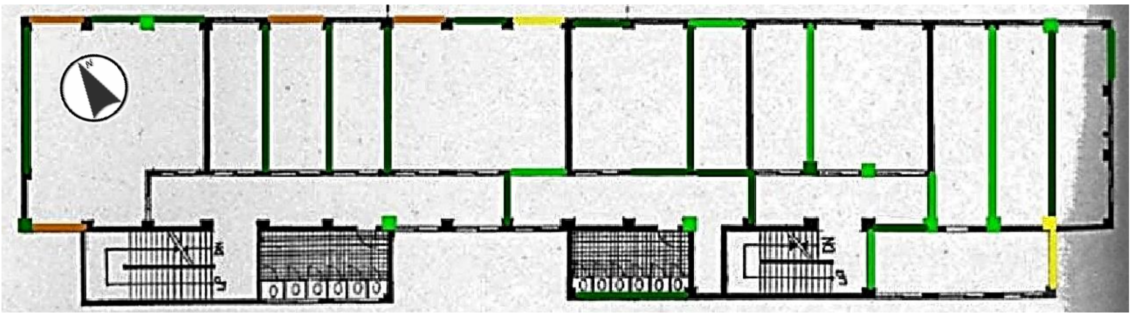

Building No.70 deterioration level distribution map (Level 3)

Figure 2-4-60 Building No.70 deterioration level distribution maps (Level 1 to Level 3)

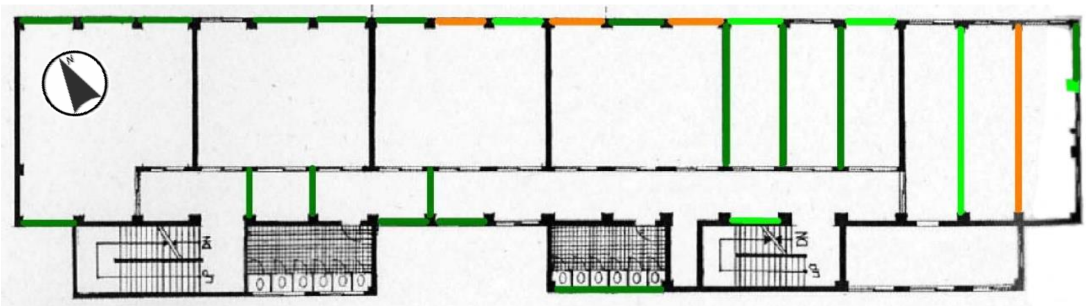

Building No.70 deterioration level distribution map (Level 4)

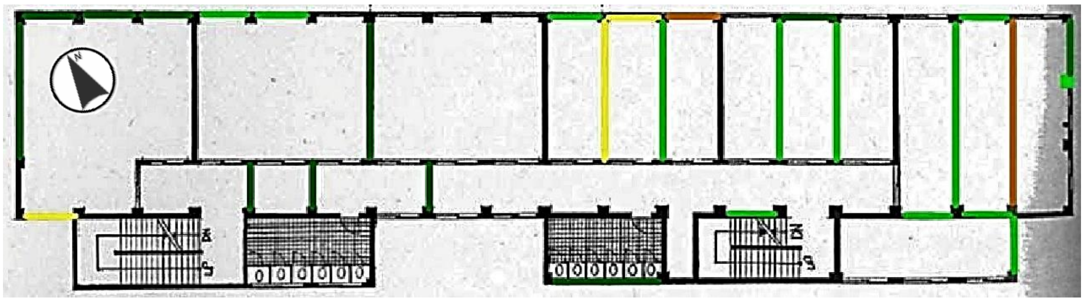

Building No.70 deterioration level distribution map (Level 5)

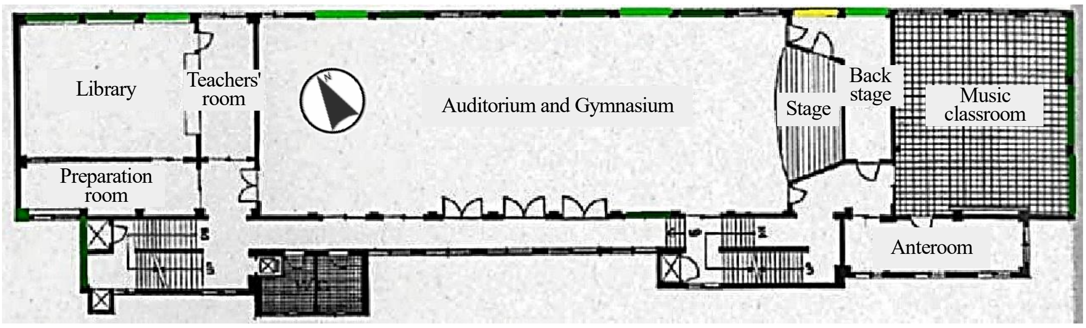

Building No.70 deterioration level distribution map (Level 6)

Figure 2-4-61 Building No.70 deterioration level distribution maps (Level 4 to Level 6)

③Structural performance grading evaluation

Visual inspection of vertical members (i.e., shear columns, bending columns, walls without a column, walls with a column on one side, and walls with columns on both sides) of the building is made, and the damage degree is evaluated on the basis of surface crack width, falling of concrete cover, and the condition of rebar. Described below are the criteria table (Table 2-4-52) and reference examples (Photo 2-4-117), as well as the results of structure grading visual inspection for Level 1 to Level 6 of Building No.70 (Figure 2-4-62 and -63). From the observation of the evaluation results, we can find that deteriorations are more serious on the east side than on the west side, with no variations in damage seen for Level 3.

Table 2-4-52 Damage degree and damage description

Damage degree	Damage
0	No damage
I	Crack width: ≤ 0.2 mm
II	Crack width: 0.2–1.0 mm
III	Crack width: 0.2–1.0 mm, limited concrete falling
IV	Crack width: ≥ 2.0 mm, concrete falling
V	Buckling or rapture / axial contraction of rebar

Damage degree III

Damage degree IV

Column: Damage degree III

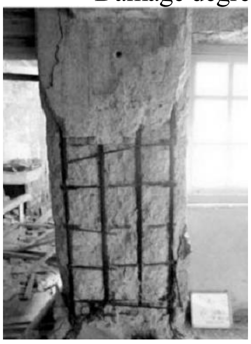

Column: Damage degree IV

Wall: Damage degree IV

Photo 2-4-117 Examples of structural performance grading

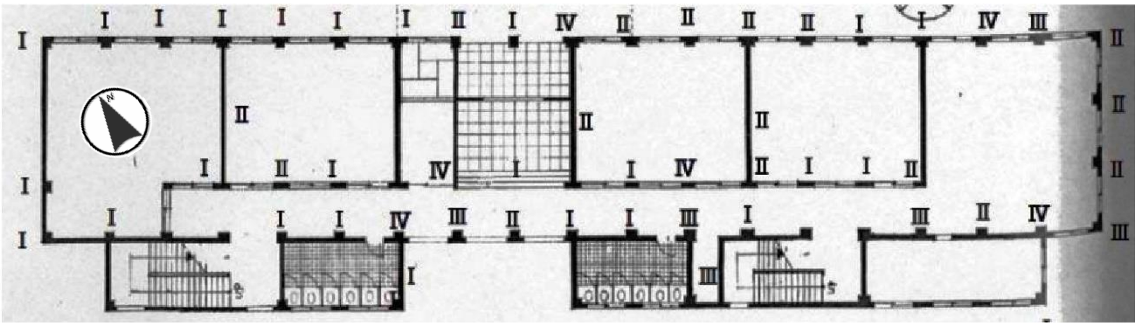

Building No.70 damage degree determination result (Level 1)

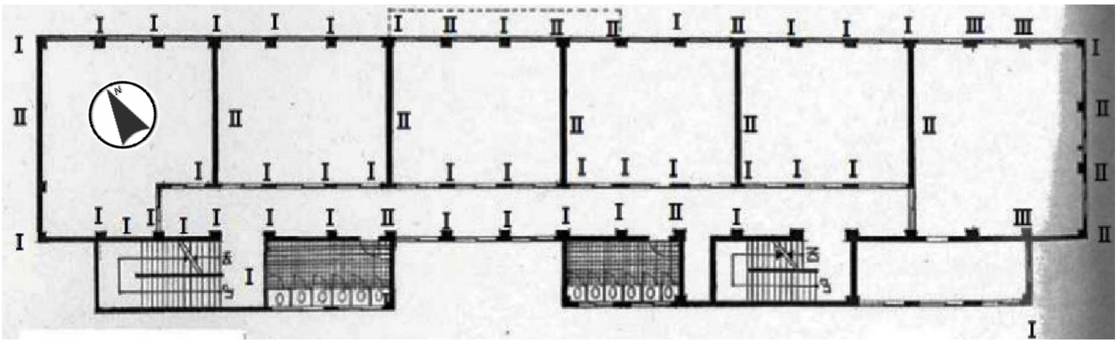

Building No.70 damage degree determination result (Level 2)

Figure 2-4-62 Building No.70 damage degree determination result (Level 1 and Level 2)

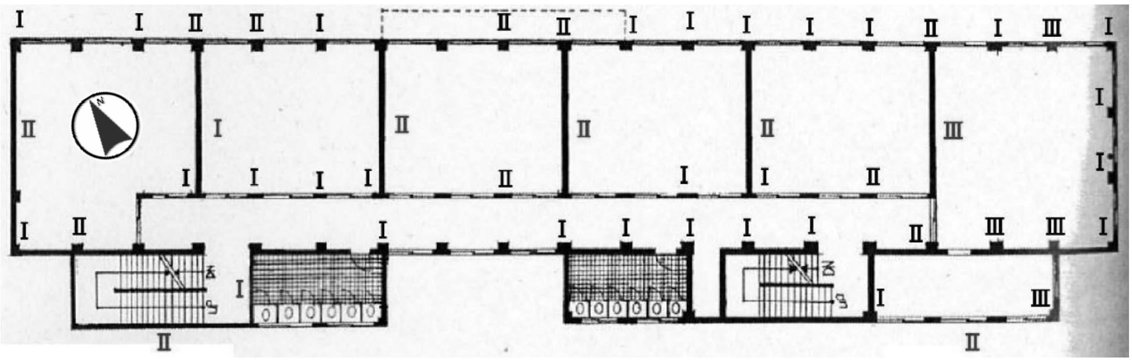

Building No.70 damage degree determination result (Level 3)

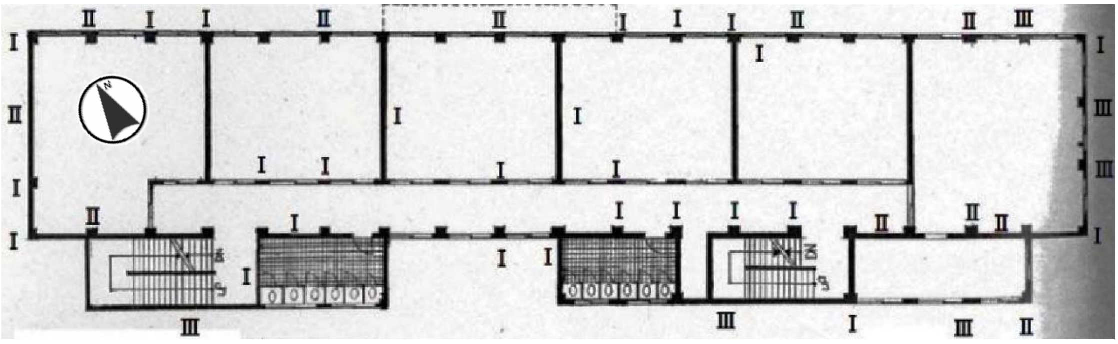

Building No.70 damage degree determination result (Level 4)

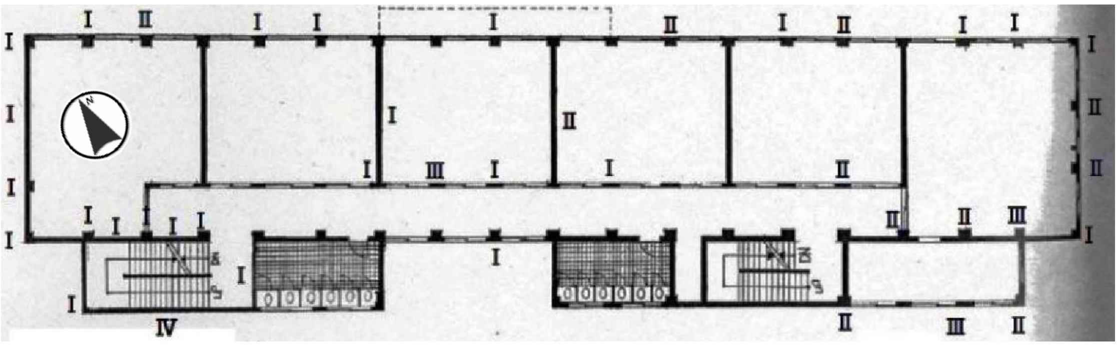

Building No.70 damage degree determination result (Level 5)

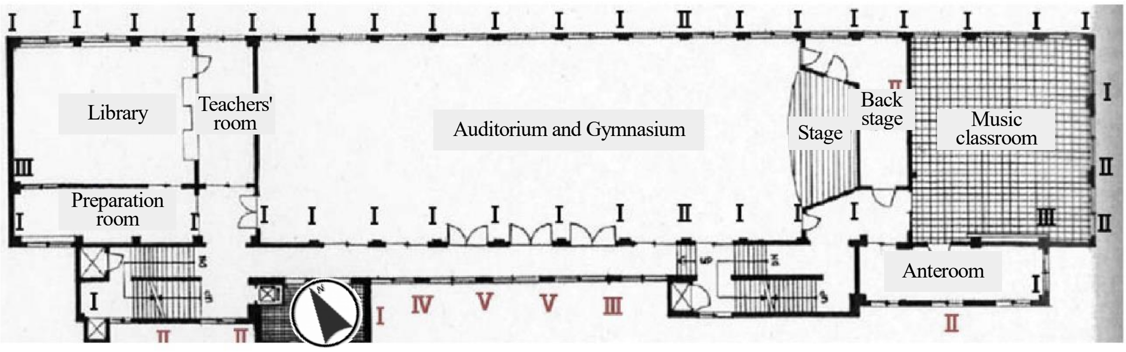

Building No.70 damage degree determination result (Level 6)

Figure 2-4-63　Building No.70 damage degree determination result (Level 3 to Level 6)

④ Calculation of deterioration grades

The tables used to calculate deterioration grades are shown below (Tables 2-4-53 and 54). From the totaled results, the residual seismic performance ratio was lowest on Level 2 at 71.7% and highest on Level 5 at 94.3%. Concerning the determination of damage, Level 2 was determined to be "Intermediate damage" and the other Levels to be "Minor damage."

Residual seismic performance ratio (R)	Damage degree
R=100	No damage
$95 \leq R < 95$	Slight
$80 \leq R < 95$	Minor damage
$60 \leq R < 80$	Intermediate damage
$R < 60$	Major damage

Table 2-4-53 Damage degree summary sheet (Level 1 to Level 3)

Table: Damage degree tabulation (Level 1)

	Shear column				Bending column				Wall without a column				Wall with a column on one side				Wall with columns on both sides				Total	
No. of total members	61			+	0			+	3			+	5			+	25			=		
No. of members surveyed	61			+	0			+	3			+	5			+	25			=		
	No. of members inspected	×	1	+	No. of members inspected	×	1	+	No. of members inspected	×	1	+	No. of members inspected	×	2	+	25	×	6	=	224	Aorg
Damage degree 0	14	×	1	+	0	×	1	+	2	×	1	+	5	×	2	+	21	×	6	=	152	A0
Damage degree I	23	×	0.95	+	0	×	0.95	+	0	×	0.95	+	0	×	1.9	+	1	×	6	=	27.55	A1
Damage degree II	14	×	0.6	+	0	×	0.75	+	0	×	0.6	+	0	×	1.2	+	3	×	4	=	19.2	A2
Damage degree III	5	×	0.3	+	0	×	0.5	+	1	×	0.3	+	0	×	0.6	+	0	×	2	=	1.8	A3
Damage degree IV	5	×	0	+	0	×	0.1	+	0	×	0	+	0	×	0	+	0	×	0	=	0	A4
Damage degree V	0	×	0	+	0	×	0.0	+	0	×	0	+	0	×	0	+	0	×	0	=	0	A5

ΣAj = A0+A1+A2+A3+A4+A5 = 200.55

Residual seismic performance ratio = ΣAj / Aorg = 89.5 Minor damage

Table: Damage degree tabulation (Level 2)

	Shear column				Bending column				Wall without a column				Wall with a column on one side				Wall with columns on both sides				Total	
No. of total members	60			+	0			+	1			+	5			+	26			=		
No. of members surveyed	60			+	0			+	1			+	5			+	26			=		
	No. of members inspected	×	1	+	No. of members inspected	×	1	+	No. of members inspected	×	1	+	No. of members inspected	×	2	+	No. of members inspected	×	6	=	227	Aorg
Damage degree 0	12	×	1	+	0	×	1	+	1	×	1	+	5	×	2	+	10	×	6	=	83	A0
Damage degree I	37	×	0.95	+	0	×	0.95	+	0	×	0.95	+	0	×	1.9	+	3	×	6	=	52.25	A1
Damage degree II	9	×	0.6	+	0	×	0.75	+	0	×	0.6	+	0	×	1.2	+	6	×	4	=	27	A2
Damage degree III	2	×	0.3	+	0	×	0.5	+	0	×	0.3	+	0	×	0.6	+	0	×	2	=	0.6	A3
Damage degree IV	0	×	0	+	0	×	0.1	+	0	×	0	+	0	×	0	+	0	×	0	=	0	A4
Damage degree V	0	×	0	+	0	×	0.0	+	0	×	0	+	0	×	0	+	0	×	0	=	0	A5

ΣAj = A0+A1+A2+A3+A4+A5 = 162.85

Residual seismic performance ratio = ΣAj / Aorg = 71.7 Intermediate damage

Table: Damage degree tabulation (Level 3)

	Shear column				Bending column				Wall without a column				Wall with a column on one side				Wall with columns on both sides				Total	
No. of total members	60			+	0			+	1			+	5			+	26			=		
No. of members surveyed	60			+	0			+	1			+	5			+	26			=		
	No. of members inspected	×	1	+	No. of members inspected	×	1	+	No. of members inspected	×	1	+	No. of members inspected	×	2	+	No. of members inspected	×	6	=	227	Aorg
Damage degree 0	21	×	1	+	0	×	1	+	1	×	1	+	3	×	2	+	19	×	6	=	142	A0
Damage degree I	26	×	0.95	+	0	×	0.95	+	0	×	0.95	+	2	×	1.9	+	2	×	6	=	39.9	A1
Damage degree II	9	×	0.6	+	0	×	0.75	+	0	×	0.6	+	0	×	1.2	+	4	×	4	=	19.8	A2
Damage degree III	4	×	0.3	+	0	×	0.5	+	0	×	0.3	+	0	×	0.6	+	1	×	2	=	3	A3
Damage degree IV	0	×	0	+	0	×	0.1	+	0	×	0	+	0	×	0	+	0	×	0	=	0	A4
Damage degree V	0	×	0	+	0	×	0.0	+	0	×	0	+	0	×	0	+	0	×	0	=	0	A5

ΣAj = A0+A1+A2+A3+A4+A5 = 204.7

Residual seismic performance ratio = ΣAj / Aorg = 90.2 Minor damage

Appendix 1

Table 2-4-54 Damage degree summary sheet (Level 4 to Level 6)

Table: Damage degree tabulation (Level 4)

	Shear column				Bending column				Wall without a column				Wall with a column on one side				Wall with columns on both sides				Total	
No. of total members	61			+	0			+	1			+	5			+	25			=		
No. of members surveyed	61			+	0			+	1			+	5			+	25			=		
	No. of members inspected	×	1	+	No. of members inspected	×	1	+	No. of members inspected	×	1	+	No. of members inspected	×	2	+	25	×	6	=	222	Aorg
Damage degree 0	28	×	1	+	0	×	1	+	1	×	1	+	2	×	2	+	19	×	6	=	147	A0
Damage degree I	22	×	0.95	+	0	×	0.95	+	0	×	0.95	+	0	×	1.9	+	3	×	6	=	38	A1
Damage degree II	8	×	0.6	+	0	×	0.75	+	0	×	0.6	+	0	×	1.2	+	3	×	4	=	15.6	A2
Damage degree III	3	×	0.3	+	0	×	0.5	+	1	×	0.3	+	0	×	0.6	+	0	×	2	=	2.7	A3
Damage degree IV	0	×	0	+	0	×	0.1	+	0	×	0	+	0	×	0	+	0	×	0	=	0	A4
Damage degree V	0	×	0	+	0	×	0.0	+	0	×	0	+	0	×	0	+	0	×	0	=	0	A5

Σ Aj = A0+A1+A2+A3+A4+A5 = 203.3

Residual seismic performance ratio = Σ Aj / Aorg = 91.6 Minor damage

Table: Damage degree tabulation (Level 5)

	Shear column				Bending column				Wall without a column				Wall with a column on one side				Wall with columns on both sides				Total	
No. of total members	60			+	0			+	1			+	5			+	26			=		
No. of members surveyed	60			+	0			+	1			+	5			+	26			=		
	No. of members inspected	×	1	+	No. of members inspected	×	1	+	No. of members inspected	×	1	+	No. of members inspected	×	2	+	No. of members inspected	×	6	=	227	Aorg
Damage degree 0	31	×	1	+	0	×	1	+	1	×	1	+	3	×	2	+	21	×	6	=	164	A0
Damage degree I	18	×	0.95	+	0	×	0.95	+	0	×	0.95	+	0	×	1.9	+	4	×	6	=	39.9	A1
Damage degree II	9	×	0.6	+	0	×	0.75	+	0	×	0.6	+	0	×	1.2	+	1	×	4	=	9	A2
Damage degree III	2	×	0.3	+	0	×	0.5	+	0	×	0.3	+	1	×	0.6	+	0	×	2	=	1.2	A3
Damage degree IV	0	×	0	+	0	×	0.1	+	0	×	0	+	1	×	0	+	0	×	0	=	0	A4
Damage degree V	0	×	0	+	0	×	0.0	+	0	×	0	+	0	×	0	+	0	×	0	=	0	A5

Σ Aj = A0+A1+A2+A3+A4+A5 = 214.1

Residual seismic performance ratio = Σ Aj / Aorg = 94.3 Minor damage

Table: Damage degree tabulation (Level 6)

	Shear column				Bending column				Wall without a column				Wall with a column on one side				Wall with columns on both sides				Total	
No. of total members	56			+	0			+	1			+	4			+	12			=		
No. of members surveyed	56			+	0			+	1			+	4			+	12			=		
	No. of members inspected	×	1	+	No. of members inspected	×	1	+	No. of members inspected	×	1	+	No. of members inspected	×	2	+	No. of members inspected	×	6	=	137	Aorg
Damage degree 0	9	×	1	+	0	×	1	+	0	×	1	+	1	×	2	+	11	×	6	=	77	A0
Damage degree I	35	×	0.95	+	0	×	0.95	+	1	×	0.95	+	0	×	1.9	+	0	×	6	=	34.2	A1
Damage degree II	5	×	0.6	+	0	×	0.75	+	0	×	0.6	+	3	×	1.2	+	1	×	4	=	10.2	A2
Damage degree III	4	×	0.3	+	0	×	0.5	+	0	×	0.3	+	0	×	0.6	+	0	×	2	=	1.2	A3
Damage degree IV	3	×	0	+	0	×	0.1	+	0	×	0	+	0	×	0	+	0	×	0	=	0	A4
Damage degree V	0	×	0	+	0	×	0.0	+	0	×	0	+	0	×	0	+	0	×	0	=	0	A5

Σ Aj = A0+A1+A2+A3+A4+A5 = 122.6

Residual seismic performance ratio = Σ Aj / Aorg = 89.5 Minor damage

⑤ Three-dimensional elastic analysis by FEM

To understand the current deterioration level of the overall structure, the deterioration level of the foundation was calculated using the three-dimensional elastic analysis by FEM, in which foundation piles and the undermost layer of the structure were modeled.

Concerning the analytical method, the three-dimensional elastic model of analysis objects (i.e., foundation piles as well as underground beams and slabs in the undermost layer of the structure) is created first, and then, the fixed load of the structure is calculated for each of a wall, column, beam, floor slab, and staircase. After that, a verification was conducted by setting analysis cases to evaluate the vertical and horizontal load-carrying capacity of the foundation of the structure, and the stability of the overall foundation was evaluated.

⑤-1 Modeling of analysis objects

The three-dimensional elastic model was created for foundation piles (made of concrete) as well as underground beams and slabs in the undermost layer of the structure as analysis objects (Table 2-4-55 and Figure 2-4-64).

Table 2-4-55 Methods for modeling members

	Member	Material	Model element	Remarks
1	Foundation pile	Reinforced concrete	Beam (bar) element	・Model each pile ・Reflect current condition ・Estimate the bar arrangement at the time of construction ・Regard a footing as a rigid body
2	Underground beam	Reinforced concrete	Beam (bar) element	・Estimate the bar arrangement of from the section size
3	Slab	Reinforced concrete	Shell element	・Do not model rebar
4	Ground	Soil	Spring element	・Consider the condition of pile embedment

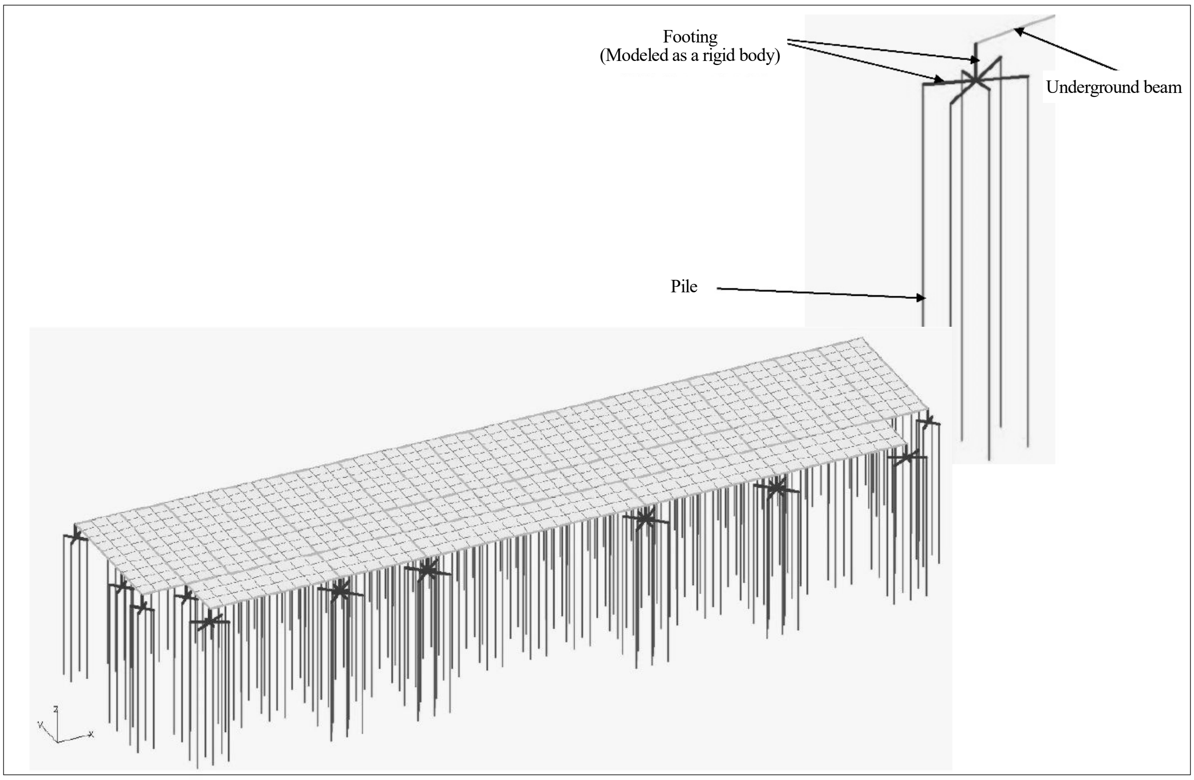

Figure 2-4-64 Model of three-dimensional elastic analysis by FEM
(the whole / foundation pile and footing)

⑤-2 Calculation of fixed load (deal load)

With regard to the fixed load of the structure, the weight was calculated for each of a wall, column, beam, floor slab, and staircase. Table 2-4-56 shows the results of fixed load calculation. In calculating the inertial force at the time of earthquake, the analysis model treats the weight shared by each Level as the weight concentrated in the location of the floor slab. For the totalization of the weight shared by each Level, the weights of the wall, column, and staircase were divided into two halves, and each half was allocated to the upper and lower Levels; then, the weights of the beam and floor slab of that Level were added. The item "Total Level weight Wi (kN)" in Table 2-4-56 shows the result of calculation performed in the manner described above. The calculation of the fixed load was mainly performed based on the assumptions of the notes ① to ⑥ for Table 2-4-56. The height of the structure was calculated through scaling based on the drawing data shown in Figure 2-4-65.

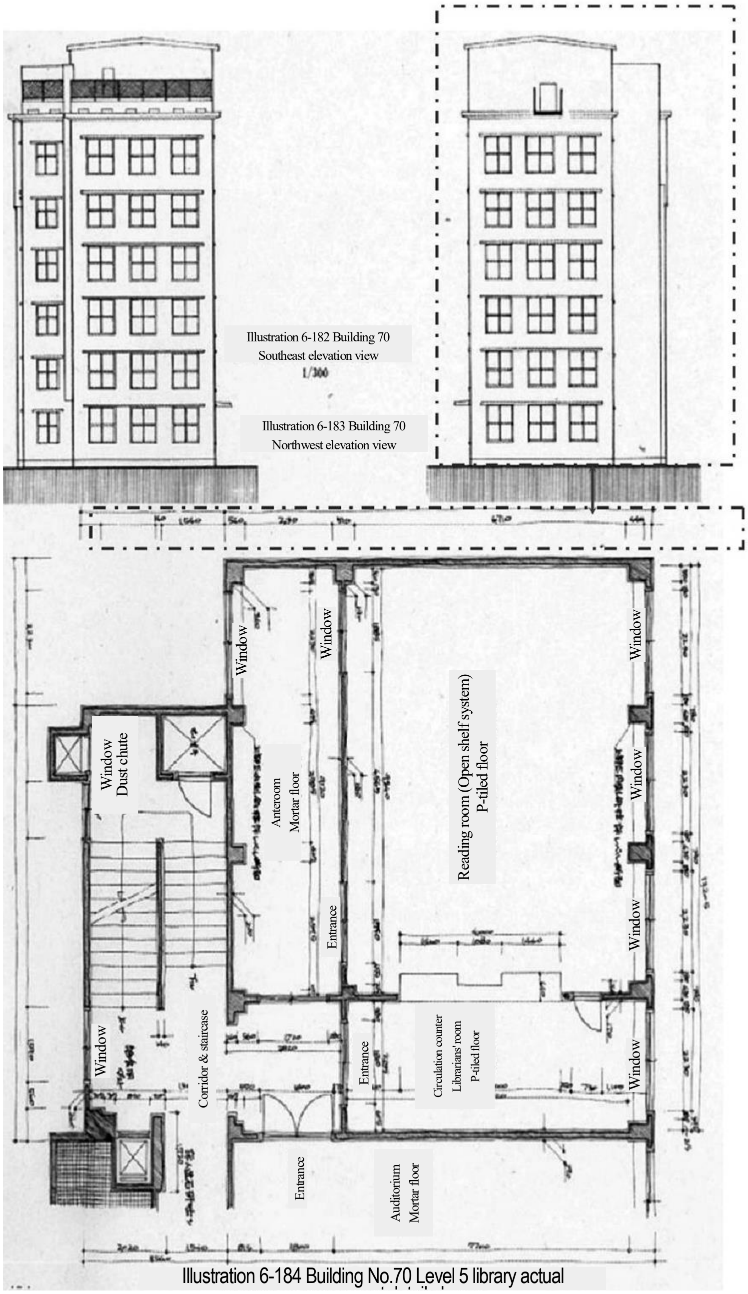

Figure 2-4-65 "Gunkanjima measurement survey data" (Akui, et al., 1984)

Table 2-4-56 Fixed load calculation result

Floor	Total Level weight Wi (kN)	Wall					Column								Beam							Floor slab							Staircase				
		Height Hw Note 7 (m)	Wall area (before deduction) Sw (m^2)	Thickness Bw Note 1 (m)	Window area (deduction) Sw (m^2)	Total volume (m^3)	Height Hp (m)	Column (type 1) Note 2			Column (type 2) Note 2			Total volume (m^3)	Longer direction (ridge direction) Note 3			Shorter direction (span direction) Note 3			Total volume (m^3)	Width Bs Note 4 (m)	Excluding restroom and preparation room		Restroom and preparation room		Total area (m^2)	Total volume (m^3)	Width HK (m)	Length LK (m)	Area AK (m^2)	Weight per unit area Note 5 (kN/m^2)	Weight WK (kN)
								Width Ap (m)	Thickness Bp (m)	No. of columns	Width Ap (m)	Thickness Bp (m)	No. of columns		Height HG (m)	Length LG (m)	Width BG (m)	Height HG (m)	Length LG (m)	Width BG (m)			Width Hs (m)	Length Ls (m)	Width Hs (m)	Length Ls (m)							
Roof	3.673																					0.10	45.825	10.53			482.54	48.25					
7 Note 6	7.489	4.30	883.62	0.15	191.16	103.87	4.30								0.35	139.86	0.32	0.65	61.99	0.25	13.69	0.20	55.01	10.53	3.56	22.65	659.89	131.98	3.56	16.61	59.13	4.80	283.83
6	7.999	5.00	920.01	0.20	214.91	141.02	5.00	0.55	0.43	46				54.40	0.35	155.40	0.32	0.65	75.39	0.25	15.94	0.20	55.01	10.53	3.56	22.65	649.01	129.80	3.56	16.61	59.13	4.80	283.83
5	7.502	3.60	727.45	0.20	231.52	99.19	3.60	0.55	0.55	48	0.30	0.30	14	56.81	0.35	155.40	0.32	0.65	75.39	0.25	15.94	0.20	55.01	10.53	3.56	22.65	644.11	128.82	3.56	16.61	59.13	4.80	283.83
4	7.502	3.60	727.45	0.20	231.52	99.19	3.60	0.55	0.55	48	0.30	0.30	14	56.81	0.35	155.40	0.32	0.65	75.39	0.25	15.94	0.20	55.01	10.53	3.56	22.65	644.11	128.82	3.56	16.61	59.13	4.80	283.83
3	7.673	3.60	727.45	0.20	231.52	99.19	3.60	0.55	0.55	48	0.30	0.30	14	56.81	0.35	155.40	0.32	0.65	75.39	0.25	15.94	0.20	55.01	10.53	3.56	22.65	644.11	128.82	3.56	16.61	59.13	4.80	283.83
2	8.442	3.60	727.45	0.20	231.52	99.19	3.60	0.70	0.55	48	0.30	0.30	14	71.06	0.35	155.22	0.32	0.65	77.03	0.25	15.88	0.20	55.01	10.53	3.56	22.65	640.15	128.03	3.56	16.61	59.13	4.80	283.83
1	16.138	4.30	900.81	0.20	216.32	136.9	4.30	0.70	0.55	48	0.30	0.30	14	84.88	1.15	155.22	0.55	1.15	77.03	0.55	99.99	0.35	55.01	10.53	3.56	22.65	640.15	224.05	3.56	16.61	59.13	4.80	283.83

Note 1: For wall thickness, concrete walls with a general thickness of 20 cm were assumed for Level 1 to Level 6. For Level 7, though containing steel members, the weight was assumed to be equivalent to that of a 15 cm thick concrete wall.

Note 2: Dimensions of columns were divided into two types for assumption on the basis of simplified measurements obtained in the on-site survey.

Note 3: Dimensions of beams were divided into two types (longer direction [ridge direction] and shorter direction [span direction]) for assumption on the basis of simplified measurements obtained in the on-site survey.

Note 4: Regarding the thickness of floor slabs, simplified measurements obtained in the on-site survey were used for Level 1; a general thickness of 20 cm were assumed for the other Levels. For the roof, the weight was assumed to be equivalent to that of 10 cm thick concrete.

Note 5: For the staircase, the weight per unit area equivalent to the weight of 20 cm thick concrete (= 24 kN/m^3 x 0.2 m = 4.80 kN/m^3)

Note 6: The weight of the steel frame part of Level 7 was calculated by assuming the dimensions on the basis of the pictures taken during the on-site survey.

Note 7: The height of the structure was calculated through scaling based on drawing data.

⑤-3 Setting of analysis cases and modeling of surcharge loads

To evaluate the vertical and horizontal load-carrying capacity required for the foundation of the structure, analysis cases were set as described in Table 2-4-57. The surcharge load was modeled using methods indicated in Table 2-4-58.

Table 2-4-57 Analysis cases

Analysis Case	Analysis condition	Items checked	Remarks
0	Restoration of the construction at the time of completion	・Stability of foundation ・Bearing capacity of pile ・Stress of pile	・Stationary (only deal load) ・Confirm a case where the foundation is sound (→ Verify the validity of modeling)
1	Current condition	・Stability of foundation ・Bearing capacity of pile ・Stress of pile	・Stationary (only deal load) ・Determine the theoretical destruction state (deterioration level) ・Identify points to note for restoration work
2	After restoration work	・Stability of foundation ・Bearing capacity of pile ・Stress of pile	・Stationary (only deal load) ・Confirm the effect of restoration work (→ Identify points to note for maintenance)
3 (3.1–3.4)	After restoration work (at the time of Level 1 earthquake)	・Bearing capacity of pile ・Stress of pile	・Stationary (only deal load) + at the time of earthquake (horizontal load) ・Input each seismic force from four directions (both longer side directions, both shorter side directions)

Table 2-4-58 Surcharge load modeling method

1	Dead load	・Calculate the weight of the upper layer part on the basis of existing data ・Uniformly distribute the weight calculated, and apply it vertically downward on the slab
2	Seismic force	・Apply the horizontal inertial force equivalent to that at the time of earthquake on each Level, and thereby calculate the shearing force and bending moment that act on the undermost layer ・Apply the shearing force and bending moment calculated to the undermost layer * Evaluate Level 1 earthquake motion in accordance with the Building Standards Act

⑤-4 Results of Analysis Case 0 (Restoration of the construction at the time of completion)

The restoration of the construction at the time of completion was performed with respect to the stationary load. In the restoration analysis of the construction at the time of completion, the live load was added in addition to the fixed load. For the live load, in accordance with the Building Standards Act, a value of 2,100 N/m^2 was used, which is the value used for “the case where structural calculations of a girder, column, or foundation are performed” and “where classroom is selected as the room type.” For the specifications of the pile, the result of the on-site survey showed that the outside diameter of the pile (D) = 500 mm. Therefore, it was assumed to be an 80 mm thick hollow prefabricated pile by taking into account the situation at that time. From the situation of exposed rebar, the bar arrangement of the pile was assumed to be eight round axial reinforcing bars with a diameter of 13 mm. Table 2-4-59 shows the settings of material property values used for the analysis, and Tables 2-4-60 to 63 indicate the items checked and results of checking.

The results of checking show that the design of the restoration of the construction at the time of completion, which was based on various assumptions, was safe as the stress and bearing capacity of piles as well as the stability of the overall foundation were all OK.

Table 2-4-59 Settings of material property values

<table>
<tr><th colspan="2">Item</th><th>Code</th><th>Long term</th><th>Short term</th><th>Remarks</th></tr>
<tr><td rowspan="4">Concrete (beam/floor slab)</td><td>Design strength (N/mm²)</td><td>σck</td><td colspan="2">24</td><td>Assumption</td></tr>
<tr><td>Elastic coefficient: E (N/mm²)</td><td>Ec</td><td colspan="2">23004</td><td>Page 51 (Explanation 5.1, AIJ Standards for Structural Calculation of Reinforced Concrete Structures, (Architectural Institute of Japan, Revised 2010)</td></tr>
<tr><td>Poisson’s ratio</td><td>ν</td><td colspan="2">0.2</td><td>Page 50 (Table 5.1, AIJ Standards for Structural Calculation of Reinforced Concrete Structures, (Architectural Institute of Japan, Revised 2010)</td></tr>
<tr><td>Unit weight (kN/m³)</td><td>γ</td><td colspan="2">24</td><td>Page 59 (Table 7.1, AIJ Standards for Structural Calculation of Reinforced Concrete Structures, (Architectural Institute of Japan, Revised 2010)</td></tr>
<tr><td rowspan="6">Concrete (pile)</td><td>Design strength (N/mm²)</td><td>σck</td><td colspan="2">40</td><td>Assumption (JIS・A・5372)</td></tr>
<tr><td>Elastic coefficient: E (N/mm²)</td><td>Ec</td><td colspan="2">28058</td><td>Page 51 (Explanation 5.2, AIJ Standards for Structural Calculation of Reinforced Concrete Structures, (Architectural Institute of Japan, Revised 2010)</td></tr>
<tr><td>Poisson’s ratio</td><td>ν</td><td colspan="2">0.2</td><td>Page 50 (Table 5.1, AIJ Standards for Structural Calculation of Reinforced Concrete Structures, (Architectural Institute of Japan, Revised 2010)</td></tr>
<tr><td>Unit weight (kN/m³)</td><td>γ</td><td colspan="2">24.5</td><td>Page 59 (Table 7.1, AIJ Standards for Structural Calculation of Reinforced Concrete Structures, (Architectural Institute of Japan, Revised 2010)</td></tr>
<tr><td>Allowable bending and compressive strength (N/mm²)</td><td>σca</td><td>13.3</td><td>26.6</td><td>Page 53 (Table 6.1, AIJ Standards for Structural Calculation of Reinforced Concrete Structures, (Architectural Institute of Japan, Revised 2010)</td></tr>
<tr><td>Allowable shearing unit stress (N/mm²)</td><td>τa</td><td>0.890</td><td>1.335</td><td>Page 53 (Table 6.1, AIJ Standards for Structural Calculation of Reinforced Concrete Structures, (Architectural Institute of Japan, Revised 2010)</td></tr>
<tr><td rowspan="2">Rebar</td><td>Material (main reinforcement, distributing bar)</td><td>SR</td><td colspan="2">235</td><td>Page 53 (Table 6.2, AIJ Standards for Structural Calculation of Reinforced Concrete Structures, (Architectural Institute of Japan, Revised 2010)</td></tr>
<tr><td>Allowable tensile/compressive stress (N/mm²)</td><td>σs, a</td><td>155</td><td>235</td><td>Page 53 (Table 6.2, AIJ Standards for Structural Calculation of Reinforced Concrete Structures, (Architectural Institute of Japan, Revised 2010)</td></tr>
</table>

Table 2-4-60 Analysis Case 0 checking results

Item checked		Checking result	Observations
1	Checking of bending stress of the pile	OK	The stress was checked with respect to the parts that yielded the maximum bending moment value, the maximum axial force value, and the minimum axial force value for each of the longer side and shorter side directions, and the results did not exceed the allowable unit stress and were considered OK. Thus, all the results of checking of bending stress is considered OK for the whole pile.
2	Checking of shear stress of the pile	OK	The stress was checked with respect to the parts that yielded the maximum shearing force value for each of the longer side and shorter side directions, and the results did not exceed the allowable unit stress and were considered OK. Thus, all the results of checking of shearing stress is considered OK for the whole pile.
3	Checking of bearing capacity of the pile	OK	As no boring data are available, the fictional resistance of the intermediate layer was ignored and it was assumed that the bearing layer is a gravel layer with an N value of 40 and the embedment of the pile is 2D (D = 500 mm pile diameter). To achieve a safe side design with this stratum structure, the allowable bearing capacity and drawing power of the pile are calculated in accordance with *Pile Foundation Design Manual* (January 2007). The FORUM8’s pile foundation calculation program calculated the allowable bearing capacity at Ra = 468 kN and the allowable drawing power at Pa = 17 kN per pile at the normal

			time. From PNmax (= 433.9 kN) < Ra (= 468 kN), the bearing capacity of all the piles is considered OK. No drawing power of the piles was generated.
4	Checking of the overall foundation stability	OK	This checking was conducted using the eccentric distance: e = M/N (M: overturning moment, N: foundation reaction force) with respect to the center of gravity of the bottom slab. For the allowable eccentric distance value, the spread foundation normal-time allowable value B/6 (B: foundation width) was used. As the result of checking, the eccentric distances of both the longer side and shorter side directions did not exceed their allowable values; thus, the stability of the overall foundation is considered OK.

Table 2-4-61 Results of checking of shear stress of the pile

1) Shorter side direction

Item		Pile cross-sectional property			Section force response	Unit stress response	Allowable unit stress	Checking result	
		Diameter Φ (m)	Wall thickness t (m)	Cross-sectional area A (m^2)	Searing force Q (kN)	Average shearing unit stress τm (N/mm^2)	Shear τa (N/mm^2)	Shear τm/τa	Checking of shear
Pile	Shearing force maximum	0.5	0.08	0.1056	0.95	0.009	0.890	0.010	OK

2) Longer side direction

Position		Pile cross-sectional property			Section force response	Unit stress response	Allowable unit stress	Checking result	
		Diameter Φ (m)	Wall thickness t (m)	Cross-sectional area A (m^2)	Searing force Q (kN)	Average shearing unit stress τm (N/mm^2)	Shear τa (N/mm^2)	Shear τm/τa	Checking of shear
Pile	Shearing force maximum	0.5	0.08	0.1056	0.35	0.003	0.890	0.004	OK

Table 2-4-62 Results of checking of bending stress of the pile

1) Shorter side direction

Item		Pile cross-sectional property			Section force response		Unit stress response			Allowable unit stress			Checking result					
		Diameter Φ (m)	Wall thickness t (m)	Cross-sectional area A (m²)	Bending moment M (kN/m)	Axial force N (kN)	Concrete compression σs (N/mm²)	Steel tension σs (N/mm²)	Steel compression σs' (N/mm²)	Concrete bending compression σca (N/mm²)	Steel tension σsa (N/mm²)	Steel compression σsa' (N/mm²)	Concrete bending compression σca/σca (N/mm²)	Concrete bending compression checking	Steel tension σs/σsa	Steel tension checking	Steel compression σs'/σsa'	Steel compression checking
Pile	Bending moment maximum	0. 5	0. 08	0. 1056	8. 53	278. 72	3. 000	Not caused	-45. 000	13. 30	155. 00	-155. 00	0. 226	OK	-	-	0. 290	OK
	Axial force maximum	0. 5	0. 08	0. 1056	0. 36	433. 91	3. 600	Not caused	-54. 000	13. 30	155. 00	-155. 00	0. 271	OK	-	-	0. 348	OK
	Axial force minimum	0. 5	0. 08	0. 1056	1. 53	135.16	1. 200	Not caused	-18. 600	13. 30	155. 00	-155. 00	0. 090	OK	-	-	0. 120	OK

2) Longer side direction

Item		Pile cross-sectional property			Section force response		Unit stress response			Allowable unit stress			Checking result					
		Diameter Φ (m)	Wall thickness t (m)	Cross-sectional area A (m²)	Bending moment M (kN/m)	Axial force N (kN)	Concrete compression σs (N/mm²)	Steel tension σs (N/mm²)	Steel compression σs' (N/mm²)	Concrete bending compression σca (N/mm²)	Steel tension σsa (N/mm²)	Steel compression σsa' (N/mm²)	Concrete bending compression σca/σca (N/mm²)	Concrete bending compression checking	Steel tension σs/σsa	Steel tension checking	Steel compression σs'/σsa'	Steel compression checking
Pile	Bending moment maximum	0. 5	0. 08	0. 1056	3. 17	272. 83	2. 500	Not caused	-37. 600	13. 30	155. 00	-155. 00	0. 188	OK	-	-	0. 243	OK
	Axial force maximum	0. 5	0. 08	0. 1056	0. 06	433. 91	3. 600	Not caused	-53. 600	13. 30	155. 00	-155. 00	0. 271	OK	-	-	0. 346	OK
	Axial force minimum	0. 5	0. 08	0. 1056	0. 97	135. 16	1. 200	Not caused	-17. 900	13. 30	155. 00	-155. 00	0. 090	OK	-	-	0. 115	OK

Table 2-4-63 Results of checking of the overall foundation stability

Foundation reaction force	Overturning moment total		Bottom slab eccentric distance		Calculated bottom slab width (pillar centerline)		Allowable eccentric distance value		Result of checking of the overall foundation stability	
N (kN)	Longer direction (kN·m)	Shorter direction (kN·m)	Longer direction ex(m)	Shorter direction ey(m)	Longer direction width Bx(m)	Shorter direction width By(m)	Longer direction Bx/6	Shorter direction By/6	Longer direction (ex<Bx/6)	Shorter direction (ey<By/6)
74,316.16	-12,265.32	-9,383.83	0.165	0.126	54.460	13.39	9.077	2.232	OK	OK

Direction of the sea →

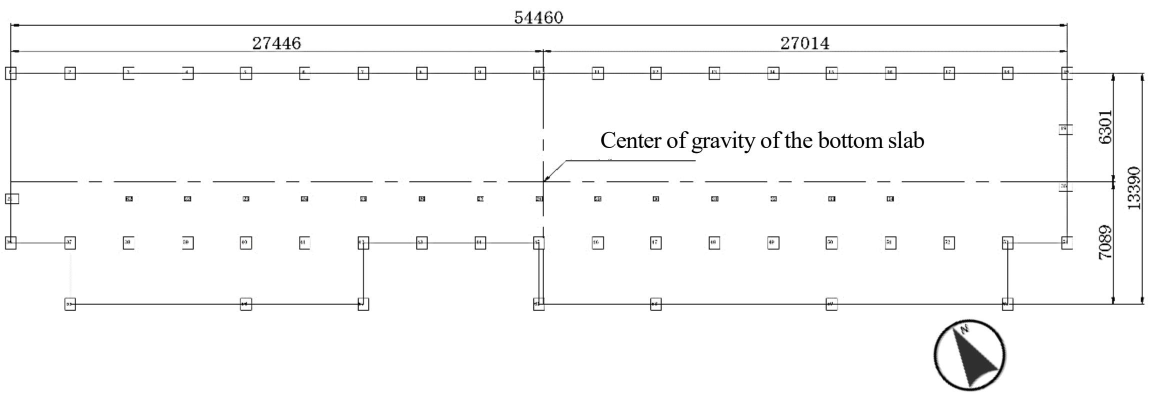

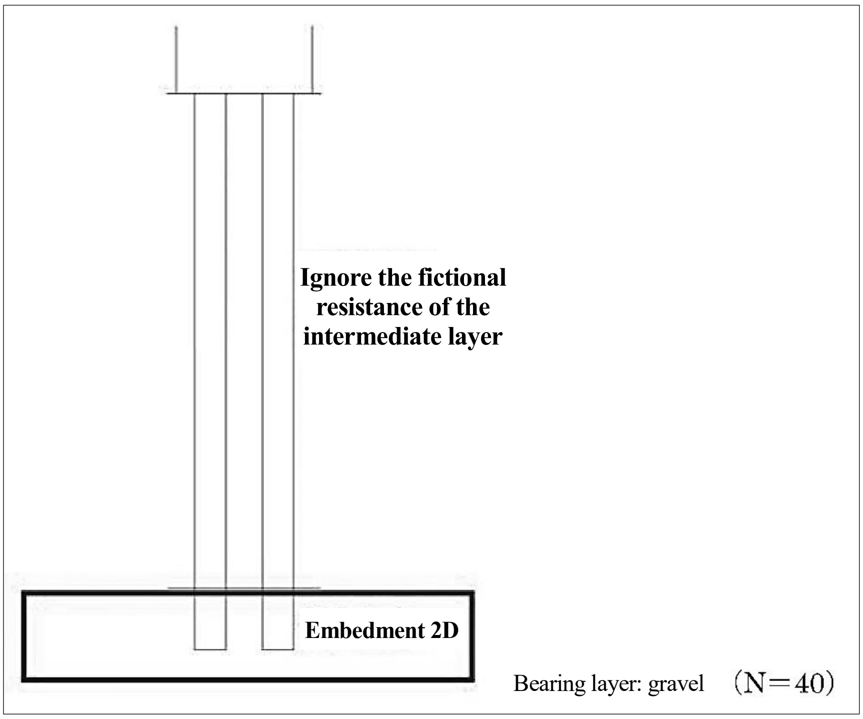

Figure 2-4-66 Assumption of stratum structure for pile bearing capacity calculation

⑤-5 Results of Analysis Case 1 (current condition)

Figure 2-4-67 shows the result of pile soundness. On the basis of the result of pile soundness, piles that have been lost and that no longer function were excluded from the model for analyzing the construction at the time of completion, and a model for analyzing the current condition was created. The analysis and checking of the current condition at the normal time were performed by considering only the fixed load because no people enter and thus the live load can be ignored. The items checked and results of checking are shown in Tables 2-4-64 to 67 and Figures 2-4-68 to 70.

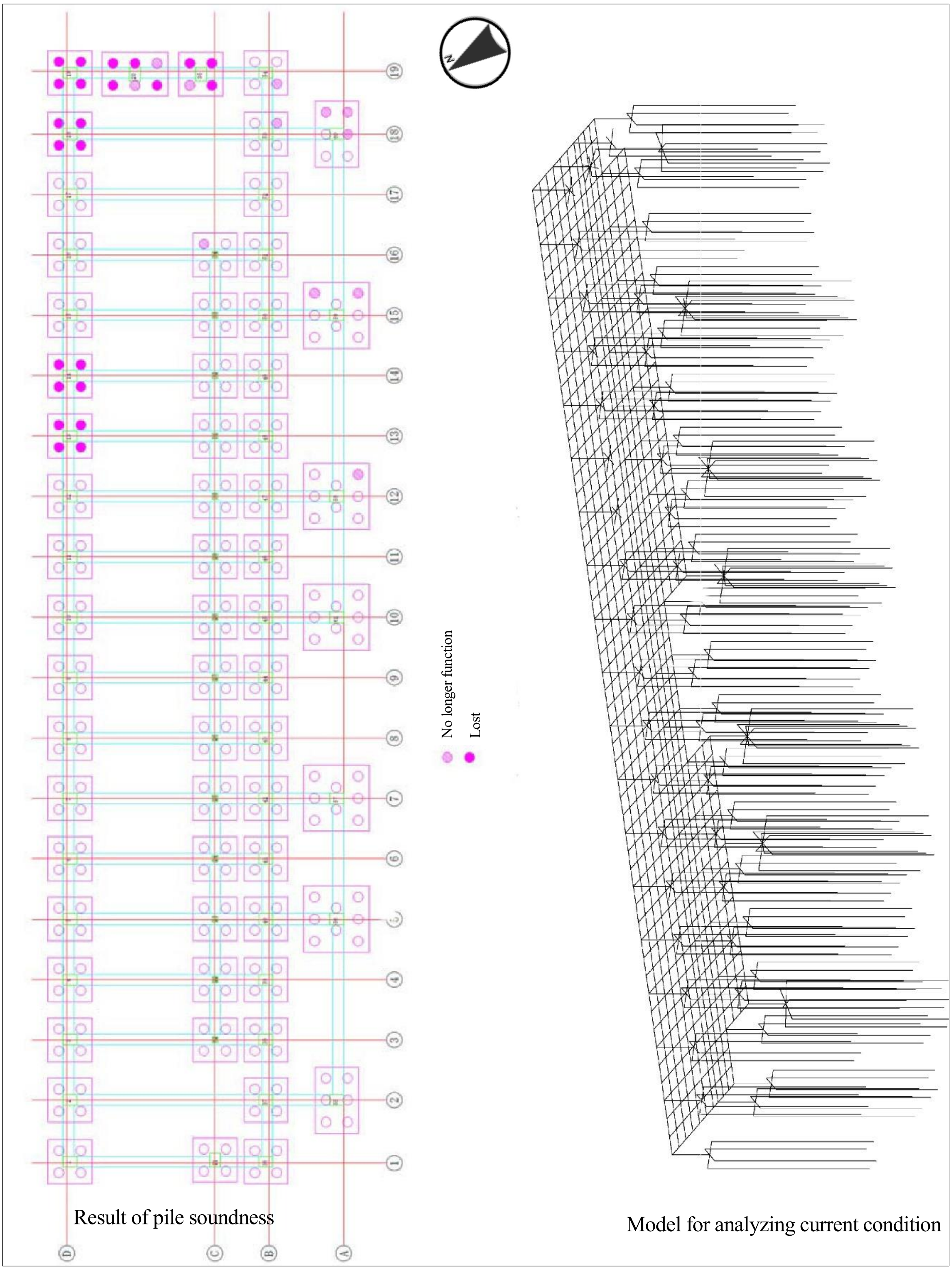

Figure 2-4-67 Result of pile soundness / Model for analyzing current condition

Table 2-4-64 Analysis case 1 checking results

Items checked		Checking result	Findings
1.	Checking of bending stress of the pile	NG	The stress was checked with respect to the parts that yielded the maximum bending moment value, the maximum axial force value, and the minimum axial force value for each of the longer side and shorter side directions, and the results exceed the allowable unit stress and were considered NG.
2.	Checking of shear stress of the pile	OK	The stress was checked with respect to the parts that yielded the maximum shearing force value for each of the longer side and shorter side directions, and the results did not exceed the allowable unit stress and were considered OK. Thus, all the results of checking of shearing stress is considered OK for the whole pile.
3.	Checking of bearing capacity of the pile	—	Some piles exceeded the allowable bearing capacity of Ra = 468 kN and the allowable drawing power of Pa = 17 kN per pile at the normal time, which were calculated in analysis case 0 (at the time of completion).
4.	Checking of the overall foundation stability	OK	As with Analysis case 0 (at the time of completion), checking was conducted using the eccentric distance: e = M/N (M: overturning moment, N: foundation reaction force) with respect to the center of gravity of the bottom slab. For the allowable eccentric distance value, the spread foundation normal-time allowable value B/6 (B: foundation width) was used. As the result of checking, the eccentric distances of both the longer side and shorter side directions did not exceed their allowable values; thus, the stability of the overall foundation is considered OK.

Table 2-4-65 Results of checking of shear stress (current condition)

1) Shorter side direction

Item		Pile cross-sectional property			Section force response	Unit stress response	Allowable unit stress	Checking result	
		Diameter Φ (m)	Wall thickness t (m)	Cross-sectional area A (m²)	Searing force Q (kN)	Average shearing unit stress τm (N/mm²)	Shear τa (N/mm²)	Shear τm/τa	Checking of shear
Pile	Shearing force maximum	0.5	0.08	0.1056	22.70	0.215	0.890	0.242	OK

2) Longer side direction

Position		Pile cross-sectional property			Section force response	Unit stress response	Allowable unit stress	Checking result	
		Diameter Φ (m)	Wall thickness t (m)	Cross-sectional area A (m²)	Searing force Q (kN)	Average shearing unit stress τm (N/mm²)	Shear τa (N/mm²)	Shear τm/τa	Checking of shear
Pile	Shearing force maximum	0.5	0.08	0.1056	18.17	0.172	0.890	0.193	OK

Table 2-4-66 Results of checking of bending stress of the pile (current condition)

1) Shorter side direction

Position		Pile cross-sectional property			Section force response		Unit stress response			Allowable unit stress			Checking result					
		Diameter Φ (m)	Wall thickness t (m)	Cross-sectional area A (m^2)	Bending moment M (kN/m)	Axial force N (kN)	Concrete compression σs (N/mm^2)	Steel tension σs (N/mm^2)	Steel compression σs' (N/mm^2)	Concrete bending compression σca (N/mm^2)	Steel tension σsa (N/mm^2)	Steel compression σsa' (N/mm^2)	Concrete bending compression σca/σca (N/mm^2)	Concrete bending compression checking	Steel tension σs/σsa	Steel tension checking	Steel compression σs'/σsa'	Steel compression checking
Pile	Bending moment maximum	0.5	0.08	0.1056	204.33	1900.60	33.600	20.200	-488.200	13.30	155.00	-155.00	2.526	OUT	0.130	OK	3.150	OUT
	Axial force maximum	0.5	0.08	0.1056	0.67	2647.47	21.900	Not caused	-327.700	13.30	155.00	-155.00	1.647	OUT	-	-	2.114	OUT
	Axial force minimum	0.5	0.08	0.1056	203.89	-774.02	27.500	2192.000	-332.100	13.30	155.00	-155.00	2.068	OUT	14.142	OUT	2.143	OUT

2) Longer side direction

Position		Pile cross-sectional property			Section force response		Unit stress response			Allowable unit stress			Checking result					
		Diameter Φ (m)	Wall thickness t (m)	Cross-sectional area A (m^2)	Bending moment M (kN/m)	Axial force N (kN)	Concrete compression σs (N/mm^2)	Steel tension σs (N/mm^2)	Steel compression σs' (N/mm^2)	Concrete bending compression σca (N/mm^2)	Steel tension σsa (N/mm^2)	Steel compression σsa' (N/mm^2)	Concrete bending compression σca/σca (N/mm^2)	Concrete bending compression checking	Steel tension σs/σsa	Steel tension checking	Steel compression σs'/σsa'	Steel compression checking
Pile	Bending moment maximum	0.5	0.08	0.1056	163.57	466.84	25.400	567.900	-351.200	13.30	155.00	-155.00	1.910	OUT	3.664	OUT	2.266	OUT
	Axial force maximum	0.5	0.08	0.1056	9.09	2647.47	22.600	Not caused	-338.100	13.30	155.00	-155.00	1.699	OUT	-	-	2.181	OUT
	Axial force minimum	0.5	0.08	0.1056	10.01	-774.02		809.100	Not caused	13.30	155.00	-155.00			5.220	OUT	-	-

Appendix 1

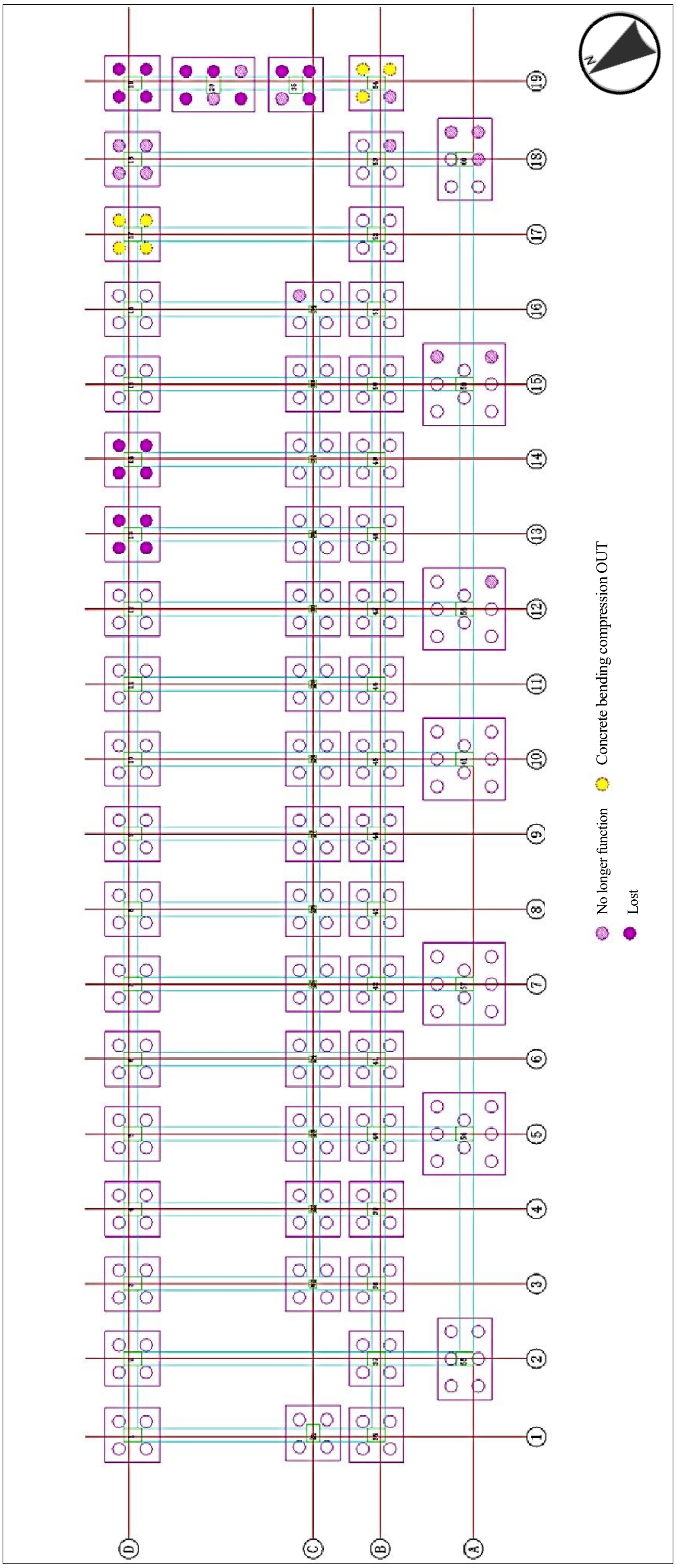

Figure 2-4-68 Current condition: Pile bending checking – concrete bending compressive stress OUT parts

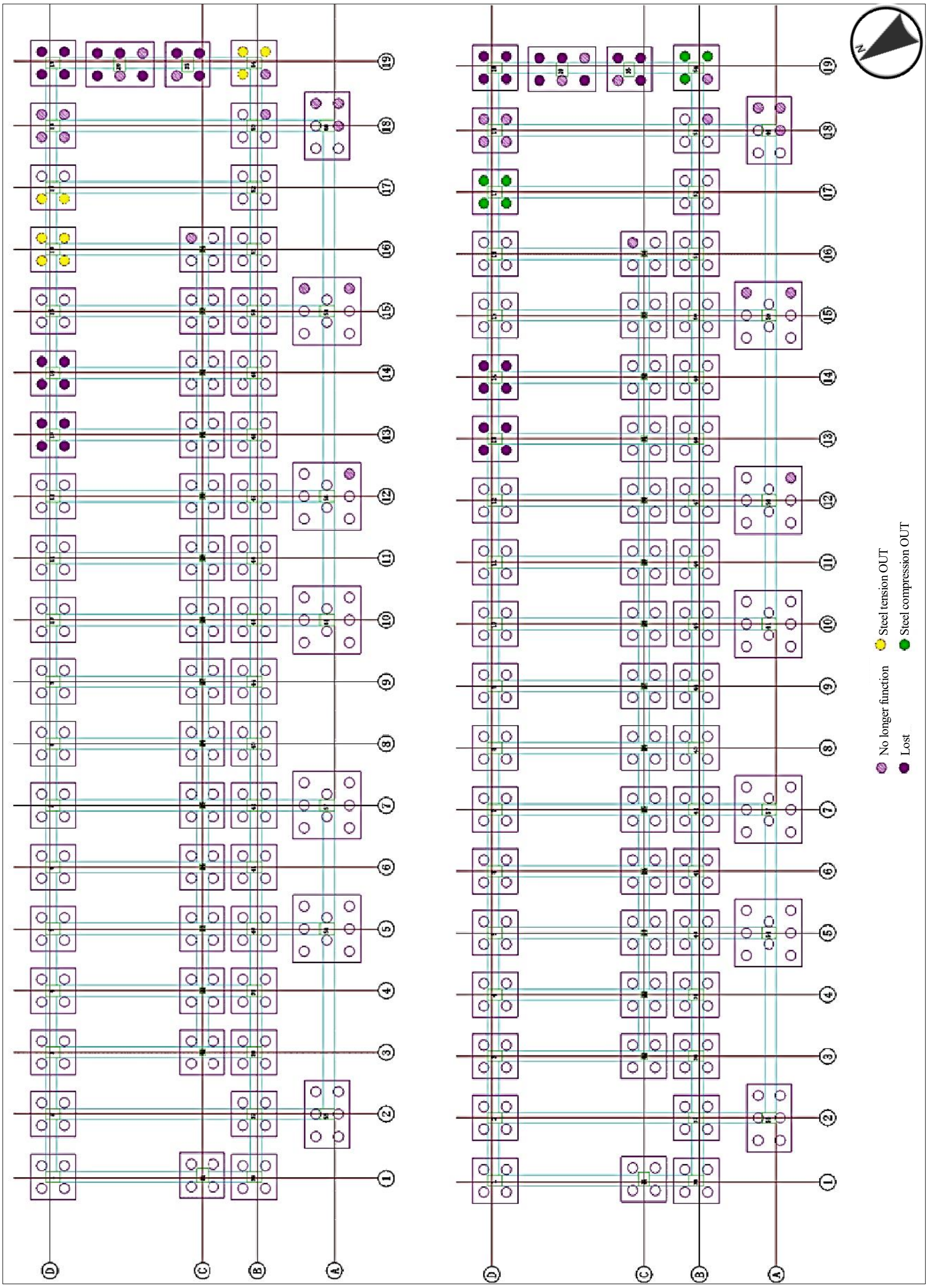

Figure 2-4-69 Current condition: Pile bending checking – Rebar tension / compressive stress OUT parts

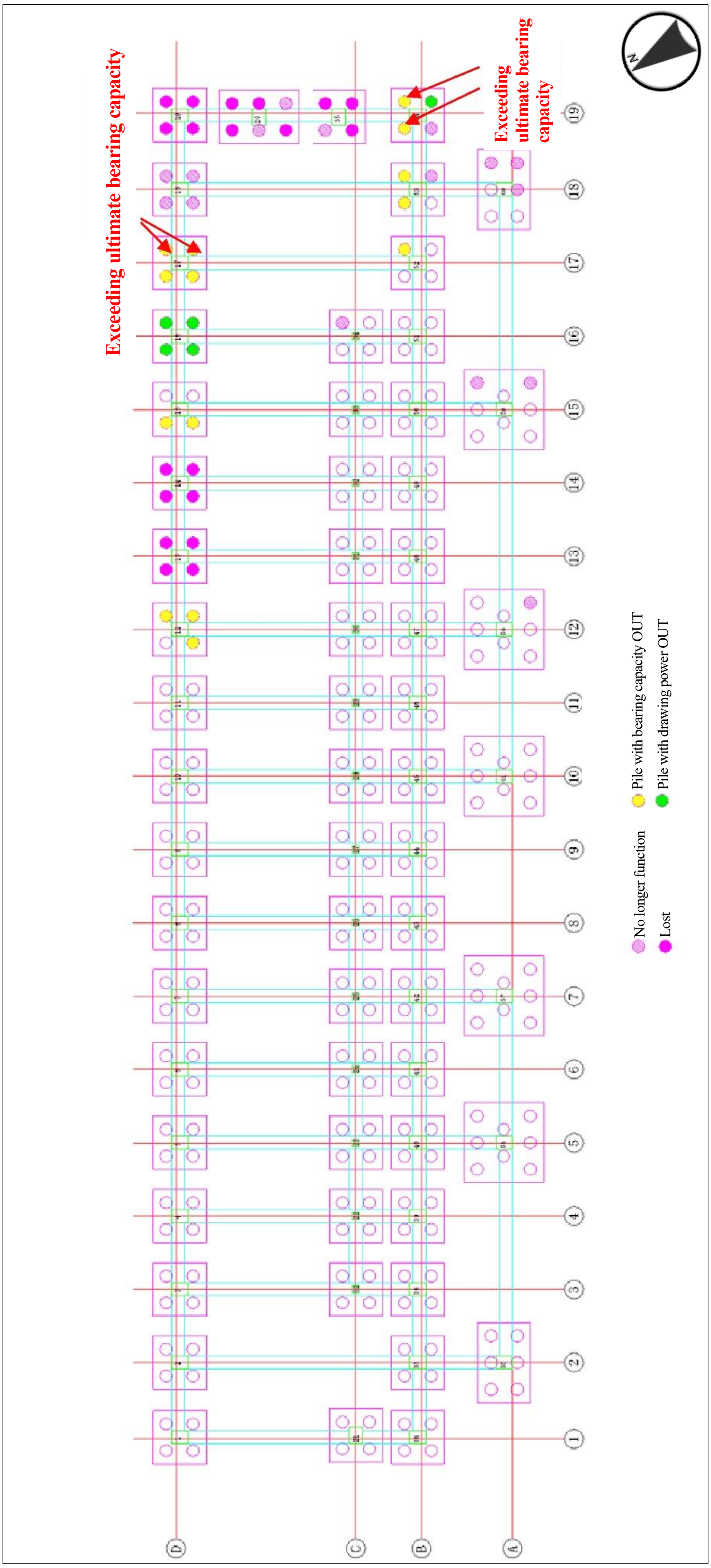

Figure 2-4-70 Pile bearing capacity / drawing power OUT parts

Table 2-4-67 Results of checking of the current overall foundation stability

Foundation reaction force	Overturning moment total		Bottom slab eccentric distance		Calculated bottom slab width (pillar centerline)		Allowable eccentric distance value		Result of checking of the overall foundation stability	
N (kN)	Longer direction (kN・m)	Shorter direction (kN・m)	Longer direction ex(m)	Shorter direction ey(m)	Longer direction width Bx(m)	Shorter direction width By(m)	Longer direction Bx/6	Shorter direction By/6	Longer direction (ex<Bx/6)	Shorter direction (ey<By/6)
64,002.74	-10,785.37	-8,112.2	0.169	0.127	54.460	13.39	9.077	2.232	OK	OK

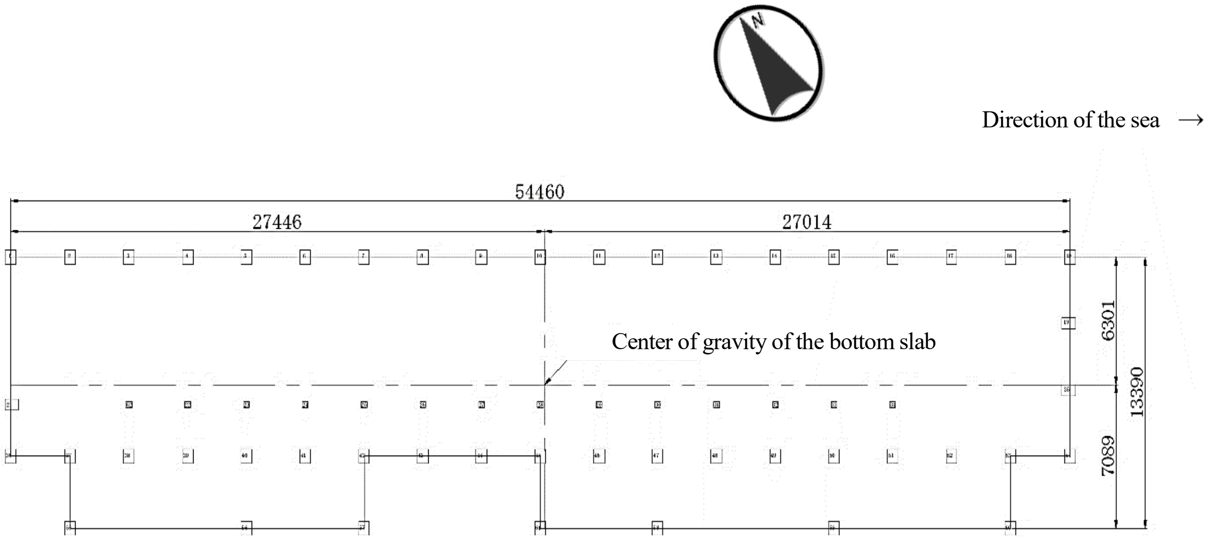

⑥ Summary

For the Building No.70, the displacement survey, slant survey using three-dimensional laser measurement, and deterioration level survey were conducted. The displacement survey did not detect displacement. Concerning the slant of the building, Level 1 was found to project to the east side by 15–20 mm compared with Level 2 and upper floors.

As for the deterioration of the building, serious deterioration was found on the east side and deterioration was more noticeable on the north side than on the south side on many Levels. This is presumably because there are no structures that block wind and rain as well as sea breezes on the east side and the north side.

Regarding seismic performance, the residual seismic performance ratio was lowest on Level 2 at 71.7% and highest on Level 5 at 94.3%. Concerning the determination of damage, Level 2 was determined to be “Intermediate damage” and the other Levels to be “Minor damage.” Therefore, seismic performance has not decreased to the level that requires emergency measures.

As for the current deterioration level of the foundation, the bending stress of the piles was determined to be NG, and the bearing capacity exceeding the allowable value was confirmed in some piles.

(2) Survey of deterioration level

1) Outline of the survey

To understand the current condition of accommodation facilities existing in the Hashima Coal Mine remains, the deterioration levels of reinforced concrete structures were visually inspected, and “Evaluation results of the residual vertical load bearing capacity ratio,”, “Evaluation results of the residual seismic performance ratio,” and Evaluation results of the future residual vertical load bearing capacity ratio and residual seismic performance ratio” were put together.

The contents of the surveys are as described below.

・The survey of deterioration condition and the prediction of durable years with respect to accommodation facilities that were not evaluated in “Report of the deterioration survey of concrete structures in Gunkanjima” (March 2013)

・The survey of deterioration condition and the prediction of durable years with respect to accommodation facilities that were evaluated in “Report of the deterioration survey of concrete structures in Gunkanjima” (March 2013), for which one of the survey of deterioration condition or the prediction of durable years was not performed.

・ The structural safety evaluation of structures to which high priority is given to delay the progress of deterioration, among accommodation facilities.

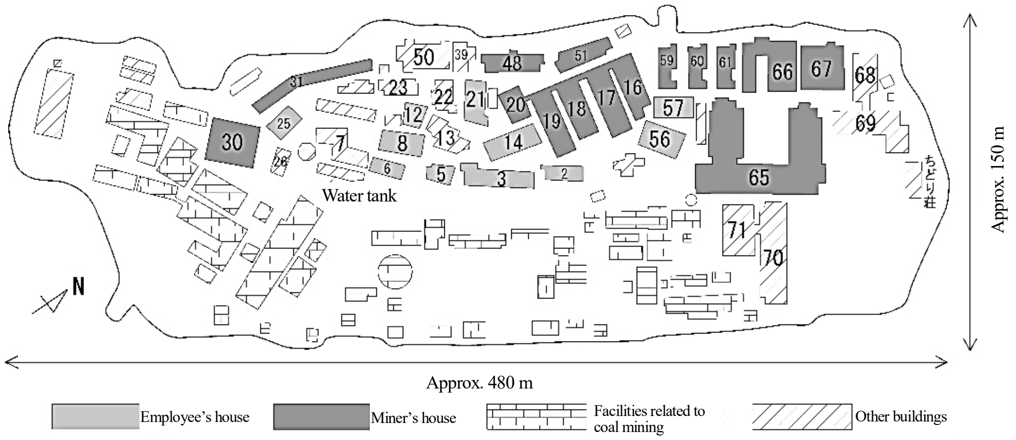

Figure 2-4-71 Map showing Hashima building numbers

Table 2-4-68 List of buildings for the deterioration level survey

Building	Constructed	Structure/Levels	Use	Building	Constructed	Structure/Levels	Use
2	1950	RC / 3 Levels + semibasement	Employee’s house	51	1961	RC / 8 Levels + semibasement	Miner’s house
3	1959	RC 4 Levels + semibasement	Employee’s house (for executives / with bath)	56	1939	RC / 3 Levels	Miner’s house
8	1919	RC + 3 story wooden house	Employee’s house / communal bath	57	1939	RC / 4 Levels	Miner’s house / shops
13	1967	RC / 4 Levels	Town-managed housing (for school personnel)	59	1953	RC / 5 Levels + basement	Miner’s house / Basement kobaikai
14	1941	RC / 5 Levels	Employee’s house (Central house)	60	1953	RC / 5 Levels + basement	Miner’s house / Basement kobaikai
16	1918	RC / 9 Levels	Miner’s house (daily wage miner’s house)	61	1953	RC / 5 Levels + basement	Miner’s house / Communal bath
17	1918	RC / 9 Levels	Miner’s house (daily wage miner’s house)	65 North	1945	RC / 9 Levels + basement	Miner’s house
18	1918	RC / 9 Levels	Miner’s house (daily wage miner’s house)	65 East	1949	RC / 9 Levels + basement	Miner’s house / Rooftop kindergarten

19	1922	RC / 9 Levels	Miner's house (daily wage miner's house)	65 South	1958	RC / 10 Levels	Miner's house
20	1922	RC / 6 Levels	Miner's house (daily wage miner's house)	66	1940	RC / 4 Levels + basement	Miner's lodging (Keimei dormitory)
21	1954	RC / 5 Levels	Miner's house / Police box	67	1950	RC / 4 Levels	Miner's lodging (bachelor dormitory)
22	1953	RC / 5 Levels	Town-managed housing (public employees) / public office, etc.	68	1958	RC / 2 Levels	Isolation ward
25	1931	RC / 5 Levels + basement	Employee's house / hostel	69	1958	RC / 4 Levels	Hashima hospital
30	1916	RC / 7 Levels	Former miner's house (contractor's house)	70	1958	RC + S / 7 Levels	Hashima Elementary School and Hashima Junior High School
31	1957	RC / 6 Levels + basement	Miner's house / Post office / Basement communal bath	71	1970	RC + S / 2 Levels	Gymnasium
39	1964	RC / 3 Levels	Public hall	Chidori-so	1958	Wood and plaster / 2 Levels	School personnel house
48	1955	RC / 5 Levels + basement	Miner's house	Water tank	-	-	-
50	1927	RC / 2 Levels	Movie theater (Showa-kan)				

2) Evaluation of member deterioration levels

① Outline

To evaluate decreases in structural performance due to the deterioration of buildings, deterioration levels were classified from the deterioration condition of structural members, which was obtained through the on-site survey, and the structural performance decreasing rate was defined for each deterioration level.

② Classification of member deterioration levels

The deterioration levels of members were classified according to the state of concrete cracks and the corrosion condition of rebar confirmed by visual inspection.

Deterioration levels were classified into eight stages (0, I, II, III one side, III both sides, IV one side, IV both sides, and V, with larger numbers indicating more serious condition) for columns; six stages (0, I, II, III, IV, and V) for beams and wallboards; and four stages (A, B, C, and D) for slabs. Criteria for classification are as described below. Note that the terms "one side" and "both sides" were used depending on "whether the deterioration condition of the deterioration level III or IV is found on one side or both sides of the member." The deterioration levels of slabs were classified into A: No deterioration; B: Rebar exposed and rusted; C: Many losses in the rebar section; or D: Fallen or lost, and then recorded.

Table 2-4-69 Deterioration level classification table

Deterioration level I	The level at which a small number of cracks are found
Deterioration level II	The level at which slight bond deterioration is seen
Deterioration level III	The level at which there is almost no concrete cover, but bond performance of the core side is likely to be provided, or the corrosion of rebar shows floating rust.
Deterioration level IV	The level at which virtually no bond appears to be present, or rebar has become iron oxide with more than around 70% of the cross section remaining.
Deterioration level V	The condition in which the concrete of the core part has fallen, or the level at which the cross section of rebar is determined to be less than 70%.

③ Examples of member deterioration levels and damaged condition

Shown below are examples of determination of deterioration levels. Values in parentheses are the long-term and seismic performance decreasing rates.

③-1 Deterioration level I (long-term: 0.95, seismic: 0.95)

The condition in which a small number of cracks are found.

Photo 2-4-118 Deterioration level I

③-2 Deterioration level II (long-term: 0.90, seismic: 0.8)

The condition in which there is a boundary crack between rebar and concrete, and slight bond deterioration is seen.

Photo 2-4-119 Deterioration level II

③-3 Deterioration level III (long-term: 0.90, seismic: 0.65 for one side/0.33 for both sides)

The condition in which concrete cover has fallen or appears to have almost fallen, and the concrete cover side of rebar virtually shows a boundary crack but the bond remains on its core side.

Photo 2-4-120 Deterioration level III

③-4 Deterioration level IV (long- term: 0.8 for column/0.5 for beam, seismic: 0.25 for one side and beam/0.10 for both sides)

The level at which strength can be expected and proof strength should not be lowered to as low as 0. Cases in which concrete cover has peeled and inside rebar has seriously deteriorated were categorized as Deterioration level IV.

Photo 2-4-121 Deterioration level IV

③-5 Deterioration level (long-term: 0.3 for shear column/0.8 for bending column/0.0 for beam, seismic: 0.0)

The condition in which either one of shear reinforcement or main reinforcement shows a loss of cross-sectional area due to corrosion, with less than 70% of that remaining.

④Shear column deterioration level classification and structural performance decreasing rate

Table 2-4-70 shows deterioration levels and condition as well as performance decreasing rates for shear columns.

Table 2-4-70 Performance decreasing rate

Deterioration level	Deterioration condition	Long-term performance	Seismic performance
0	There is no deterioration	1.00	1.00
I	Crack width is approx. 1 mm or less; rebar is unlikely to have bond deterioration	0.95	0.95
II	Corrosion has caused a boundary crack between rebar and concrete; slight bond deterioration is seen	0.90	0.80
III one side	The concrete cover on one side of the member has fallen and the concrete cover side of rebar virtually shows a boundary crack, but the bond remains on the core side of rebar, with floating rust observed on the whole surface of rebar	0.90	0.65
III both sides	The concrete cover on both sides of the member has fallen and the concrete cover side of rebar virtually shows a boundary crack, but the concrete of the core part is sound, and the bond remains on the core side of main reinforcement, with floating rust observed on the whole surface of rebar	0.90	0.33
IV one side	The concrete cover on one side of the member has fallen, there is a boundary crack between rebar and concrete, and there is almost no adhesion force; however, the cross-sectional area of rebar is determined to be approx. 70% or greater, or iron oxide is determined to be present only on the surface	0.90	0.25
IV both sides	The concrete cover on both sides of the member has fallen, there is a boundary crack between rebar and concrete, and there is almost no adhesion force; however, the cross-sectional area of rebar is determined to be approx. 70% or greater, or iron oxide is determined to be present only on the surface	0.80	0.10
V	The boundary crack between rebar and concrete is so complete that even the core part concrete is missing, and there is no adhesion force; the cross-sectional area of rebar is determined to be less than 70%, or rebar is splitting in layers	0.30	0.00

3) Evaluation of the structural performance deterioration level of the entire building

① Outline

Here, we describe methods for evaluating the structural performance deterioration level of the entire building using the deterioration level classification shown in “2) Evaluation of member deterioration levels” and performance reduction coefficient.

② Basic policy for the structural performance evaluation of the entire frame

In the survey of reinforced concrete structure ("RC structure") architectural buildings in Hashima, which was conducted in September 2015, deterioration levels were evaluated with respect to vertical load bearing performance and seismic performance as structural performance. To evaluate structural performance deterioration levels, we used a principle for RC structure buildings, which is provided in "Criteria for determination of quake-hit building damage degree categories ("Damage degree determination criteria") published by the Japan Building Disaster Prevention Association. In the Damage degree determination criteria, the degree of damage of a quake-hit building is determined through quantitative evaluation using the residual seismic performance ratio: R (the ratio of the post-quake seismic performance to pre-quake seismic performance).

Figure 2-4-72 is a conceptual drawing of the relationship between the damage degree of member and deformation under load, which was cited from the Damage degree determination criteria. For damage degrees (0 and I to V) of columns, beams, walls, etc., the degree of structural performance degrease (seismic performance reduction coefficient: η) is numerically expressed by estimating the maximum deformation caused in the member at the time of earthquake on the basis of damaged condition, including cracks in the member. It is thought that the residual seismic performance ratio R for the entire building can be roughly calculated from the proof strength ratio between each member (shear column: bending column: wall without a column: wall with a column on one side: wall with columns on both sides = 1 : 1 : 1 : 2 : 6) and the seismic performance reduction coefficient η.

It should be noted that the residual seismic performance ratio R does not evaluate the absolute value of structural performance but does evaluate the residual rate as compared with the initial performance (degree of decrease). In this survey, the principle of the residual seismic performance ratio R, which is intended for earthquake damage, was applied to the structural performance decrease of buildings in Hashima, which have deteriorated over time.

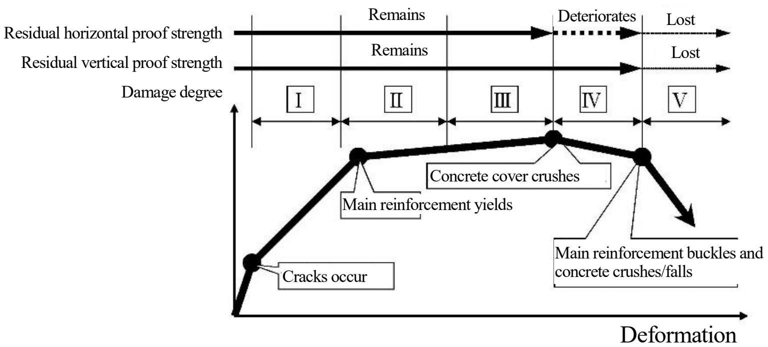

(a) Members with high plastic deformation capacity (bending member)

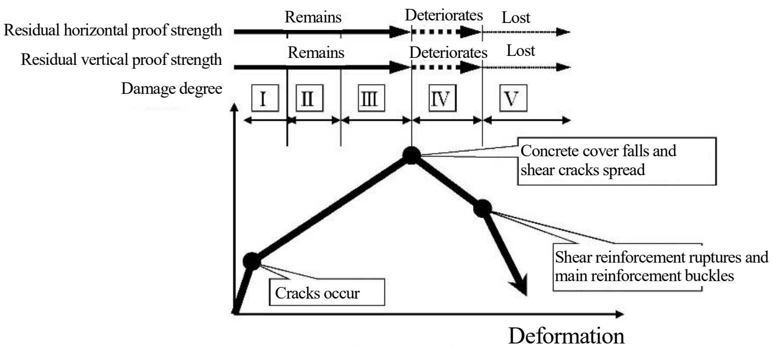

(b) Members which cause brittle fracture (shear member)

Figure 2-4-72 Deterioration level calculation methods for walls and beams

③ Evaluation of the residual structural performance ratios R_L and R_E of RC structure buildings that have deteriorated with time

As described above, in this survey, the principle of the residual seismic performance ratio R in the Damage degree determination criteria was applied to evaluate the structural performance of RC structure buildings in Hashima, which have deteriorated over time. The two kinds of structural performance (vertical load bearing performance and seismic performance) were set as evaluation objects; deterioration levels were classified into five stages (I to V) on the basis of the condition of damage of members due to age deterioration; the performance reduction coefficient was established for each deterioration level in accordance with the Damage degree determination criteria; and the residual performance ratio of the entire building was calculated. The details are as described below.

③-1 Vertical load bearing performance

The capacity to bear long-term loads including axial force is one of the important structural performance elements; it was called the vertical load bearing performance and evaluated as the residual ratio R_L in this survey. Since it is the capacity to bear the vertical load, the residual ratio for the entire frame was basically calculated on the basis of the deterioration levels (I to V) of vertical members (i.e., columns, bearing walls) that bear axial force; the calculation of the residual ratio R_L did not take into consideration the deterioration levels of beams. However, for the parts where the deterioration levels of beams and floor slabs are high (Deterioration level of IV and higher), their locations and damaged condition were separately recorded in light of dangers including local floor collapse.

The residual vertical load bearing performance ratio R_L for the entire frame was calculated using Table 2-4-71 and the formula below. The evaluation objects of this survey were buildings in Hashima, which were designed in accordance with the former earthquake resistance standards; therefore, we did not differentiate between bending columns and shear columns and treated all the columns as shear columns.

$$R_L = \frac{\sum A_j}{A_{org}} \times 100 = \frac{(\quad)}{(\quad)} \times 100 = (\qquad)$$

Table 2-4-71 Calculation table for the residual vertical load bearing performance ratio R_L due to deterioration

	Shear column	~~Bending column~~	Wall without a column	Wall with a column on one side	Wall with columns on both sides	Total	
No. of total members	( ) +	( ) +	( ) +	( ) +	( ) =	( )	
No. of members surveyed	( )① +	( )② +	( )③ +	( )④ +	( )⑤ =	( )	
	①×1 +	②×1 +	③×1 +	④×2 +	⑤×6 =	( )	$=A_{org}$
Deterioration level 0	( ) +	( ) +	( ) +	( )×2 +	( )×6 =	( )	$=A_0$
Deterioration level I	( )×0.95 +	( )×0.95 +	( )×0.95 +	( )×1.9 +	( )×5.7 =	( )	$=A_1$
Deterioration level II	( )×0.9 +	( )×0.9 +	( )×0.9 +	( )×1.8 +	( )×5.4 =	( )	$=A_2$
Deterioration level III	( )×0.9 +	( )×0.9 +	( )×0.9 +	( )×1.8 +	( )×5.4 =	( )	$=A_3$
Deterioration level IV	( )×0.8 +	( )×0.8 +	( )×0.8 +	( )×1.6 +	( )×4.8 =	( )	$=A_4$
Deterioration level V	( )×0.3 +	( )×0.8 +	( )×0.8 +	( )×1.6 +	( )×4.8 =	( )	$=A_5$

$$\sum A_j = A_0+A_1+A_2+A_3+A_4+A_5 = (\qquad)$$

③-2 Seismic performance

The residual seismic performance ratio R_E due to age deterioration for the entire frame was basically calculated on the basis of the method provided in the Damage degree determination criteria (the performance reduction coefficients of members are different). When the deterioration level of a beam was higher than that of a vertical member (i.e., column, bearing wall) to which the member clung, the deterioration level of the beam was replaced by that of the vertical member concerned, and the residual seismic performance ratio R_E for the entire frame was calculated using Table 2-4-72 and the formula below.

$$R_E = \frac{\sum A_j}{A_{org}} \times 100 = \frac{(\quad\quad)}{(\quad\quad)} \times 100 = (\quad\quad)$$

Table 2-4-72 Calculation table for the residual seismic performance ratio RE due to deterioration

	Shear column	~~Bending column~~	Wall without a column	Wall with a column on one side	Wall with columns on both sides	Total	
No. of total members	( ) +	~~( )~~ +	( ) +	( ) +	( ) =	( )	
No. of members surveyed	( )① +	~~( )②~~ +	( )③ +	( )④ +	( )⑤ =	( )	
	①×1 +	~~②×1~~ +	③×1 +	④×2 +	⑤×6 =	( )	$=A_{org}$
Deterioration level 0	( ) +	~~( )~~ +	( ) +	( )×2 +	( )×6 =	( )	$=A_0$
Deterioration level I	( )×0.95 +	~~( )×0.95~~ +	( )×0.95 +	( )×1.9 +	( )×5.7 =	( )	$=A_1$
Deterioration level II	( )×0.6 +	~~( )×0.75~~ +	( )×0.6 +	( )×1.2 +	( )×3.6 =	( )	$=A_2$
Deterioration level III	( )×0.65 ( )×0.33 +	~~( )×0.5~~ ~~( )×0.2~~ +	( )×0.65 ( )×0.33 +	( )×1.3 ( )×0.66 +	( )×3.9 ( )×1.98 =	( )	$=A_3$
Deterioration level IV	( )×0.25 ( )×0.1 +	~~( )×0.25~~ ~~( )×0.1~~ +	( )×0.25 ( )×0.1 +	( )×0.5 ( )×0.2 +	( )×1.5 ( )×0.6 =	( )	$=A_4$
Deterioration level V	( )×0 +	~~( )×0~~ +	( )×0 +	( )×0 +	( )×0 =	( )	$=A_5$

* Damage degree III and IV: the top indicates falling on one side of the concrete cover, the bottom shows falling on both sides of the concrete cover

$$\Sigma A_j = A_0 + A_1 + A_2 + A_3 + A_4 + A_5 = (\quad\quad)$$

4) Survey of bar arrangement

① Outline of the survey

For the structural safety evaluation of buildings to which high priority is given to delay the progress of deterioration, among accommodation facilities, a survey of bar arrangement was conducted using various non-destructive inspection equipment to collect data necessary for the evaluation of the structures.

The survey was conducted for 10 of the 11 buildings listed in Table 2-4-73, which shows buildings for structural safety evaluation; Building 16 was excluded from this survey as a bar arrangement survey was conducted in 2012 for this building.

Table 2-4-73 Buildings for the bar arrangement survey

Building	Structure / No. of Levels
3	RC structure / 4 Levels + semibasement
16	RC structure / 9 Levels
17	RC structure / 9 Levels
18	RC structure / 9 Levels
19	RC structure / 9 Levels
20	RC structure / 6 Levels
50	S structure / 2 Levels (Level 1 front chamber RC structure)
65 North	RC structure / 9 Levels + basement
65 East	RC structure / 9 Levels + basement
65 South	RC structure / 10 Levels
70	RC structure / 6 Levels + S structure roof floor (extension)

*RC structure: Reinforced concrete structure. S structure: Steel structure

② Survey methods

The bar arrangement survey was conducted by focusing on columns and walls that are set as survey objects in the Damage degree determination criteria as well as in the secondary diagnosis of the standard for seismic diagnosis.

In addition, by assuming the conduct of the third diagnosis of the standard for seismic diagnosis as well as push-over analysis, beams and floors were also surveyed in a simplified manner to the extent possible.

②-1 Policy for selecting members to be surveyed

The policy for selecting members to be surveyed is as described below.

1. For each building, the columns, beams, and walls of the same section size are grouped on the basis of past drawing data.
2. The columns, beams, and walls of the same section size are assumed to have the same bar arrangement, and a member code is given to each of them. However, even when a corner pillar and a center pillar have the same section size, the bar arrangement is assumed to be different and different column codes are given, unless drawing data show that the bar arrangement is the same. In some cases, it is impossible to differentiate between an RC wall and a brick wall from past drawing data; the walls that were assumed to be RC walls and given the relevant code need to be verified on site if they were RC walls or not.
3. The on-site bar arrangement survey is conducted for one member per member code, with the location of the member being arbitrary. Measuring planes are four sides for columns, and one plane or two sides for walls depending on the thickness. As a rule, beams are visually inspected, and one side (the bottom) is inspected to the extent possible. When the bar arrangement cannot be confirmed with one member, multiple members are surveyed.

②-2 Items surveyed

The items surveyed are as described below.

・Rebar diameter (column/beam: main and shear reinforcements, wall: vertical and horizontal reinforcements)
・No. of rebars (column/ beam: main reinforcement)
・Reinforcement interval (column/beam: shear reinforcement, wall: vertical and horizontal reinforcements)
・Section size (column, beam, wall, and floor)
・Depth of concrete cover (column, beam, and wall)

For the items above, beams were surveyed through visual inspection as a rule to the extent possible.

②-3 Survey methods

To understand bar arrangement condition and member sections, the survey was conducted for each part using the method described in Table 2-4-74.

For the use of non-destructive inspection equipment, a policy that can serve as the standard was established to ensure that measurement results do not vary depending on the inspector. The survey was conducted by changing the policy as necessary, taking into account the condition of measurement instrument used by the inspector and circumstances at the site.

Table 2-4-74 Survey methods

Method used with equipment	Item	Part surveyed
Electromagnetic wave radar method	No. and interval of rebars	Column, wall
Electromagnetic induction method	Diameter*, numbers, and interval of rebars, Depth of concrete cover	
Measure / visual inspection	Member size, etc.	Beam, floor

③ Results

③-1 Survey of bar arrangement using the electromagnetic wave radar method

Figure 2-4-73 shows the result of an exploration using the electromagnetic wave radar method, which was conducted for a column of Building No.70. In an image obtained from an exploration using the electromagnetic wave radar method, rebar is usually shown as “mountain shapes” as in the image (a). The image (b) does not clearly show “mountain shapes” that were seen in the image (a), and rebar inside the member was extremely corroded at this part. These images indicate that the depth of concrete cover is greater in (a), but at the same time confirms that even if the depth of concrete cover is small, reinforcement corrosion can make an image unclear. Reinforcement corrosion has progressed in most of the buildings in Hashima, which prevented the confirmation of rebar with the electromagnetic wave radar method in some cases. In a survey using the electromagnetic induction method too, the location of rebar was not accurately detected in some cases when rebar was corroded or the depth of concrete cover was great. With these fundamental limits of measuring instruments, individual inspectors conducted the exploration by adapting to circumstances at the site.

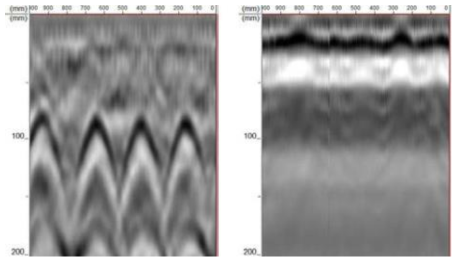

(a)Waveform of sound reinforcement (b)Waveform of corroded reinforcement

Figure 2-4-73 Electromagnetic wave radar image

③-2 Member section

A list of members was created using information obtained from the survey of bar arrangement. As mentioned earlier, from its fundamental limits, the reinforcement exploration with non-destructive testing did not confirm the condition of bar arrangement for all members. Moreover, due to circumstances including the accuracy of formwork at the time of construction, the same member on a drawing sometimes had different sizes; thus, the size of each member was checked for the survey at the site.

As an example of the results, the member structure of a column from Building No.17 is shown in Figure 2-4-74. While (a) shows the result obtained through the survey, (b) is a reinforcement plan for the member, which was confirmed in “Gunkanjima measurement survey data: Supplement revision - Empirical study of modern buildings in the Taisho and early Showa periods” (Akui, et. al, 2005). Concerning this particular member, both the data indicated the same size, and rebar was also confirmed to be the same.

In this way, a list of members was created to the extent possible with respect to those that could be explored at each building, as information used for the evaluation of structural safety.

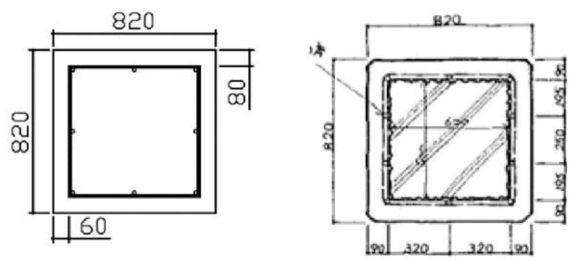

(a)Survey result (b)Data

Figure 2-4-74 Electromagnetic wave radar image

③-3 Problems

The survey of bar arrangement was conducted for various buildings in Hashima through visual inspection and using non-destructive inspection equipment; as a result, the problems below emerged, which need to be solved to identify the condition of bar arrangement.

- Structural drawings do not survive.
- The change of design during construction and repeated reinforcement after completion led to a low degree of regularity in cross-sectional shape/condition of bar arrangement.
- Construction accuracy is not high, causing significant variations in cross-sectional shape/condition of bar arrangement.
- Conducting a reinforcement exploration using non-destructive inspection equipment is difficult for parts where a wall is clung to a column as well as parts where finishing material is thick on a member.
- In exposed rebar, expansion and a loss of cross-sectional area have progressed due to corrosion; the original reinforcement diameter cannot be identified.
- Reinforcement corrosion sometimes prevents non-destructive testing from producing accurate exploration results.

5) Survey and deterioration level of Building No.3

① Outline of the survey

To maintain and conserve RC structure buildings that have markedly deteriorated, it is necessary to evaluate structural safety performance by taking into account the deterioration level of each building and to use the results to consider proper repair measures. To this end, a survey was conducted for Building No.3 to understand deterioration levels and assess their effects on structural performance.

Standing at the highest altitude in Hashima, Building No.3 is a symbolic building. Photo 2-4-122 shows the appearance from the south, and Figure 2-4-75 indicates the location of Building No.3 within the island. Building No.3 has a semibasement, but it has not been investigated in detail; therefore, the survey covers the four Levels above ground excluding the semibasement. Table 2-4-75 provides an overview of the building. A framing plan was developed on the basis of “Gunkanjima measurement survey data: Supplement revision - Empirical study of modern buildings in the Taisho and early Showa periods” (Akui, et. al, 2005) and the survey results. It is common to all Levels, and Figure 2-4-76 shows the framing plan with member codes for the reference floor. As the figure indicates, the ridge direction (long axis) is X and the span direction (short axis) is Y.

Photo 2-4-122 Building No.3 appearance

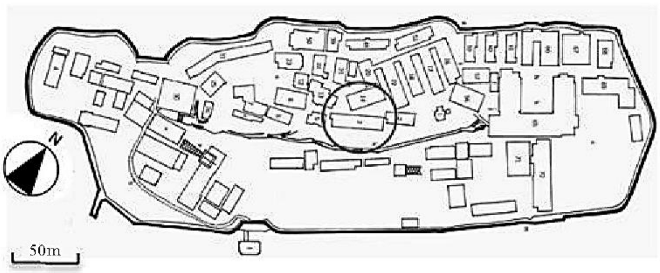

Figure 2-4-75 Building No.3 location map

Table 2-4-75 Building overview

Building		3
Constructed		1959
Use		Employee’s house
Structure classification	Ridge direction	RC rigid-framed structure
	Span direction	RC rigid-framed structure with quake resisting walls
No. of Levels		Above ground 4 Levels + 1 semibasement Level
Total floor area		1,588 ㎡

Figure 2-4-76 Reference floor framing plan

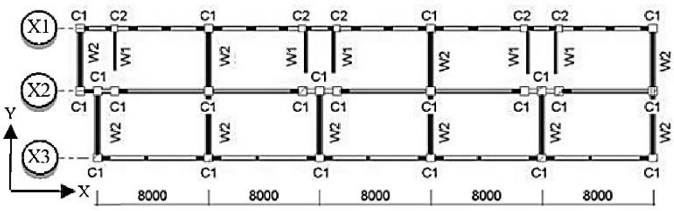

Floor height	1–4 Levels: 2.9 m
Ground and foundation type	Onto rocks, spread foundation

② Survey

②-1 Member information

From the results of major frame dimensional measurement and reinforcement exploration, the column, beam, and wall were assumed as described in Table 2-4-76. The bar arrangement is unknown for floor slabs. Figures 2-4-77 and 2-4-78 show frame drawings for the base lines X1 and X3, respectively, which were created from the assumed member dimensions and the results of a non-structural wall location survey. The shaded areas represent openings. As an example, the measurement of beam dimensions is shown in Photo 2-4-123.

②-2 Deterioration conditions of structural members

In accordance with the standard described earlier, the deterioration levels of columns, walls, and beams were surveyed on each Level. The results are shown in Figure 2-4-79. The deterioration level of colorless members is 0. Damage of Deterioration level III or higher was not found in the columns, and damage of Deterioration level IV was confirmed in beams on Level 2 to Level 4 on the west side of the building.

Table 2-4-76 Building overview

Code	Column C1	Column C2	Ridge direction Beam	Span direction Beam
Cross section	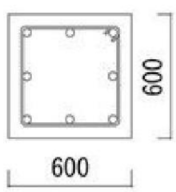	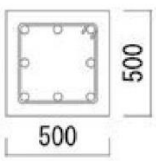	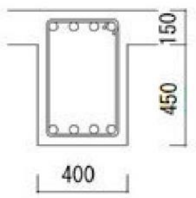	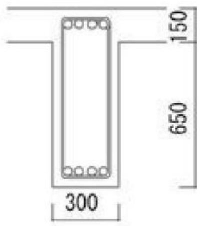
Dimen-sions	600×600	500×500	400×600	300×800
Main reinfo-rcement	8-19Φ	8-19Φ	8-19Φ	8-19Φ
Hoop	□-Φ9@220	□-Φ9@220	□-Φ9@250	□-Φ9@250

Code	Quake resisting wall W1	Quake resisting wall W2
Thickness	200	250
Vertical reinforcement	Φ9@230	Φ9@230
Horizontal reinforcement	Φ9@230	Φ9@230

(mm)

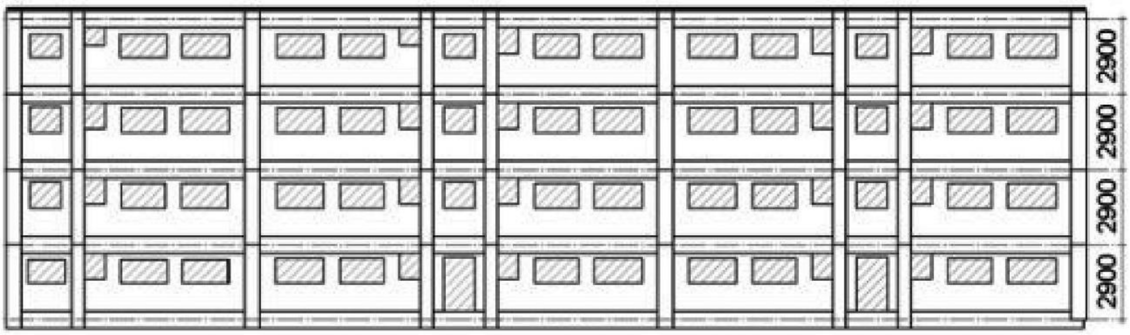

Figure 2-4-77 Frame drawing on base line X1

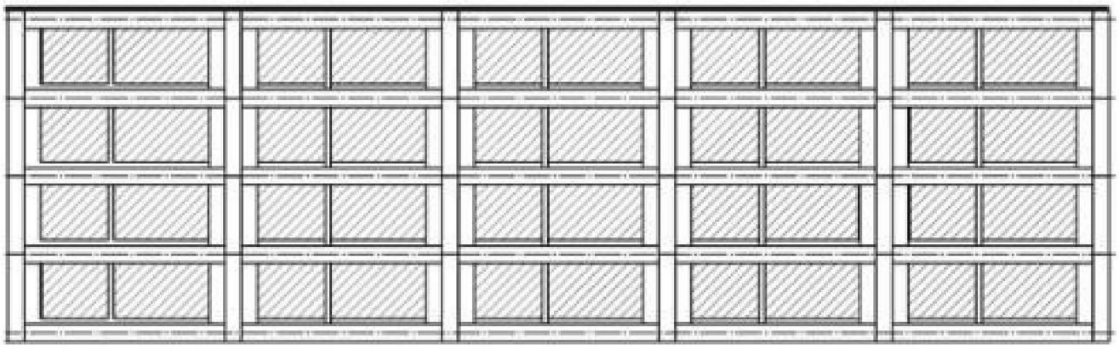

Figure 2-4-78 Frame drawing on base line X3

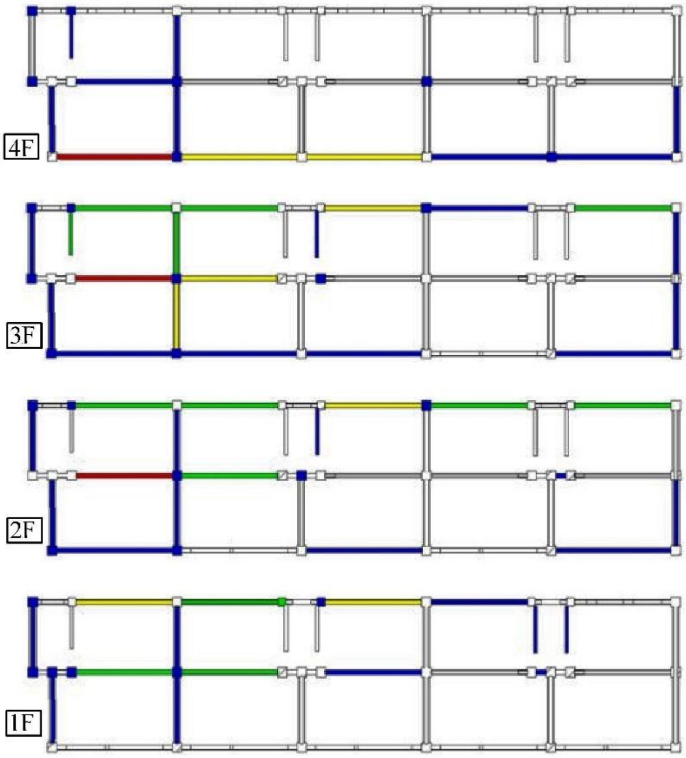

Figure 2-4-79 Structural member deterioration condition

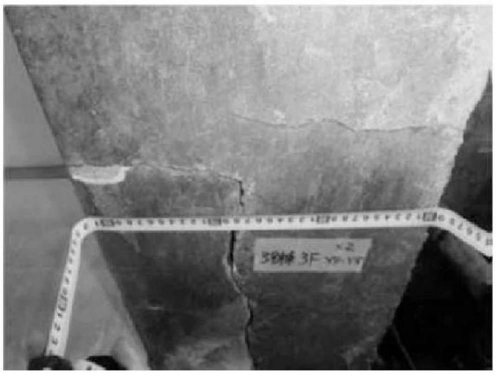

Photo 2-4-123 Beam dimension measurement

Photo 2-4-124 Interior fixture deterioration condition

③ Decrease in structural performance due to deterioration

Table 2-4-77 shows the residual vertical load bearing performance ratio R_L and the residual seismic performance ratio R_E of Building No.3, which were obtained using the methods described earlier. R_L is the lowest for Level 2 at 98%, indicating that deterioration had a small effect. Meanwhile, R_E is lower in the X direction than in Y direction, with a lowest ratio of 83%, which was obtained for Level 2 X direction. As Photo 2-4-124 shows, interior wooden fixtures are markedly deteriorated and damaged, but the progress of deterioration was relatively slow with respect to the structure.

Possible reasons for the relatively minor deterioration of the Building No.3 structure are that the building was completed in 1959 and is relatively new among the buildings in the island, and that it stands on high ground in the center of the island, making the building less likely to be affected by sea breezes than other buildings.

Table 2-4-77 Residual vertical load bearing performance ratio R_L / Residual seismic performance ratio R_E

Level		1	2	3	4
R_L		99%	98%	99%	99%
R_E	X direction	90%	83%	85%	87%
	Y direction	97%	96%	97%	98%

④ Summary

For Building No.3 in Hashima, the residual structural performance ratio was determined by surveying member details and deterioration levels. The results found that the deterioration of Building No.3 was relatively minor compared with that observed at other buildings.

6) Seismic diagnosis and static incremental analysis of Building No.3

① Outline of the survey

To maintain and conserve Hashima's RC buildings of high historical value, it is necessary to evaluate structural performance by taking into account deterioration levels. To this end, the seismic diagnosis and static incremental analysis of Building No.3 were performed to understand the seismic performance of target structures at the time of construction. The target structures are four Levels above ground, and a semibasement is excluded; only the weight is considered for the penthouse. Because material strength has not been surveyed, concrete and rebar are assumed to be Fc15 and SR235, respectively.

② Seismic diagnosis

The secondary seismic diagnosis is conducted in accordance with the "Standard and Technical Manual for Seismic Evaluation of Existing Reinforced Concrete Buildings" (Japan Building Disaster Prevention Association, 2001). To understand the seismic performance at the time of construction, the aging indicator $T = 1.0$ is used here. The evaluation results are shown in Table 2-4-78. The failure type and ductility index F of the member with respect to the X direction are shown in Figure 2-4-80, and the C_T-F relationship is shown in Figure 2-4-81. The Y direction, which has a large number of quake resisting walls, was determined to be Safe, with the seismic index of structure (Is) exceeding the seismic determination index of structure Iso (which was set at 0.6). Meanwhile, the X direction, which has a small number of quake resisting walls, was determined to be Questionable for Level 1 and Level 2 as many ultra-brittle columns were found on the north side X1 structure plane. However, the Is value is relatively high for a building constructed between 1955 and 1964.

Table 2-4-78 Residual vertical load bearing performance ratio R_L / Residual seismic performance ratio R_E

Direction	Level	E0	SD	T	IS	CTU・SD	Determination
X (ridge)	4	1.11	1.00	1.00	1.11	0.91	Safe
	3	0.76			0.76	0.48	Safe
	2	0.59			0.59	0.48	Questionable
	1	0.54			0.54	0.44	Questionable
Y (span)	4	2.53	1.00	1.00	2.53	2.53	Safe
	3	1.47			1.47	1.47	Safe
	2	1.02			1.02	1.02	Safe
	1	0.86			0.86	0.86	Safe

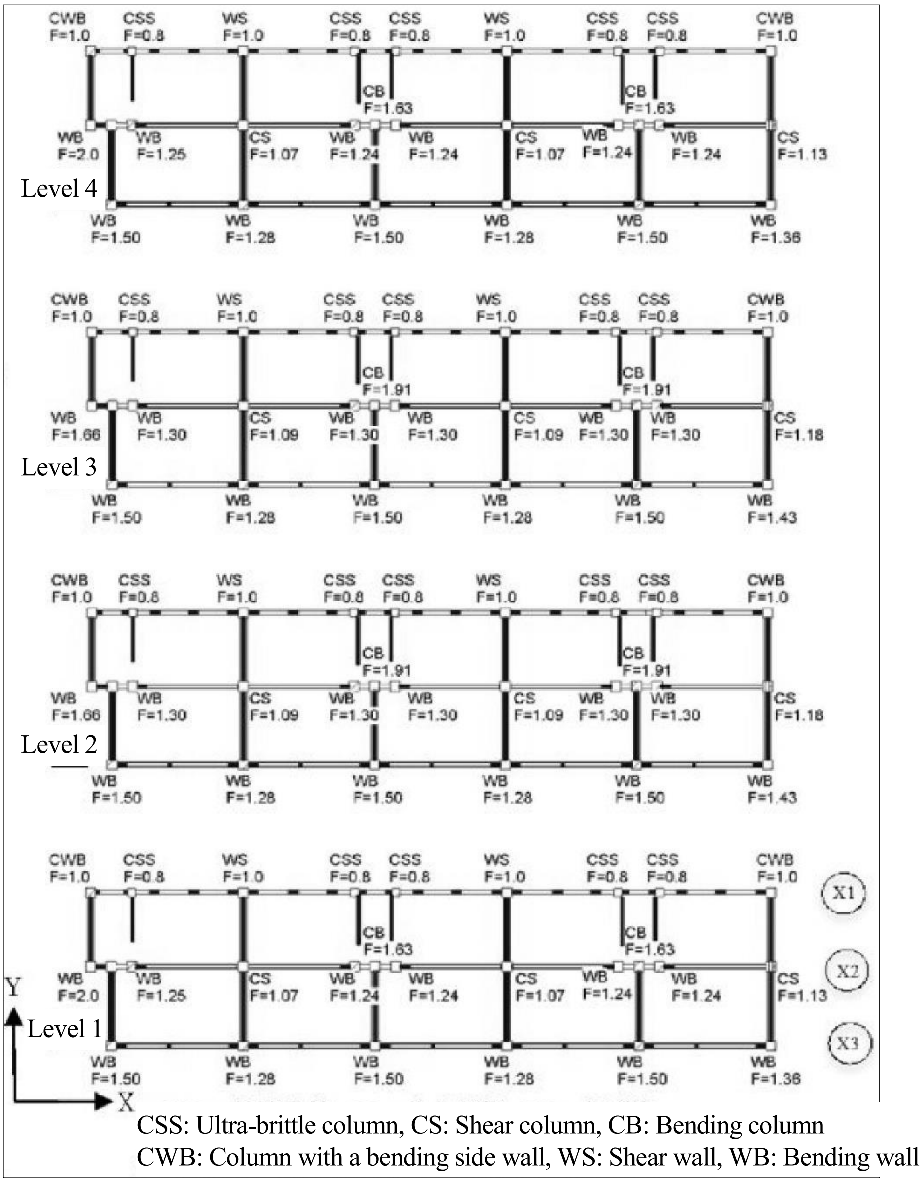

Figure 2-4-80 Failure type and ductility index F of the member (X direction)

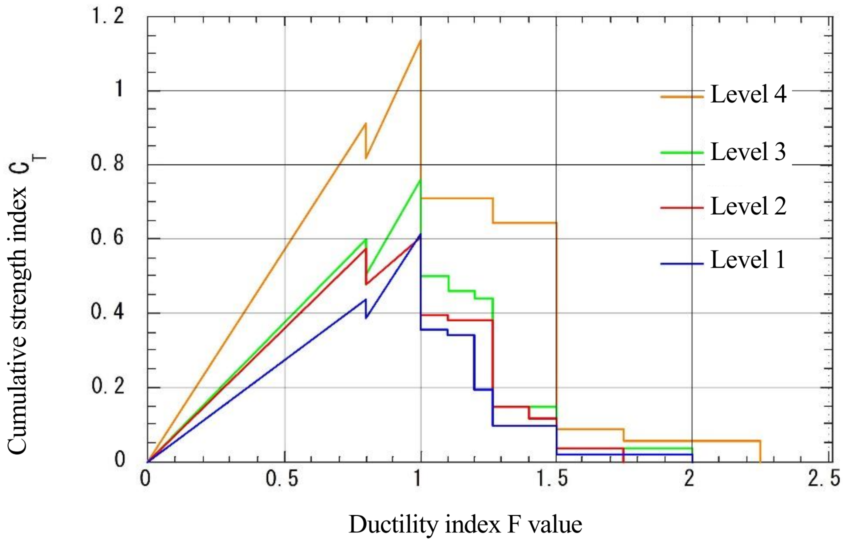

Figure 2-4-81 C_T-F relationship drawing (X direction)

③Analysis

The target structure Building No.3 was replaced by a three-dimensional frame model as shown in Figure 2-4-82, and elastoplastic response analysis was performed using analysis software SNAP Ver. 6.0.1.3 (Kozo System Inc.)

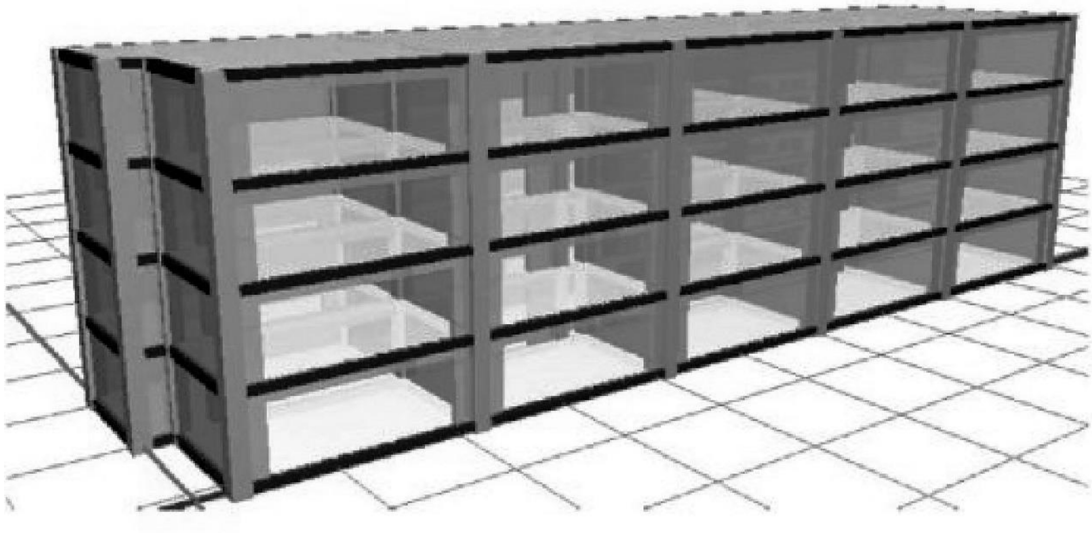

Figure 2-4-82　Three-dimensional frame model for analysis

③-1　Member model

Figure 2-4-83 shows a member spring model. For the column and beam, it is a composite model of a bending spring, shear spring, and axle spring as indicated in Figure 2-4-83 (a), while a quake resisting wall is replaced by three columns and rigid beams as shown in Figure 2-4-83 (b). For restoring force characteristics, based on the assumption of earthquake response analysis in the future, the Takeda model (Figure 2-4-84(a)) is adopted for the bending spring, the origin oriented type model (Figure 2-4-84 (b)), which considers proof strength deterioration, for the shear spring, and the linear elastic model for the axle spring. The flexural strength and shear capacity of a member are the same as values of the seismic evaluation.

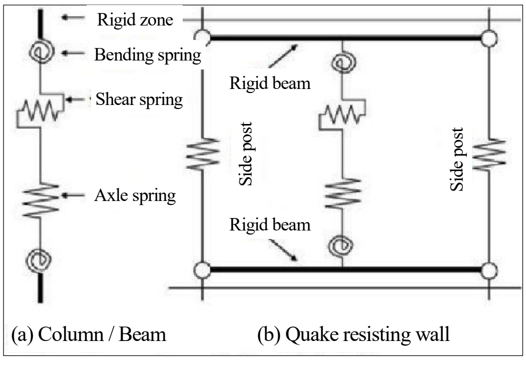

Figure 2-4-83　Member spring model

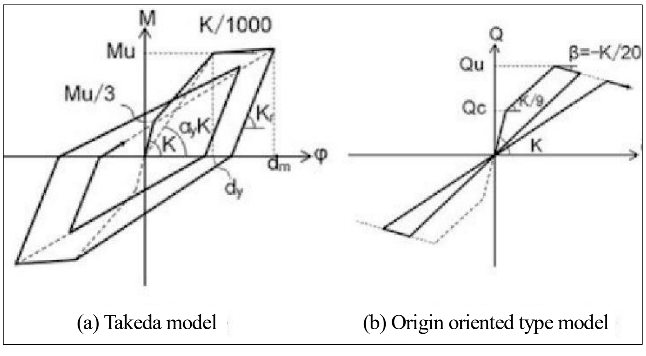

Figure 2-4-84　Restoring force characteristics

③-2 Static incremental analysis

The static incremental analysis was performed using incremental displacement until one of the stories reaches a story deformation angle of 1/200. Figure 2-4-85 shows the relationship between the story-shearing force of each story Q and the story deformation angle R with respect to the X direction. It indicates Level 1, which showed the minimum Is value in the seismic diagnosis, first achieved R = 1/200. Figure 2-4-86 shows the damaged condition of the X3 frame, which had the most noticeable damage. This figure reveals that damage is concentrated in beam ends and gradually exhibiting a beam yielding preceding total collapse mechanism. However, floor slabs have not been surveyed, and thus the beam model for analysis does not consider rebar of a floor slab, etc. under the current condition; detailed studies are required in the future.

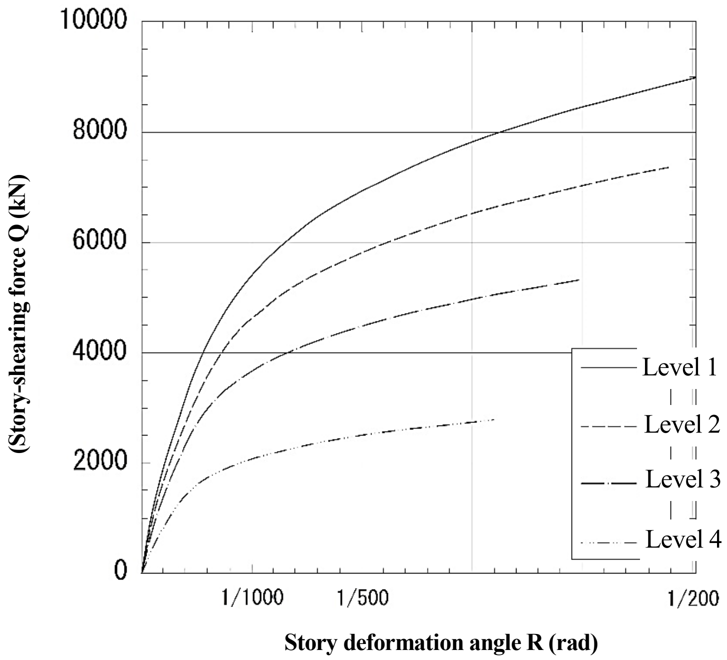

Figure 2-4-85 Story-shearing force Q - Story deformation angle R relationship (X direction)

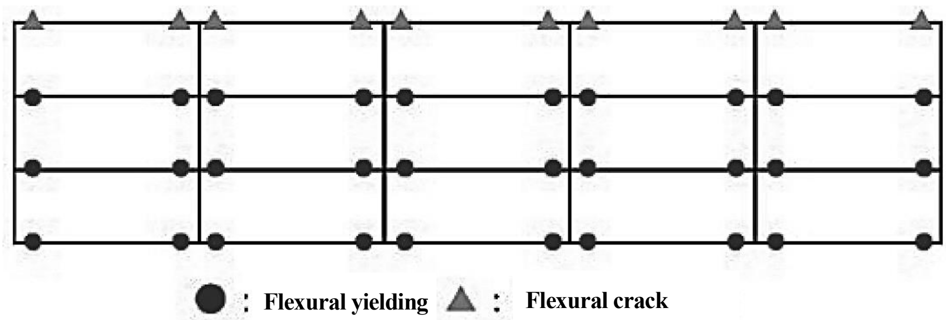

Figure 2-4-86 X3 frame damaged condition

④ Summary

For the maintenance and conservation of RC buildings in Hashima, the seismic performance of Building No.3 at the time of construction was evaluated. The seismic diagnosis revealed that seismic performance is insufficient in the ridge direction on Level 1 and Level 2, and the static incremental analysis found that the evaluation needs to be conducted using a beam model that considers floor slabs. This study evaluated the structural performance at the time of construction, but it is essential to conduct performance evaluations in the future by taking into account deterioration condition.

7) Structural performance decreasing rates for other buildings

① Outline

The structural performance decreasing rates for other buildings in Hashima were calculated using the method for classifying member deterioration levels described in “3) Evaluation of the structural performance deterioration level of the entire building” and the methods for calculating long-term performance and seismic performance decreasing rates shown in “4) Survey of bar arrangement,” as explained in 5) and 6) by taking Building No.3 as an example. The buildings surveyed were the 30 buildings listed in Table 2-4-79, among the buildings that constitute Hashima. The number of Levels ranges from one to ten. Some buildings have a semibasement, which was treated as Level 1 above ground in the calculation of decreasing rates. The long-term performance of Building No.2 and the seismic performance (X direction) of Building 66 were excluded as it was difficult to conduct on-site surveys.

Table 2-4-79 Buildings surveyed and the calculation results of decreasing rates

Building	No. of Levels	Long-term performance	Seismic performance		
			X direction	Y direction	Minimum value
Building No.2	4	–	83%	100%	83%
Building No.3	4	98%	83%	96%	83%
Building No.8	1	72%	40%	17%	17%
Building No.13	4	95%	79%	83%	79%
Building No.16	9	73%	24%	30%	24%
Building No.17	9	79%	48%	20%	20%
Building No.18	9	81%	61%	50%	50%
Building No.19	9	82%	60%	56%	56%
Building No.20	6	77%	54%	51%	51%
Building No.21	5	78%	56%	26%	26%
Building No.25	4	66%	30%	6%	6%
Building No.30	7	44%	3%	3%	3%
Building No.31	6	73%	11%	26%	11%
Building No.39	3	88%	49%	73%	49%
Building No.50	1	75%	15%	27%	15%
Building No.51	9	83%	42%	18%	18%
Building No.56	3	83%	65%	57%	57%
Building No.57	6	42%	4%	13%	4%
Building No.60	5	83%	23%	25%	23%
Building No.61	5	77%	45%	27%	27%
Building No.66	5	76%	—	40%	40%
Building No.67	1	37%	1%	4%	1%
Building No.68	2	97%	78%	73%	73%
Building No.70	6	92%	66%	72%	66%
Building No.71	2	67%	35%	18%	18%
Building No.65 North	9	56%	12%	12%	12%
Building No.65 East	10	68%	20%	24%	20%
Building No.65 South	10	88%	80%	68%	68%
Chidori-so	2	46%	0%	86%	0%
Water tank	1	69%	18%	37%	18%

② Survey methods

In the survey, the deterioration levels of columns, beams, and bearing walls on each Level of each building were classified using the method described in "3) Evaluation of the structural performance deterioration level of the entire building" and recorded. The deterioration levels of the lower faces of the slabs were also classified although they are not used this time. The deterioration levels of walls were classified by dividing the walls into three types: walls with columns on both sides, walls with a column on one side, and walls without columns. Figure 2-4-87 shows the method for totaling the deterioration levels of wall and beam. First, the deterioration level of each member is recorded in a framing plan that is prepared in advance. When deterioration levels were calculated for long-term performance, only the deterioration levels of vertical members such as columns and walls were used without considering the influence of beams. This was based on the assumption that the vertical load acting on a slab can transfer mainly through the slab, even if the beams are deteriorated.

Meanwhile, concerning the seismic performance decreasing rate, the deterioration level of a beam is considered only when it works in the direction of consideration; when the deterioration level of a beam is greater than those of vertical members connecting to the both ends of the beam, the deterioration levels of those vertical members are replaced by the deterioration level of the beam. For example, if the deterioration level of each member is classified as shown in Figure 2-4-87 (a), in considering the seismic performance in the X direction, the deterioration levels of Column b (IV) and Column c (III) are replaced by V because the deterioration level of Beam 1 is ⑤ as shown in Figure 2-4-87(b). Further, when the seismic performance of a quake resisting wall is considered, the deterioration level is evaluated by including the side posts; it is replaced by the deterioration level of the column or the wall slab, whichever is greater, and determined to be V comprehensively as shown in Figure 2-4-87 (b). Note that Column d is not affected by the deterioration level of Beam 2 when the X direction is considered.

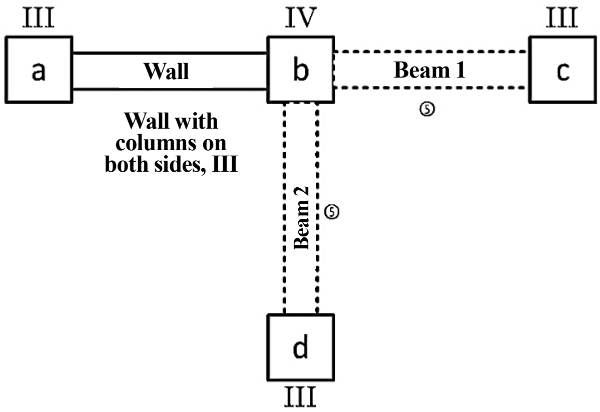

(a) Classification of member deterioration levels

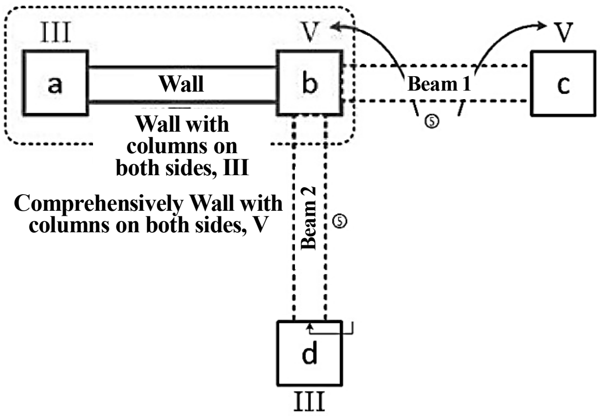

(b) Totalization of the seismic performance in the X direction

Figure 2-4-87 Method for totalizing the deterioration levels of wall and beam

③ Calculation results of decreasing rates

Table 2-4-79 and Figure 2-4-88 shows the calculation results of long-term performance decreasing rates and seismic performance decreasing rates, respectively. For the long-term performance, decreasing rates are shown to be relatively low, with the exception of some buildings including Building No.30. For the seismic performance, decreasing rates are low around Building No.3, which is located in the center of the island; however, deterioration is noticeable particularly along the coast, with single-digit decreasing rates obtained for Buildings No.25, 30, 57, 67, and Chidori-so, indicating extremely low residual seismic performance.

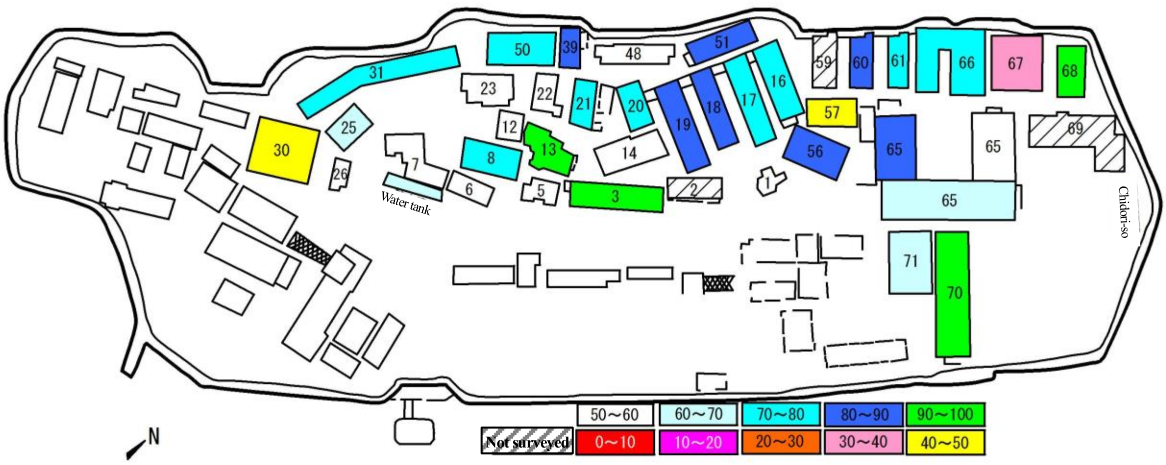

(a) Long-term performance decreasing rate

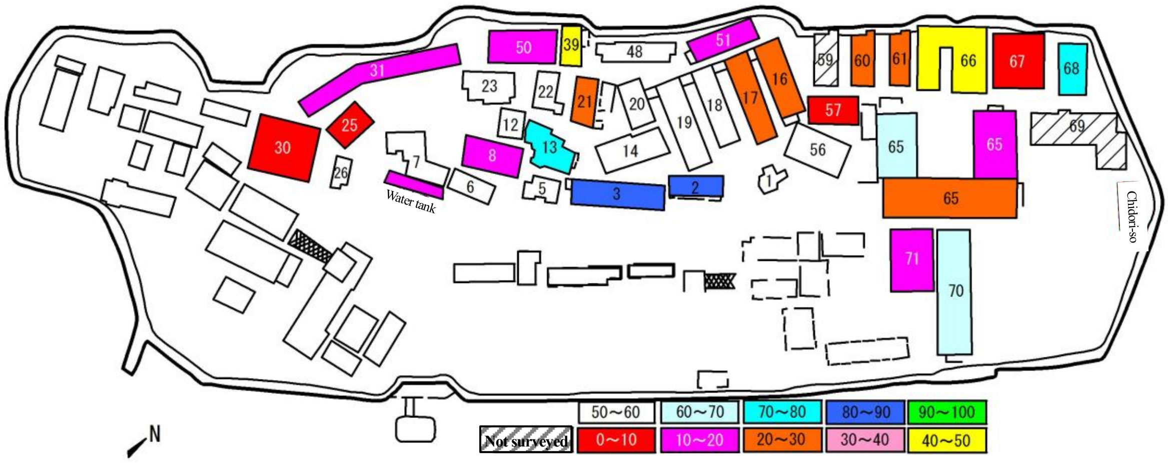

(b) Short-term performance decreasing rate

Figure 2-4-88 Long-term and short-term performance decreasing rates calculated

8) Predictions of deterioration/structural performance decrease with the Markov chain based on the deterioration environment classification

① Outline

As mentioned in the section 2), the deterioration levels of RC structure buildings in Hashima were visually inspected. Among those buildings, Buildings No.16 to 20 (Figure 2-4-89) were selected to make predictions of member deterioration based on the Markov chain. In addition, the structural performance decrease was predicted for the buildings by calculating the future residual vertical load bearing performance ratio R_L and the residual seismic performance ratio R_E..

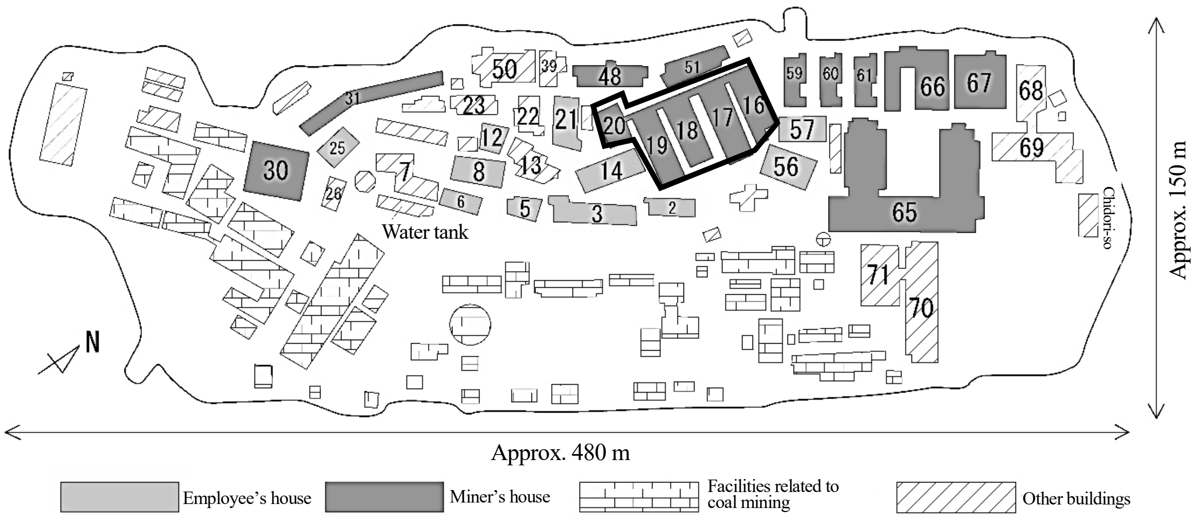

Figure 2-4-89　Buildings No.16 to 20 layout drawing

② Markov chain application method

②-1　Creation of a matrix

The deterioration transition matrix based on the Markov chain was set as Equation (1). It was assumed that the deterioration levels were 0 at the time of construction completion for all members and that the deterioration levels of the members that were repaired/reinforced at some point in time were 0 for that year. That is, assuming $X_0' = 1$ and $X_{I\text{–}V}' = 0$, the number of years elapsed to date was substituted for t, and the transition probabilities $P_{0\text{–}4}$ were calculated so that they are consistent with the percentage of current deterioration level $X_{0\text{–}V}$.

$$\begin{pmatrix} X_0 \\ X_{I} \\ X_{II} \\ X_{III} \\ X_{IV} \\ X_{V} \end{pmatrix} = \begin{pmatrix} 1-P_0 & 0 & 0 & 0 & 0 & 0 \\ P_0 & 1-P_1 & 0 & 0 & 0 & 0 \\ 0 & P_1 & 1-P_2 & 0 & 0 & 0 \\ 0 & 0 & P_2 & 1-P_3 & 0 & 0 \\ 0 & 0 & 0 & P_3 & 1-P_4 & 0 \\ 0 & 0 & 0 & 0 & P_4 & 1 \end{pmatrix}^{t} \begin{pmatrix} X_0' \\ X_{I}' \\ X_{II}' \\ X_{III}' \\ X_{IV}' \\ X_{V}' \end{pmatrix}$$

Equation (1) :

$X_{0\text{–}V}$: Percentage of current deterioration level　　*$P_{0\text{–}4}$: Transition probability*
$X_{0\text{–}V}'$: Percentage of deterioration level for t years ago　　*t: Number of years elapsed*

②-2　Classification of deterioration environments

In applying the Markov chain to the prediction of deterioration progress, it is necessary to assume that the members in question are in the same deterioration environment. That is, for members having distinct rates of deterioration progress, their transition probabilities should be separately calculated. Since the corrosion of rebar plays a dominant role in the deterioration progress of RC members, the deterioration environments were classified by focusing on factors related to the corrosion rate of rebar. Although there are wide-ranging, direct and indirect factors related to the corrosion of rebar, water content, salt content, and the depth of concrete cover were considered in this survey. The other factors were regarded as factors that should be included in the probability and evaluated because these factors are considered the same between members, or a clear difference cannot be found for these factors.

From the survey of Building No.16, there were differences between column and beam members in the frequency of the depth of concrete cover (Figure 2-4-90). Because Buildings No.16 to 20 were constructed in almost the same form in almost the same period, the depth of concrete cover was assumed to be similar across all the buildings, and the classification was made with respect to column and beam members. As environments related to water content and salt content, the presence or absence of areas exposed to the rain as well as the incoming salt amount were considered. In classifying incoming salt environments, we used the salinity transport equations for Hashima (Equations 2-1 and 2-2) (Shun Shimizu, et al., “Discussions on the state of incoming salt transport in Gunkanjima, Nagasaki Prefecture” 2015 / Shun Shimizu, et al., “Salt damage in Gunkanjima, Nagasaki Prefecture: Result of a three-year survey and creation of an incoming salt transport estimation map”), and tried to minimize variations in the number of members surveyed between classifications. From these, the deterioration environments in Hashima were classified as shown in Table 2-4-80.

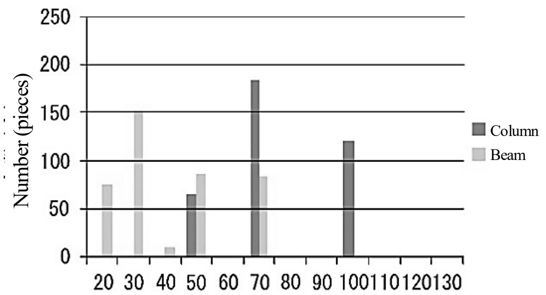

Table 2-4-80 Deterioration environment classification

Presence or absence of areas exposed to the rain	Annual average incoming salt amount	Effect of the depth of concrete cover
Outside	High (20 mdd～)	Column, beam
	Medium (4～20 mdd)	
	Low (～4 mdd)	
Inside	Hardly reaches due to the external wall	Column, beam

$$A_0 = 2.2784\times(V_a-1)^2 \quad (V_a \geq 1) \qquad \text{Equation (2-1)}$$

$$A = A_0 \left(\frac{D \cdot H}{D_0 \cdot H_0}\right)^{-\alpha} \qquad \text{Equation (2-2)}$$

A_0: Incoming salt amount generated at a given point (mg/dm²/day) Va: Average wind speed(m/s)
A: Incoming salt amount at a given point (mg/dm²/day) D: Distance from the coast at a given point (m)
H: Altitude of a given point (m) D_0: Distance from the coast at the hospital (m)
H_0: Altitude of the hospital (m) α: Attenuation coefficient (1.47)

Figure 2-4-90 Frequency distribution of the depth of concrete cover for Building No.16

③ Transition probabilities and deterioration curves

Figure 2-4-91 shows the transition probabilities for columns (including walls without a column) and beams calculated using the method described above. Figure 2-4-92 shows the deterioration curves drawn by the expected values, which are calculated from each transition probability and deterioration level. The expected values were rounded off to the closest whole number.

As a general trend, members existing outside rather than inside and those in severer incoming salt environments were shown to have higher transition probabilities and deterioration progress rates. The deterioration curves indicated that the deterioration progress is faster in beams than in columns for all the classifications.

The areas that do not follow the trend above may have members that do not fit the environments classified in this survey. For example, even members that are determined to be inside could have areas exposed to the rain or salt adhesion if there are large openings around them, or even areas that are determined to have a large incoming salt amount could have a small amount of salt adhesion depending of the direction of the building or wind conditions in the neighborhood.

Therefore, it is important to have more appropriate environment classifications to obtain more reliable transition probabilities, but members in severer deterioration environments are predicted to be faster in deterioration progress and those in milder deterioration environments are forecast to be lower in deterioration progress (Figures 2-4-91 and 2-4-92); thus, the predictions can be at least more realistic than a case where no classification is made.

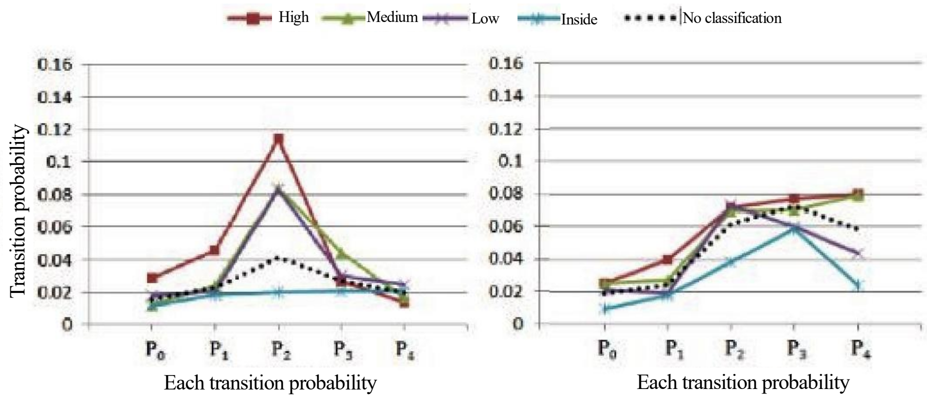

Figure 2-4-91 Transition probability (left: column, right: beam)

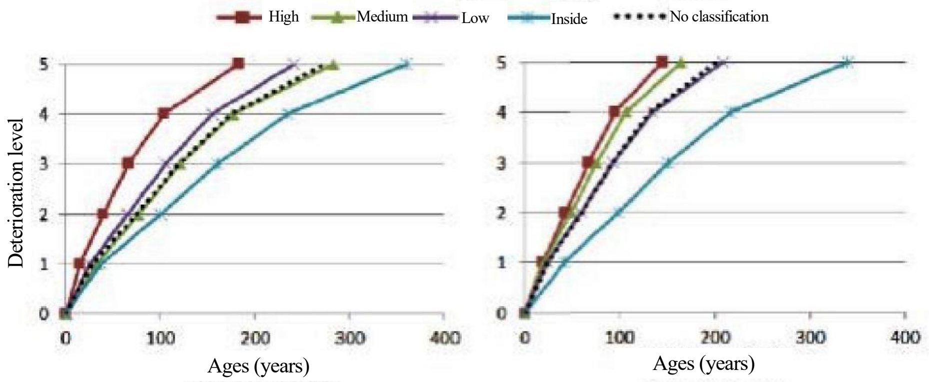

Figure 2-4-92 Deterioration curve (left: column, right: beam)

④ Prediction results for structural performance

Figure 2-4-93 shows the results of calculation and prediction of R_E for all Levels. For each building, the long-side direction is the X direction and the short-side direction the Y direction. The figure indicates that the Y direction has higher values of R_E and is lower in deterioration progress than the X direction across all the buildings. This is attributed to the fact that in the Y direction there are many inside wall members that have a low deterioration progress rate. Figure 2-4-94 shows the results of calculation and prediction of R_L for all Levels. Concerning R_L values, it was predicted that the values will not significantly change over the next 30 years for all the buildings, and after that, Building No.16 will deteriorate at a relatively high rate while Building No.20 will deteriorate at a relatively low rate. This difference may be affected by the distances from the coast.

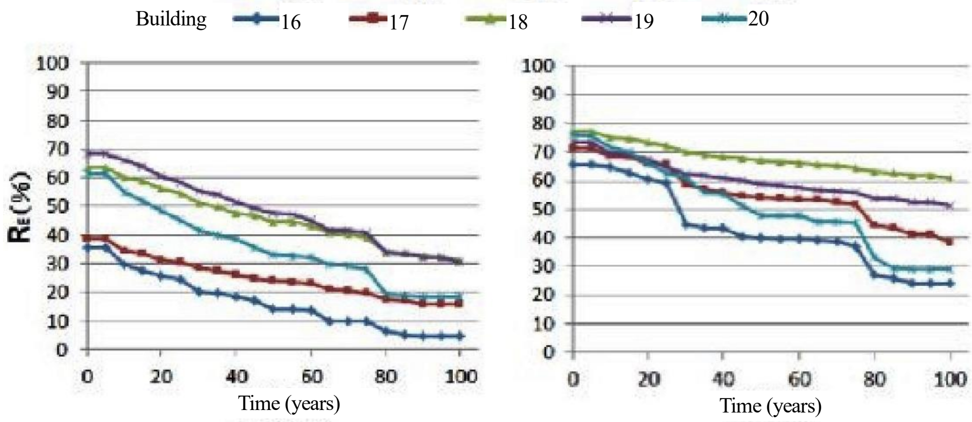

Figure 2-4-93 Prediction of residual seismic performance ratio R_E (left: X direction, right: Y direction)

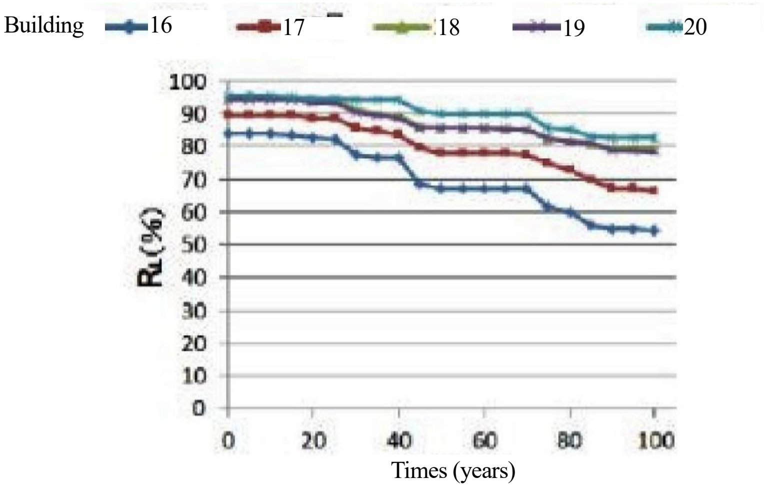

Figure 2-4-94　Prediction of residual vertical load bearing performance ratio R_L

⑤ **Summary**

1. The deterioration environments of RC members in Hashima were classified by the presence or absence of areas exposed to the rain, the incoming salt amount, and the depth of concrete cover. As a result, members having areas exposed to the rain and larger incoming salt amounts tended to show higher deterioration progress rates. In a comparison between columns and beams, deterioration progress was confirmed to be faster in beams. This may be affected by the depth of concrete cover.
2. The residual seismic performance ratio R_E was predicted for Buildings No.16 to 20. As a result, it was predicted that the Y direction will show greater values and be slower in progress of decrease than in the X direction across all the buildings.
3. The residual vertical load bearing performance ratio R_L was predicted for Buildings No.16 to 20. As a result, it was predicted that current residual ratio will not significantly change over the next 30 years for all the buildings, and after that, R_L will decrease relatively fast for Building No.16 while it will decrease relatively slowly for Building No.20.

9) Effect of material properties on the deterioration rate

① Outline

Since it is important to understand factors affecting deterioration in order to conserve buildings in Hashima, the degree of effect of material properties on the deterioration rate was evaluated. As material properties of members, the items listed in Table 2-4-81 were evaluated, and their measurement points are as shown in Table 2-4-82.

Table 2-4-81 Material properties

Code	Item	Measurement method
a	Initial total chloride ion concentration	Calculated through regression analysis using Fick's diffusion equation from the EPMA result of drilled core, and averaged for each building
b	Apparent diffusion coefficient of chloride ion	Same as above
c	Mass moisture content	A concrete piece near the rebar location was collected; then calculated by measuring the mass immediately after collection and absolute dry condition after drying it using a 105°C dryer
d	Surface air permeability coefficient	Measured using a Torrent tester
e	Depth of concrete cover	Measured through core drilling and chipping, or using an RC radar
f	Total pore quantity	A concrete piece near the rebar location was collected; then measured using the mercury press-in method

Table 2-4-82 Measurement point

Code	Location	Material age at survey (y)	Deterioration level	Items measured					
①	Level 1 of Building No.30	99	V	a	b	c	d	e	f
②	Level 1 of Building No.16	97	III	○		○	○	○	○
③	Level 3 of Building No.16	97	III	○	○	○	○	○	○
④	Level 3 of Building No.16	97	III	○	○	○	○	○	○
⑤	Level 1 of Building No.25	84	V	○	○	○	○	○	○
⑥	Level 1 of Building No.57	76	0	○	○	○	○	○	○
⑦	Level 1 of Building No.65 North	70	V	○	○	○	○	○	○
⑧	Level 1 of Building No. 65 North	70	IV	○	○	○	○	○	○
⑨	Level 1 of Building No.65 North	70	II			○	○		
⑩	Level 1 of Building No.65 East	66	I	○	○	○	○	○	○
⑪	Level 1 of Building No.65 East	66	V				○		
⑫	Level 2 of Building No.65 East	66	0			○	○		
⑬	Level 2 of Building No.65 East	66	II				○		
⑭	Level 1 of Building No.59	62	I				○		
⑮	Level 1 of Building No.59	62	0				○		
⑯	Level 1 of Building No.59	62	I			○			
⑰	Level 1 of Building 65 No.South	57	I	○	○	○	○	○	○

② Deterioration rate

②-1 Transition probability

The transition probability of each building is shown in Figure 2-4-95. This transition probability was calculated on the basis of the deterioration levels of a shear column, wall without a column, wall with a column on one side, wall with columns on both sides, and beam. To obtain accurate transition probabilities, only the buildings that had at least one member for each of all the deterioration levels were surveyed.

The transition probability is a probability of an increase in the deterioration level in a certain unit of time; in other words, it is a value that has a relationship with a kind of deterioration rate (Kenichi Komure, et al, "Development of a deterioration progress model due to salt damage at landing bridge upper part work," 2002). Figure 2-4-95 indicates that each deterioration level has a different rate of transition to the following deterioration level. Particularly, they tend to be $P_1 < P_2 < P_3$, that is, the transition of deterioration levels accelerates from Deterioration level I to IV. Toyoaki Miyagawa, et al argue that the corrosion rate increases after corrosion cracks are caused; the characteristics of the transition probabilities obtained in this study are thought to have a trend similar to that (Toyoaki Miyagawa, et al, "Life prediction and durability design of concrete structures in a saline atmosphere," 1988) .

②-2 Expected value of the deterioration level

In an attempt to eliminate the influence of aging in deterioration, the future deterioration level of each member was predicted as an expected value and adjusted to the same material age. Equation (1) is used to obtain the expected value of the deterioration level for the member that was determined to be Deterioration level II in 2015.

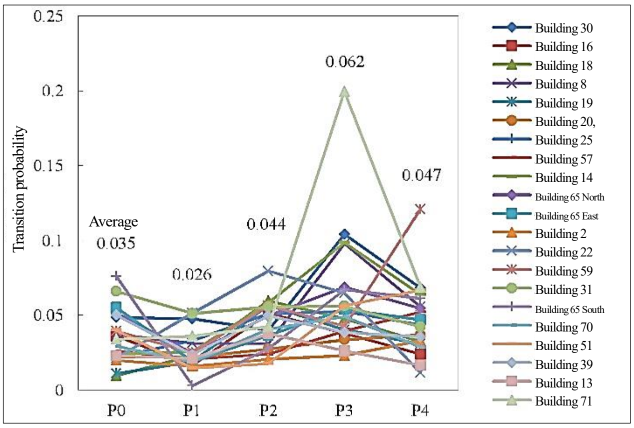

Figure 2-4-95 Transition probability

$$E = \begin{pmatrix} 0 & 1 & 2 & 3 & 4 & 5 \end{pmatrix} \begin{pmatrix} 1-P_0 & 0 & 0 & 0 & 0 & 0 \\ P_0 & 1-P_1 & 0 & 0 & 0 & 0 \\ 0 & P_1 & 1-P_2 & 0 & 0 & 0 \\ 0 & 0 & P_2 & 1-P_3 & 0 & 0 \\ 0 & 0 & 0 & P_3 & 1-P_4 & 0 \\ 0 & 0 & 0 & 0 & P_4 & 1 \end{pmatrix}^{t-t_{2015}} \begin{pmatrix} 0 \\ 0 \\ 1 \\ 0 \\ 0 \\ 0 \end{pmatrix} \qquad \text{Equation (1)}$$

where,

E : Expected value of the deterioration level

$P_0 \sim P_4$: Transition probabilities for buildings

t : A given material age

t_{2015} : Material age at 2015

③ Material properties and deterioration rates

③-1 Initial total chloride ion concentration and transition probability

Figures 2-4-96 to 2-4-100 show the relationship between the initial total chloride ion concentration and each transition probability. As these figures indicate, the higher initial total chloride ion concentration was, the higher P_1 to P_4 tended to become. Higher initial total chloride ion concentrations seem to have shorter time to reach the chloride ion threshold for corrosion and hence higher deterioration rates. It should be noted that many buildings in Hashima have chloride ion concentrations that already exceed the chloride ion threshold for corrosion provided in the "Standard Specifications for Concrete Structures" (Japan Society of Civil Engineers, 2012). No correlation was seen for P_0, for which further studies are required.

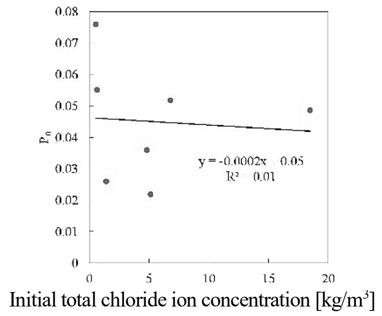

Figure 2-4-96 Initial total chloride ion concentration and P_0

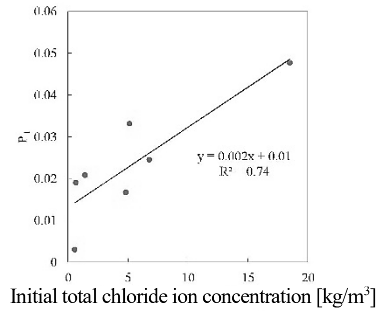

Figure 2-4-97 Initial total chloride ion concentration and P_1

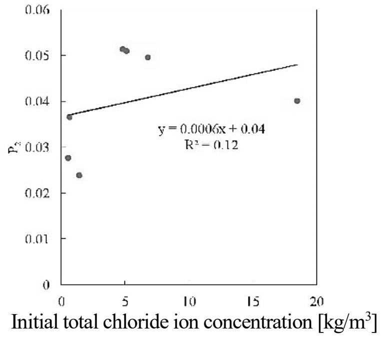

Figure 2-4-98 Initial total chloride ion concentration and P_2

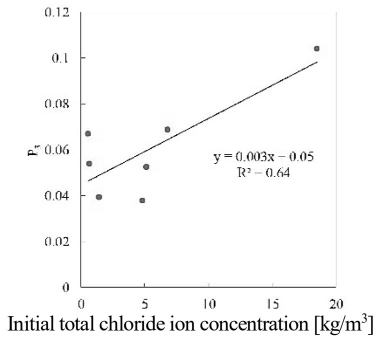

Figure 2-4-99 Initial total chloride ion concentration and P_3

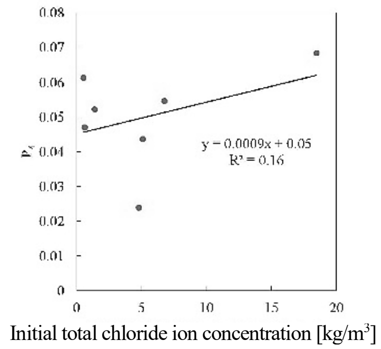

Figure 2-4-100 Initial total chloride ion concentration and P_4

③-2 Other material properties and expected values of deterioration levels

Figures 2-4-101 to 105 show the relationships between the expected values of deterioration levels and the apparent diffusion coefficient of chloride ion, mass moisture content, surface air permeability coefficient, and depth of concrete cover. Here, the expected values of deterioration levels were calculated for each member by excluding Buildings No.30 and 16, for which repair records remain, and by adjusting the material ages to 84 years, which is the material age of Building No.25, the oldest building. As these figures indicate, the higher the mass moisture content and the surface air permeability coefficient are, the greater the expected values of deterioration levels at material age 84 tended to become. The mass moisture content seems to affect the flowability of corrosion current, while the surface air permeability coefficient is considered to influence the degree of ease of the ingress of oxygen, which is a steel corrosion factor, into members. A mortar finish has been applied to all of these members with the exception of Member ⑭, which is exposed concrete. No clear trend was shown in the apparent diffusion coefficient of chloride ion, depth of concrete cover, or total pure quantity.

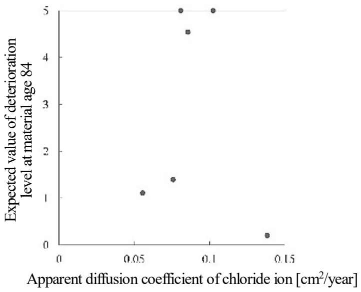

Figure 2-4-101 Apparent diffusion coefficient of chloride ion and expected value of deterioration level

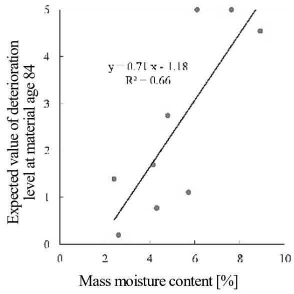

Figure 2-4-102 Mass moisture content and expected value of deterioration level

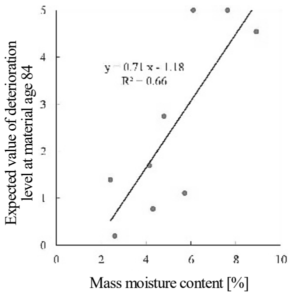

Figure 2-4-103 Surface air permeability coefficient and expected value of deterioration level

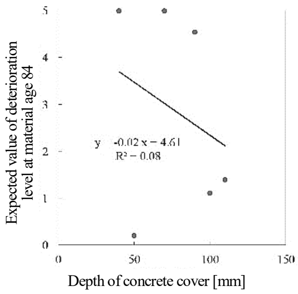

Figure 2-4-104 Surface air permeability coefficient and expected value of deterioration level

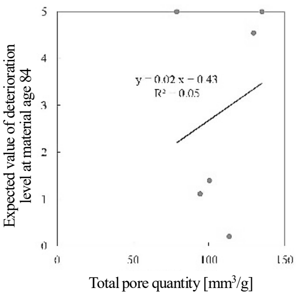

Figure 2-4-105 Surface air permeability coefficient and expected value of deterioration level

④ Summary

Table 2-4-83 shows the correlation coefficients obtained from the studies described above. The initial total chloride ion concentration, mass moisture content, and surface air permeability coefficient were found to have a relatively large effect on the deterioration rate.

Table 2-4-83 Correlation coefficient

Item	Correlation coefficient
Initial total chloride ion concentration	0.01–0.74
Apparent diffusion coefficient of chloride ion	-
Mass moisture content	0.66
Surface air permeability coefficient	0.35
Depth of concrete cover	0.08
Total pore quantity	0.05

10) Summary and future tasks

All of the reinforced concrete structures that exist today in the Hashima Coal Mine remains have damage in reinforced concrete members caused by reinforcement corrosion and are in a condition that requires repair/reinforcement. However, the degrees of reinforcement corrosion and damage of reinforced concrete members vary depending on the number of years that have elapsed since construction, the incoming salt amount, and the state of water supply to reinforced concrete members. Some buildings, including Building No.3, which is a reinforced concrete structure with a small number of years elapsed and a small amount of incoming salt, have high residual vertical load bearing performance ratios and residual seismic performance ratios, maintaining the structural safety at the time of construction to some degree. On the other hand, in some of the reinforced concrete structures built in locations where there is a large amount of incoming salt, reinforcement corrosion has excessively progressed, and part of members has collapsed; there are even buildings that are considered to barely maintain vertical load bearing performance without any seismic performance (Buildings No.25, 30, 57, 67, and Chidori-so).

However, in order to properly evaluate the vertical load bearing performance and seismic performance of the reinforced concrete structures that exist today in the Hashima Coal Mine remains, it is necessary to evaluate the vertical load bearing performance and seismic performance in the condition at the time of construction, in which no deterioration is caused. To do that, the concrete strength and the condition of bar arrangement need to be accurately understood for each reinforced concrete structure. On the basis of these data, the current vertical load bearing performance and seismic performance need to be estimated by considering the residual vertical load bearing performance ratio and residual seismic performance ratio that reflect the state of deterioration progress.

(3) Material strength testing

To understand the present condition of accommodation facilities in the Hashima Coal Mine remains, the surveys below were conducted with the aim of scientifically studying/analyzing the current deterioration state.

1) Studies including concrete compressive strength for accommodation facilities (Buildings No.3, 16, and 65)
2) Distributions of pH and chloride ion in concrete as the present condition of accommodation facilities
3) Deterioration prediction using the Markov chain

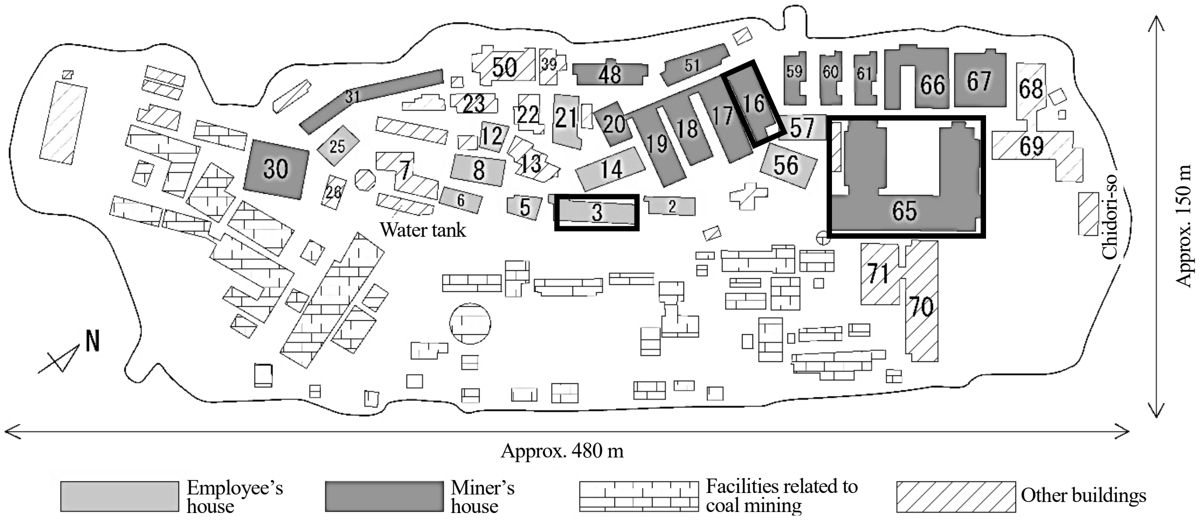

Figure 2-4-106　Location map of buildings surveyed

1) Results of concrete compressive testing for Buildings No.3, 16, and 65

Concrete cores were sampled at Buildings No.3, 16, and 65 and compressive testing was conduct. Core sampling locations and results of compressive testing at each building are shown in Figures 2-4-107 to 109 and Tables 2-4-84 to 86, respectively. Despite a large standard deviation noted for all the buildings, the average compressive strength was 18.4 (N/mm^2) for Building No.3, 21.6 (N/mm^2) for Building No.16, and 15.2 (N/mm^2) for Building No.65, showing values equivalent or superior to concrete strength generally seen at the time of construction. When the structural safety is evaluated by considering the current deterioration state, Building No.3 has almost no problems in light of the current earthquake standards and is unlikely to collapse in case of a moderate earthquake, although there is a concern in case of a large earthquake.

On the other hand, Buildings No.16 and 65 have insufficient structural performance and there is a fear of suffering huge damage even from a moderate earthquake.

Building 3

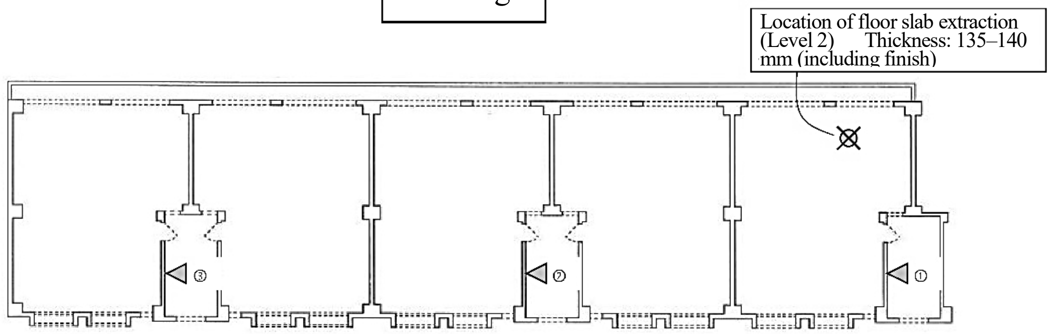

Level 2 to Level 4 plan

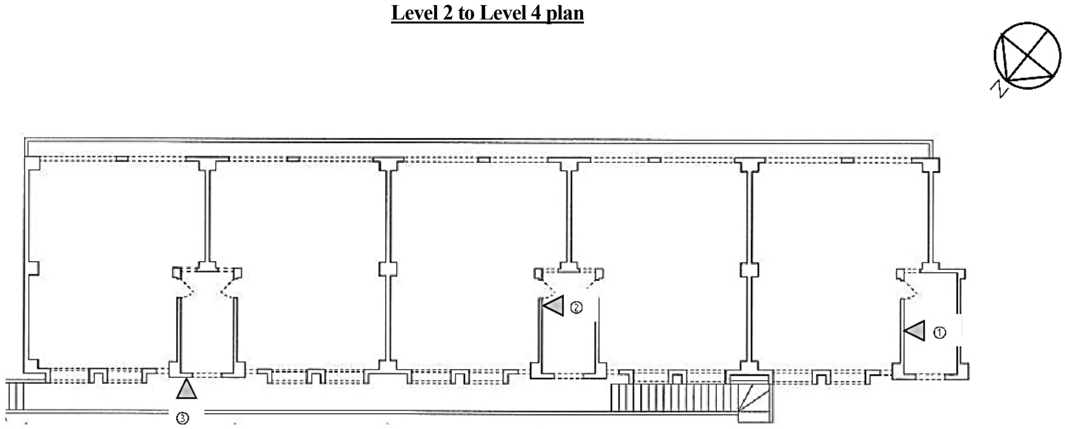

Level 1 plan

Figure 2-4-107 Locations of concrete core sampling for compressive testing at Building No.3

Table 2-4-84 Results of concrete compressive testing (Building No.3)

Level	Core number	Diameter d (mm)	Height h (mm)	h/d	Correction coefficient JISA 1107	Compressive strength (N/mm2) Before correction	Compressive strength (N/mm2) After correction	Young's modulus (104N/mm2)
4	①	103	113	1.10	0.893	31.2	27.8	1.32
	②	103	129	1.26	0.931	15.4	14.3	1.46
	③	103	133	1.29	0.935	19.6	18.3	1.65
					Average	22.0	20.1	1.48
3	①	104	136	1.31	0.937	22.3	20.9	1.30
	②	103	131	1.27	0.932	21.0	19.6	1.86
	③	104	132	1.28	0.933	13.8	12.9	1.58
					Average	19.0	17.8	1.58
2	①	103	137	1.33	0.939	20.6	19.3	2.37
	②	103	137	1.33	0.940	20.3	19.0	1.57
	③	103	125	1.21	0.921	17.5	16.1	1.15
					Average	19.4	18.1	1.70
1	①	103	145	1.41	0.949	18.3	17.4	1.70
	②	103	150	1.46	0.955	19.0	18.1	1.89
	③	103	124	1.21	0.919	18.7	17.2	1.09
					Average	18.7	17.6	1.56
					Over-all average	19.8	18.4	1.58
					Standard deviation	4.3	3.7	0.36

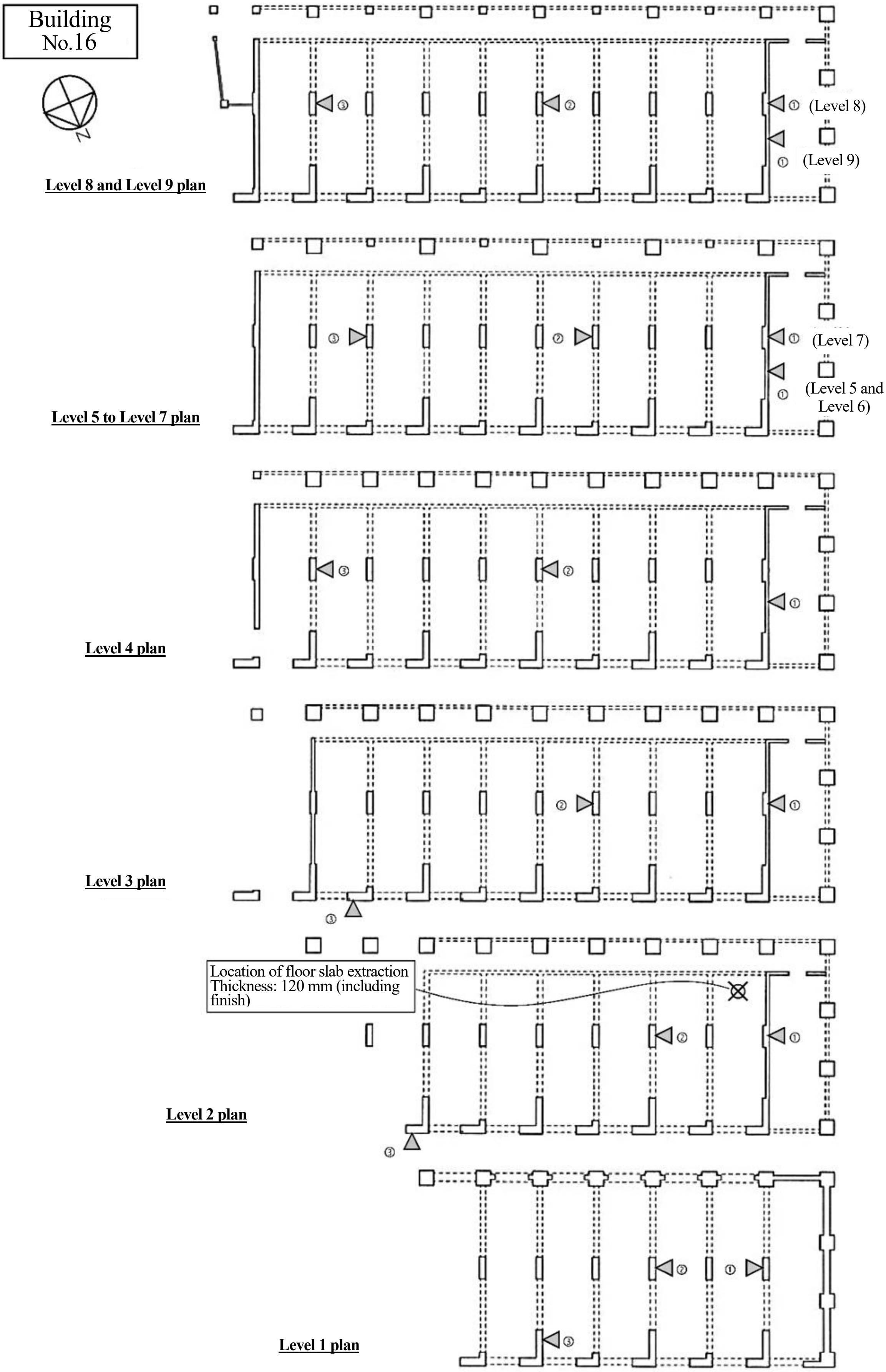

Figure 2-4-108 Locations of concrete core sampling for compressive testing at Building No.16

Appendix 1

Table 2-4-85 Results of concrete compressive testing (Building No.16)

Level	Core number	Diameter d (mm)	Height h (mm)	h/d	Correction coefficient JISA 1107	Compressive strength (N/mm2)	
						Before correction	After correction
9	①	104	207	1.99	1.000	24.3	24.3
	②	104	193	1.86	0.989	17.8	17.6
	③	104	174	1.67	0.974	24.5	23.8
					Average	22.2	21.9
8	①	104	180	1.74	0.979	18.5	18.1
	②	104	171	1.64	0.971	18.4	17.9
	③	104	178	1.72	0.977	29.0	28.3
					Average	22.0	21.4
7	①	104	190	1.83	0.986	27.2	26.8
	②	104	192	1.84	0.987	15.9	15.7
	③	104	171	1.65	0.972	16.9	16.4
					Average	20.0	19.6
6	①	104	146	1.41	0.949	27.6	26.1
	②	104	204	1.97	1.000	23.6	23.6
	③	104	192	1.84	0.988	27.4	27.1
					Average	26.2	25.6
5	①	104	141	1.35	0.943	27.8	26.2
	②	104	212	2.04	1.000	20.0	20.0
	③	104	201	1.93	1.000	15.8	15.8
					Average	21.2	20.6
4	①	104	138	1.33	0.939	20.0	18.8
	②	104	145	1.40	0.948	32.8	31.1
	③	104	126	1.22	0.922	34.2	31.6
					Average	29.0	27.1
3	①	104	145	1.39	0.947	13.1	12.4
	②	104	208	2.00	1.000	18.6	18.6
	③	104	164	1.58	0.966	22.5	21.8
					Average	18.1	17.6
2	①	104	157	1.51	0.961	22.1	21.2
	②	104	148	1.43	0.951	23.5	22.4
	③	104	203	1.96	1.000	15.2	15.2
					Average	20.3	19.6
1	①	104	190	1.83	0.987	26.1	25.7
	②	104	195	1.87	0.990	13.9	13.7
	③	104	209	2.01	1.000	24.4	24.4
					Average	21.5	21.3
					Over-all average	22.3	21.6
					Standard deviation	5.60	5.30

Building 65

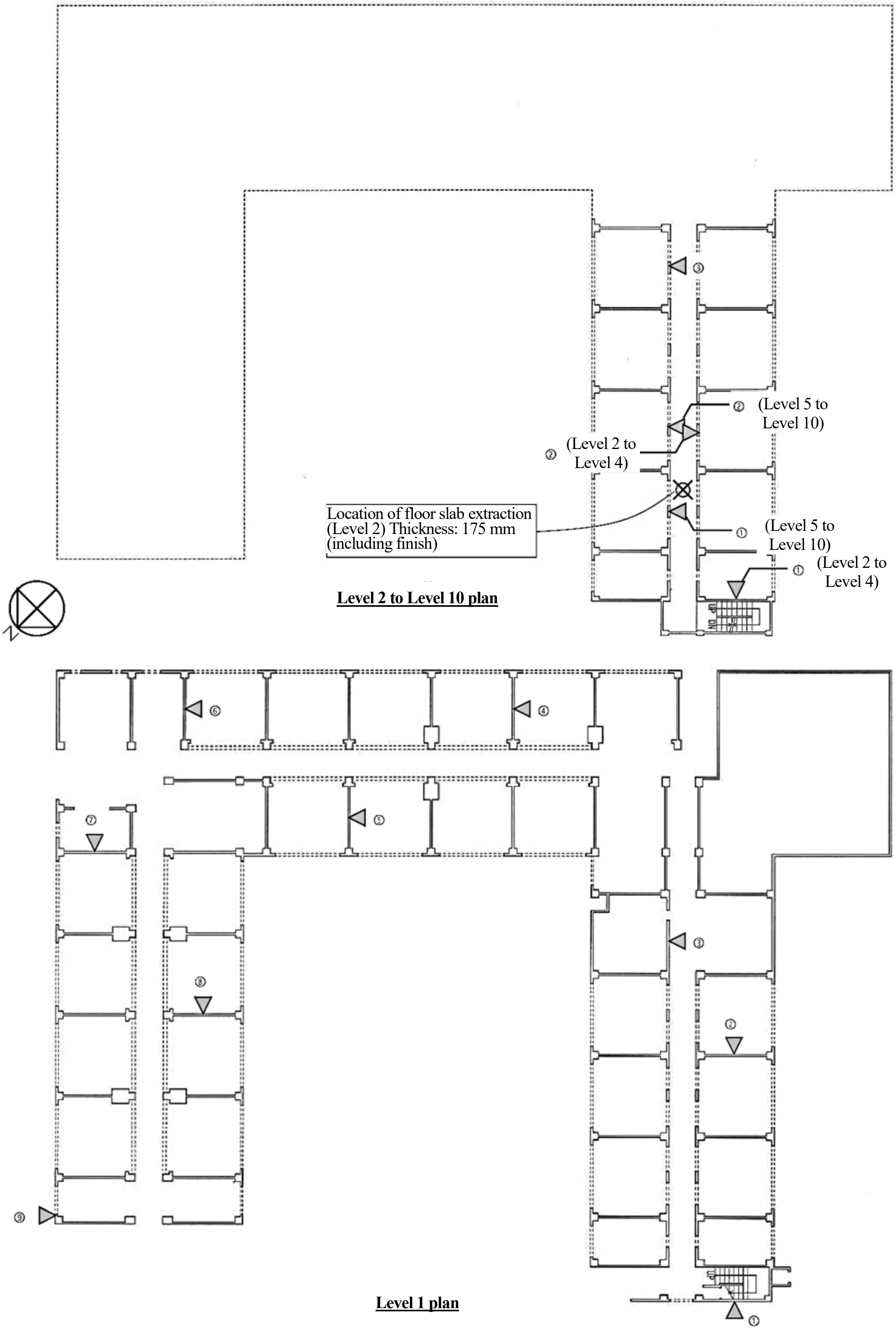

Figure 2-4-109 Locations of concrete core sampling for compressive testing at Building No.65

Table 2-4-86 Results of concrete compressive testing (Building No.65)

Level	Core number	Diameter d (mm)	Height h (mm)	h/d	Correction coefficient JIS A 1107	Compressive strength (N/mm2)		Young's modulus (104N/mm2)
						Before correction	After correction	
10	①	84	96	1.15	0.907	15.7	14.2	1.33
	②	84	96	1.15	0.905	7.2	6.5	1.11
	③	84	102	1.23	0.924	10.3	9.5	2.28
	Average					11.1	10.1	1.57
9	①	84	113	1.36	0.943	17.3	16.3	1.09
	②	84	106	1.27	0.932	20.3	18.9	1.93
	③	83	107	1.28	0.934	14.5	13.5	1.66
	Average					17.4	16.3	1.56
8	①	84	106	1.27	0.932	11.8	11.0	1.77
	②	83	110	1.32	0.939	13.3	12.5	3.74
	③	84	99	1.18	0.914	15.0	13.7	1.61
	Average					13.4	12.4	2.37
7	①	84	111	1.32	0.939	14.0	13.2	0.97
	②	83	92	1.1	0.895	16.9	15.1	1.09
	③	83	101	1.21	0.92	11.5	10.5	0.93
	Average					14.1	12.9	1.00
6	①	83	113	1.36	0.943	12.5	11.8	6.84
	②	84	95	1.14	0.903	11.6	10.5	2.93
	③	84	109	1.3	0.937	15.2	14.3	1.95
	Average					13.1	12.2	3.91
5	①	84	111	1.32	0.938	25.4	23.8	1.95
	②	84	102	1.22	0.923	23.9	22.1	2.27
	③	84	110	1.32	0.938	15.8	14.9	2.16
	Average					21.7	20.2	2.13
4	①	83	152	1.82	0.986	24.9	24.5	1.70
	②	84	86	1.02	0.876	18.1	15.9	0.67
	③	83	100	1.19	0.917	17.5	16.0	2.72
	Average					20.2	18.8	1.70
3	①	83	171	2.05	1.000	13.9	13.9	1.29
	②	83	95	1.14	0.903	21.2	19.1	1.38
	③	104	95	0.92		16.6	—	1.56
	Average					17.3	16.5	1.41
2	①	104	181	1.74	0.979	15.1	14.7	1.50
	②	84	93	1.11	0.896	17.3	15.5	1.02
	③	104	92	0.89		11.9	—	0.54
	Average					14.7	15.1	1.02
1	①	104	187	1.8	0.984	20.1	19.8	1.89
	②	84	172	2.05	1.000	14.9	14.9	1.32
	③	104	205	1.98	1.000	12.7	12.7	1.09
	④	104	129	1.24	0.927	23.4	21.7	2.61
	⑤	103	192	1.85	0.988	11.5	11.4	1.93
	⑥	104	183	1.76	0.981	13.9	13.6	1.97
	⑦	104	192	1.85	0.988	8.3	8.2	1.13
	⑧	104	185	1.79	0.983	15.7	15.4	1.96
	⑨	84	118	1.41	0.949	26.9	25.5	1.96
	Average					16.4	15.9	1.76
Over-all average						16.0	15.2	1.83
Standard deviation						4.7	4.5	1.08

2) Distributions of pH and chloride ion in concrete as the present condition of accommodation facilities

Concrete cores were sampled at Buildings No.3, 16, and 65, and the distribution of chloride ion was measured. Regarding core codes at each building, "3-1-1C" represents "Building No.3, Level 1, ①" for example. A vertical dotted line indicated neutralization depth, and hatching shows an area that has not been neutralized yet.

For all of the Buildings No.3, 16, and 65, the surface parts of an area facing the outside of the building had higher chloride ion content, which demonstrates the influence of incoming salt. In terms of the amount of salt contained, at Building No.3, chloride ion content is not more than 1kg/m3 for the inside of the building as well as parts that are deep from the surface layer, and thus the amount of salt contained is estimated to be small.

At Building No.16, chloride ion content varies among different locations even inside the building, indicating that the amount of salt contained varies depending on the location.

As for Building No.65, although chloride ion content is high on the outdoor side, indoor chloride ion content is low at each construction period, and therefore, chlorides derived from incoming salt are estimated to be dominant.

As described below, there are three possible factors for very high concentrations of salt contained; however, in-depth studies need to be conducted to reach a conclusion in the future.

・Seawater may have been used as water for concrete mixing.
・Unwashed sea sand/sea gravel may have been used as concrete aggregate.
・Seawater have splashed over the building many times at high tide and may have penetrated inside.

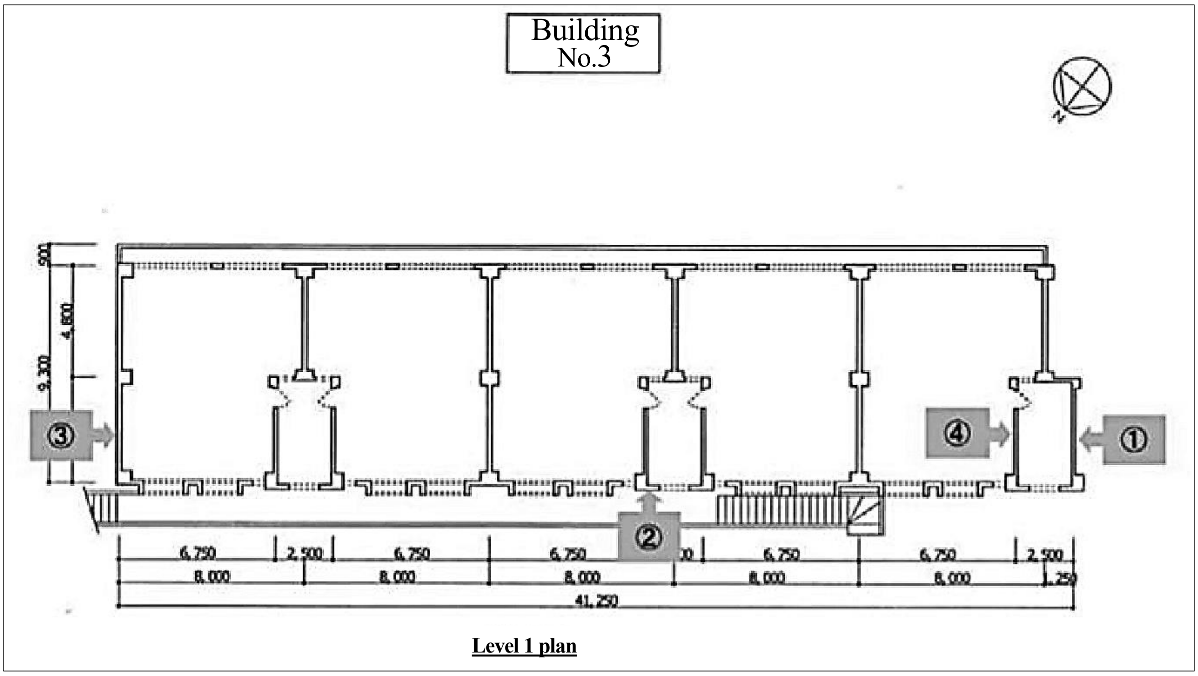

Figure 2-4-110 Locations of concrete core sampling at Building No.3

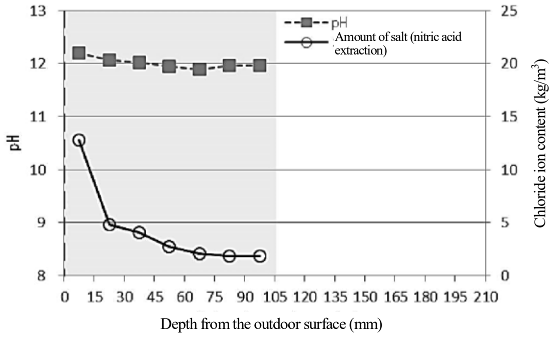

3-1-1C

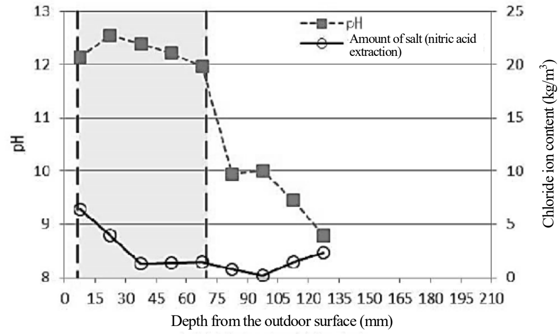

3-1-2C

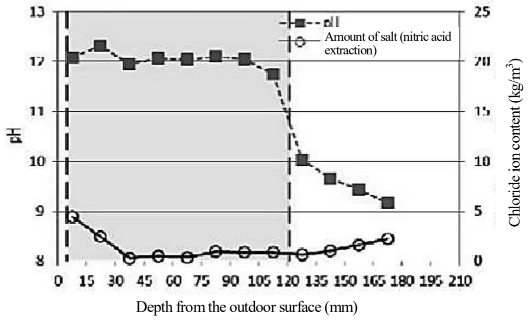

3-1-3C

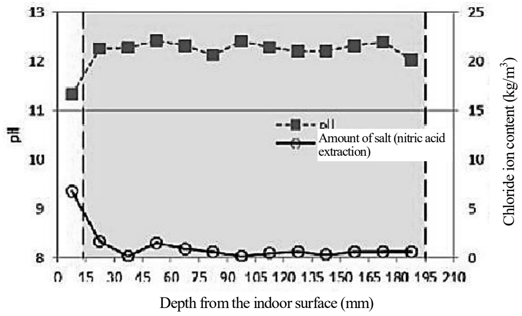

3-1-4C

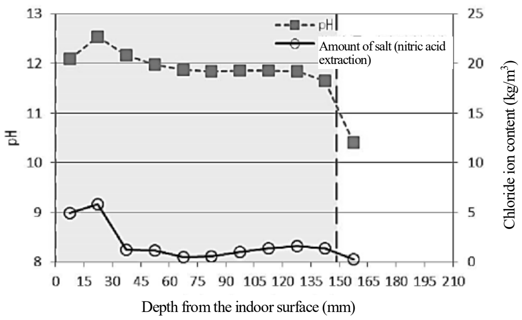

3-B1-1C

Figure 2-4-111 Distribution of chloride ion in concrete at Building No.3

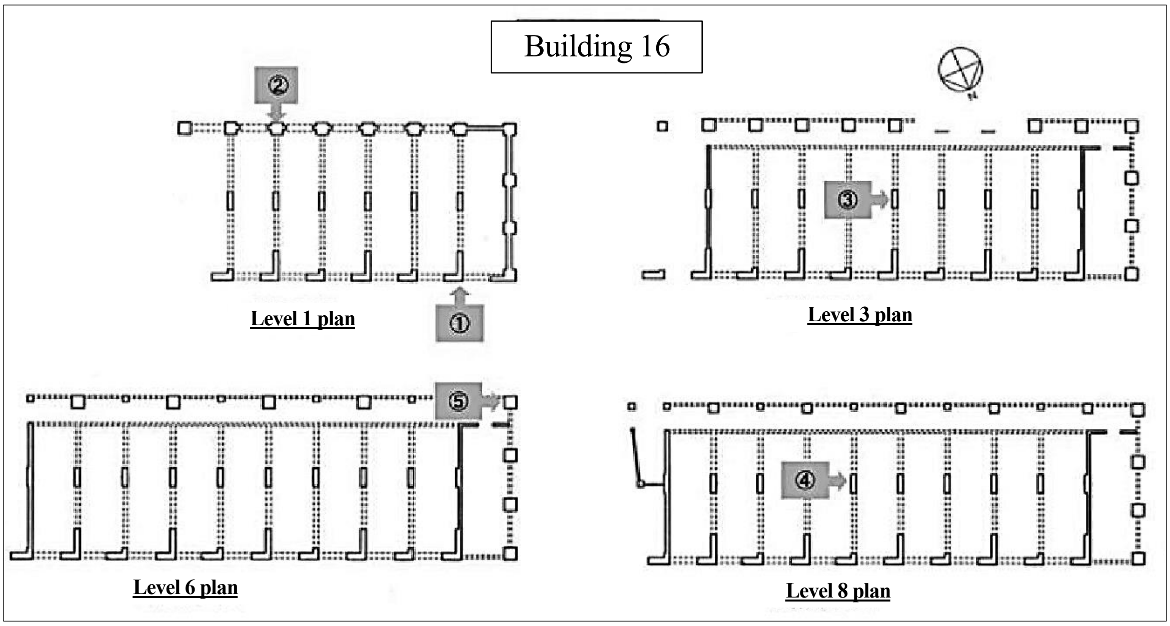

Figure 2-4-112 Locations of concrete core sampling at Building No.16

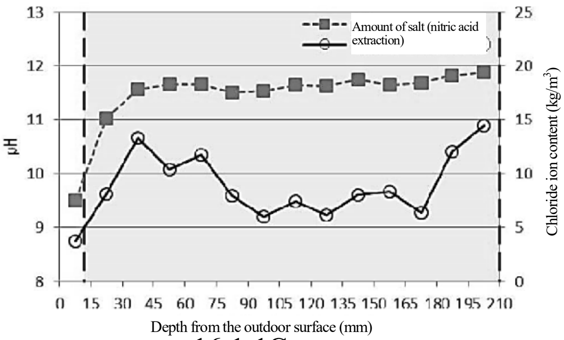

16-1-1C

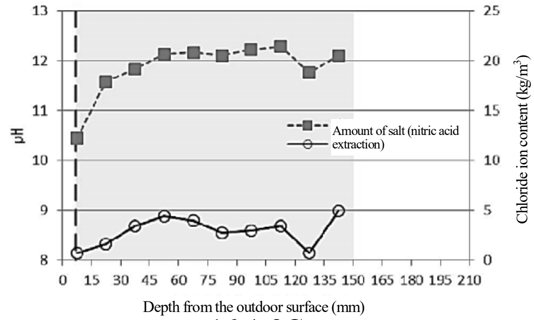

16-1-2C

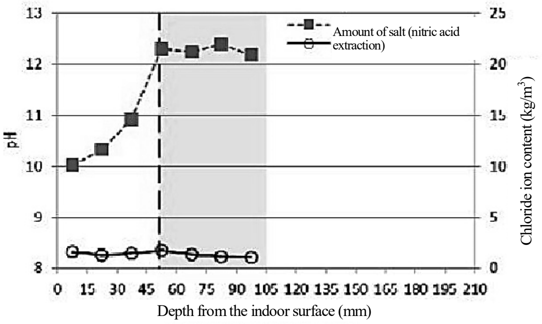

16-3-C

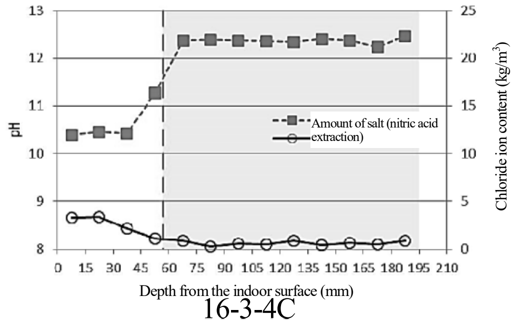

16-3-4C

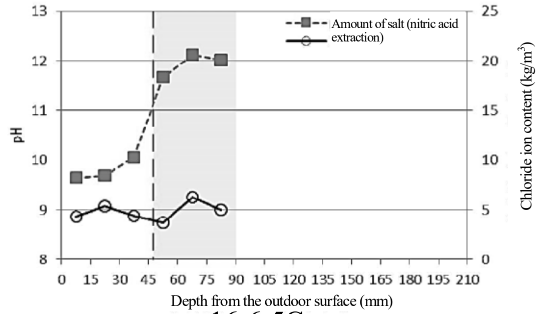

16-6-5C

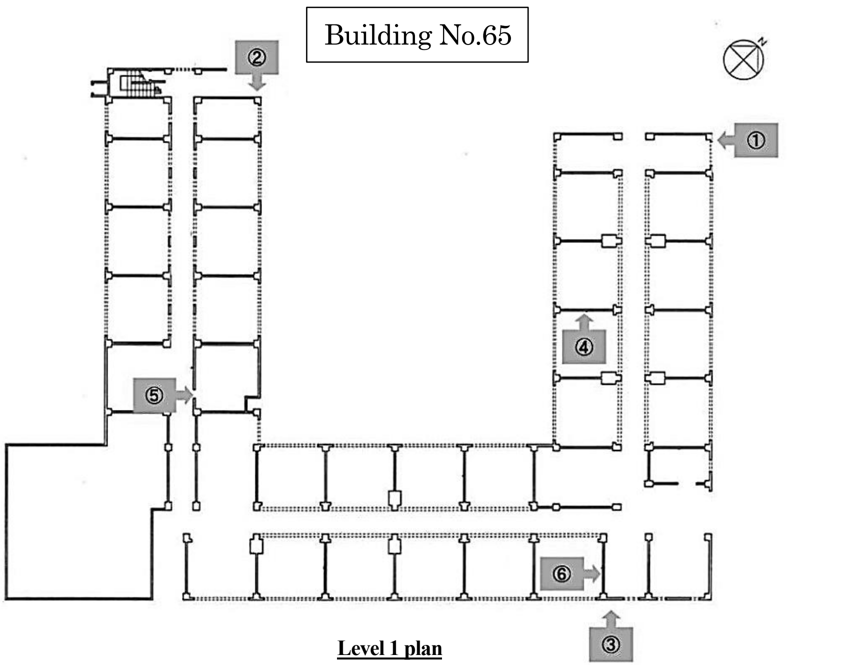

Figure 2-4-114 Locations of concrete core sampling at Building No.65

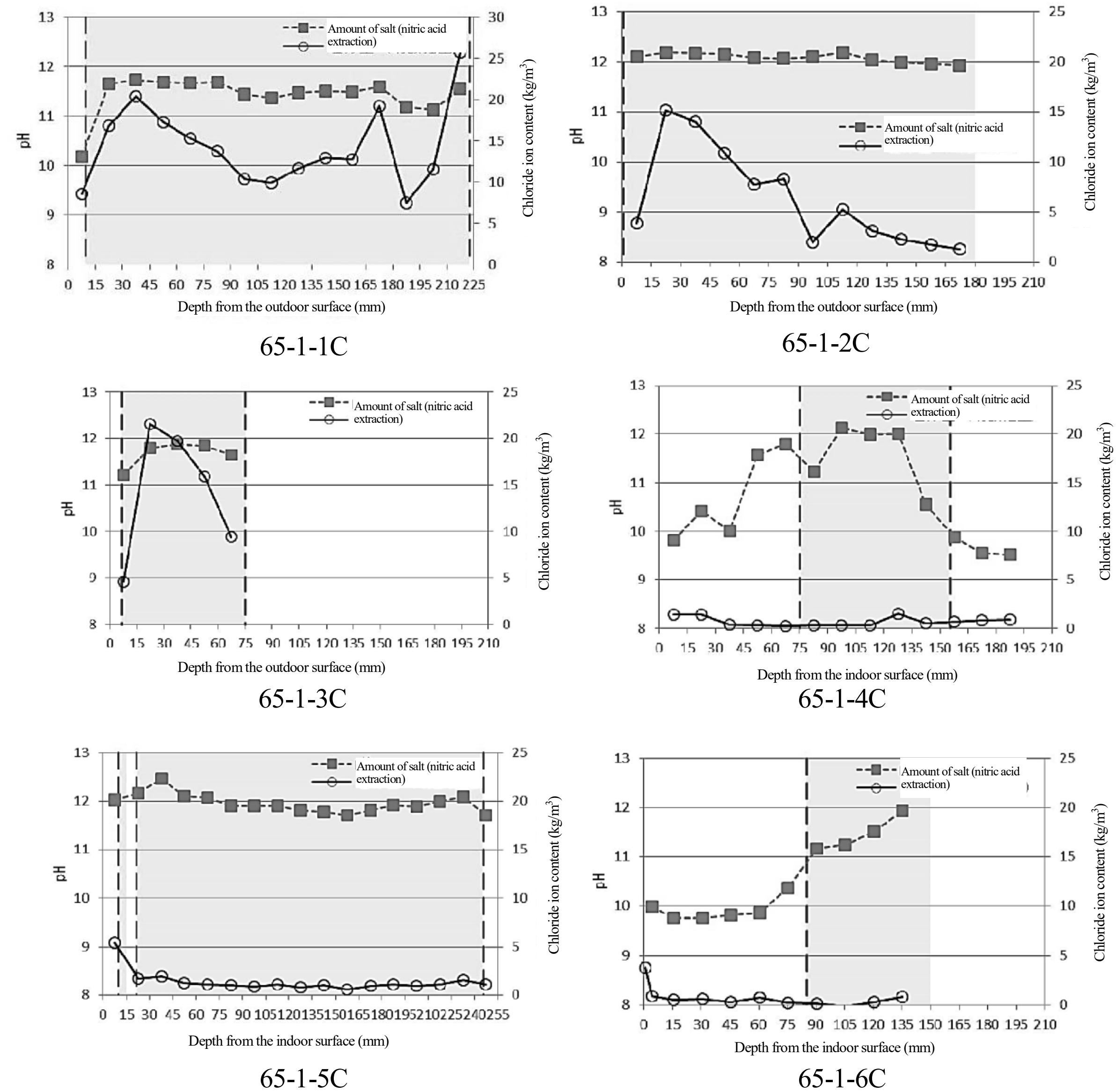

Figure 2-4-115 Distribution of chloride ion in concrete at Building No.65

3) Deterioration prediction using the Markov chain

In regard to reinforced concrete structure buildings in the Hashima Coal Mine remains, we studied a method for predicting deterioration of reinforced concrete members using the Markov chain, which are based on the classification of deterioration environments, and predicted the future residual structural performance ratios of buildings through on-site surveys, in order to calculate the years of structural performance limit and determine repair priority for Buildings No.3, 16, 17, 18, 19, 20, 65, and 70.。

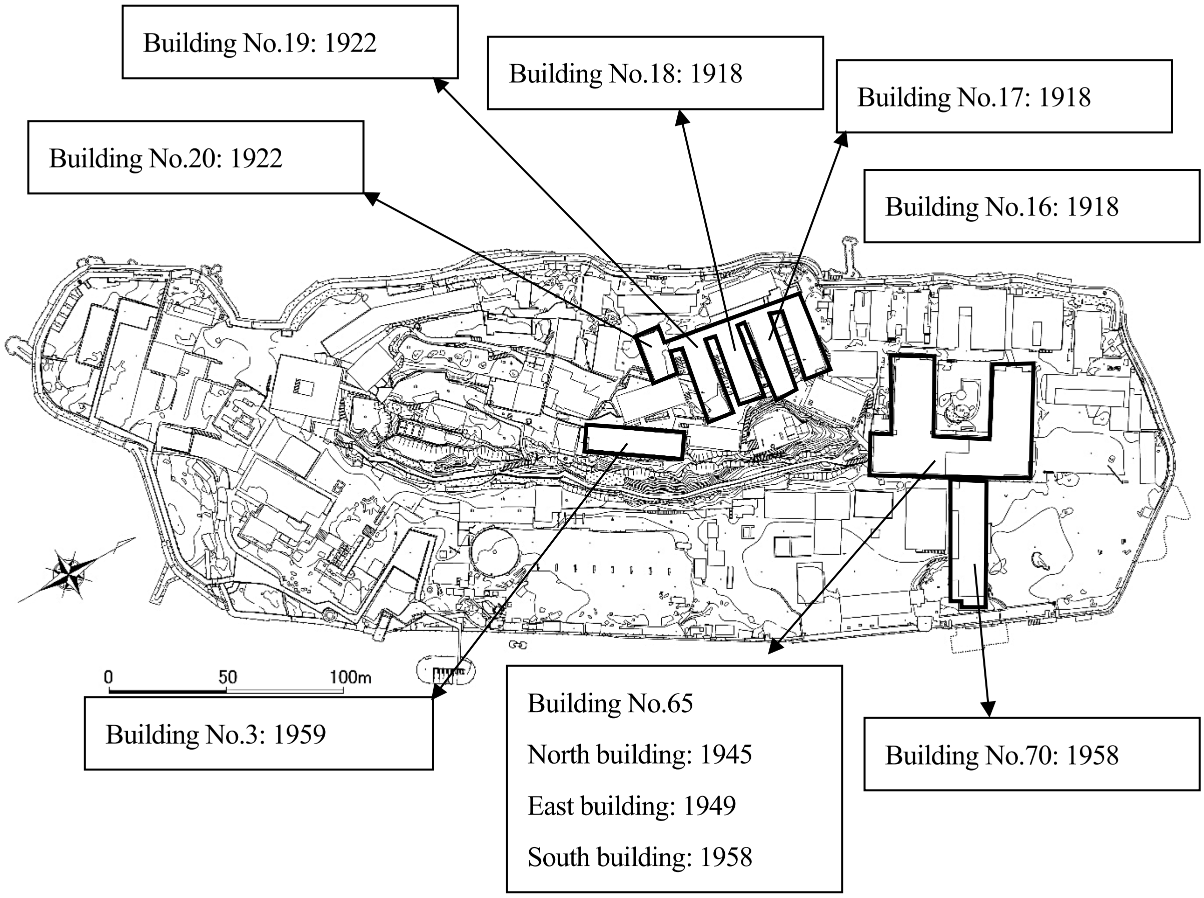

Figure 2-4-116 Location map and construction year for buildings surveyed

① Survey of deterioration levels and environments of members of the buildings in Hashima

To devise a method for classifying the deterioration environments of members, we organized information on member deterioration levels, depth of concrete cover, amount of rain received by members, and incoming salt environments, through on-site surveys and by using past literature as a reference.

In fiscal 2015, the survey of deterioration levels of columns, beams, and wall members for all of the 27 buildings in Hashima as well as the bar arrangement survey for major buildings were conducted. Moreover, in fiscal 2016, the projection lengths of eaves in the upper parts of members were measured, and shields against raindrops such as shutter boxes were visually inspected; further, the yearly amounts of rain received by members were calculated using the past literature "Estimation of the tilt angle of a raindrop colliding against a wall surface: Basic study on the assessment of a rainfall load acting on an external wall surface" (Ishikawa, et al., 2007) as a reference. In addition, the annual average incoming salt amount in Hashima was determined using "Discussions on the state of incoming salt transport in Gunkanjima, Nagasaki Prefecture" (Shimizu et al., 2015) and "Salt damage environment in Gunkanjima, Nagasaki Prefecture" (Shimizu) as references. For data on the amount of rainfall and wind conditions, we referred to Meteorological Agency's data (Nomozaki, 2006 to 2015).

② Results: Relationships between member deterioration levels and depth of concrete cover / yearly amounts of rain received by members / annual average incoming salt amount

Only the results for Buildings No.16, 17, 18, 19, and 20 are shown here as survey results are similar for the other buildings. Figure 2-4-117 shows the relationship between the graph gradient (ζ) of the expected deterioration level (an expected value calculated from the ratios of deterioration level for different members in the same area exposed to the rain within the same building) and the average annual incoming salt amount.

In almost all cases, the graph gradient shows a positive value; the greater annual average incoming salt amount is, the higher the expected deterioration level becomes. Figure 2-4-118 shows the relationship between the yearly amount of rain received and the mean value of expected deterioration level in the total incoming salt range. Basically, the smaller the depth of concrete cover is and the larger the yearly amount of rain received is, the higher the expected deterioration level becomes; however, the larger the depth of concrete cover is, the smaller the increment of the expected deterioration level with respect to an increase in the yearly amount of rain received becomes, with the depth of concrete cover as great as around 80 mm being hardly affected by the amount of rain received.

Depth of concrete cover: ■ 20mm ■ 40mm ■ 60mm ■ 80mm ■ ≥100 mm

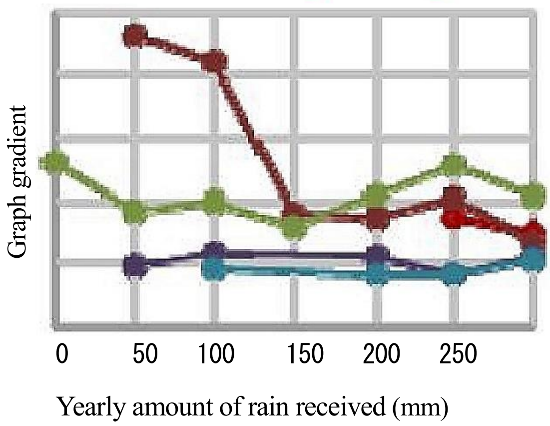

Figure 2-4-117 Yearly amount of rain received and graph gradient

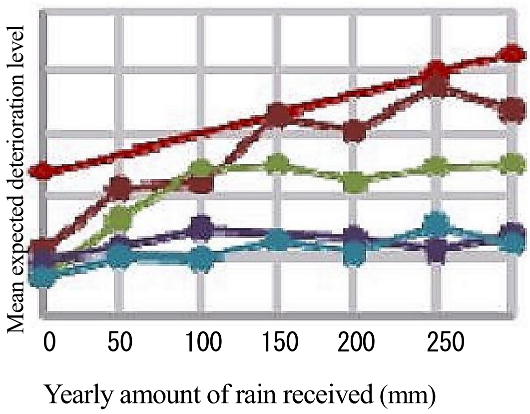

Figure 2-4-118 Yearly amount of rain received and mean expected deterioration level

③ Deterioration environment classification with the deterioration environment grade G_E

As an index to determine the severity of deterioration environment for each member, the deterioration environment grade G_E was created by following the steps below.

1. The equations were formulated using survey results and reinforcement corrosion rate evaluation equations in the past as references and based on the assumption that the depth of concrete cover acts as resistance against the ingress of substances causing corrosion including salt content and water content. In addition, it was assumed that the depth of concrete over equal to or greater than 80 mm is not affected by the amount of rain received.
2. For data on the annual average incoming salt amount, annual average amount of rain received, depth of concrete cover, and expected deterioration levels, the data for Buildings No.16, 17, 18, 19, and 20, which have the largest number of data, were used, and each coefficient was obtained using multiple regression analysis. In this step, the expected deterioration level ≒ G_E was used.
3. The equation for evaluating G_E was formulated in a similar manner also for cases in which no data are available concerning the depth of concrete cover.

Equations 1 and 2 show the evaluation equations derived for G_E. Figure 2-4-119 shows a comparison between the calculated value of G_E and the actual expected deterioration level. While proper evaluations were generally made in the case of Equation 1, slightly large variations were shown in the case of Equation 2. Therefore, data on the depth of concrete cover should not be omitted in essence in order to properly evaluate G_E. Table 2-4-87 shows the transition probabilities obtained for each value of G_E using Equation 3, after the deterioration environment grade GE was calculated for members using Equations 1 and 2. The value of transition probability increases as the value of GE increases, suggesting that an appropriate classification of deterioration environments has been made.

1 When data on CI, R, and C are available,

$$\begin{cases} G_E = \dfrac{3.07\,C\xi^{-} + 0.139R + 42.1}{C} & (C < 80) \\[2ex] G_E = \dfrac{1.16C\xi^{-} + 69.8}{C} & (C \geq 80) \end{cases} \qquad \text{Equation 1}$$

2 When data on C is not available,

$$G_E = 0.00159\,C\xi^{-} + 0.00174R + 0.91 \qquad \text{Equation 2}$$

G_E : Deterioration environment grade

Cl : Annual average incoming salt amount [mmd]

R : Yearly amount of rain received [mm]

C : Depth of concrete cover [mm]

$$\begin{bmatrix} X_0 \\ X_I \\ X_{II} \\ X_{III} \\ X_{IV} \\ X_V \end{bmatrix} = \begin{bmatrix} 1-P_0 & 0 & 0 & 0 & 0 & 0 \\ P_0 & 1-P_1 & 0 & 0 & 0 & 0 \\ 0 & P_1 & 1-P_2 & 0 & 0 & 0 \\ 0 & 0 & P_2 & 1-P_3 & 0 & 0 \\ 0 & 0 & 0 & P_3 & 1-P_4 & 0 \\ 0 & 0 & 0 & 0 & P_4 & 1 \end{bmatrix}^{t} \begin{bmatrix} 1 \\ 0 \\ 0 \\ 0 \\ 0 \\ 0 \end{bmatrix} \qquad \text{Equation 3}$$

$X_{0\sim V}$: Percentage of the current deterioration level

$P_{0\sim 4}$: Transition probability

t : Years since construction

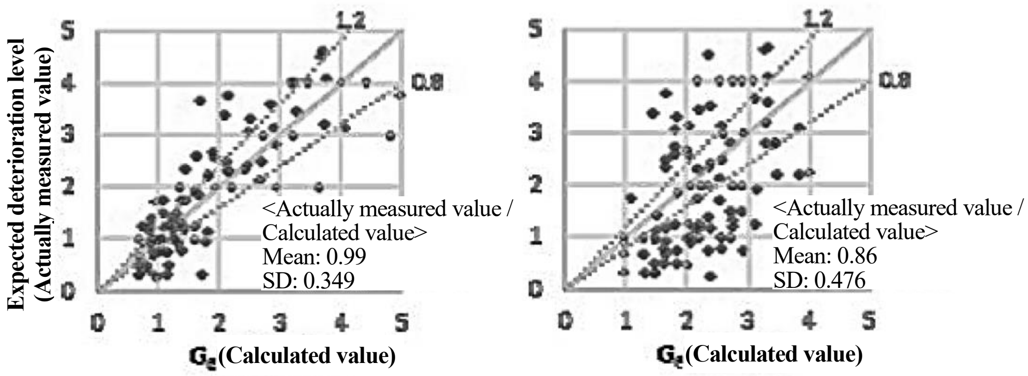

(a) Application of Equation 1

(b) Application of Equation 2

Figure 2-4-119 Comparison between actually measured values and calculated values: Buildings No.16 to 20

Appendix 1

Table 2-4-87 Transition probability for each building after deterioration environment classification

GE	Transition probability	Buildings No.16 to 20	Building No.3	Building No.65 (North)	Building No.65 (East)	Building No.65 (South)	Building No.70	Average value
	P0	0.0088	0.0079	0.0109	0.0075	0.0104	0.0136	0.0099
	P1	0.0179	0.0172	0.0378	0.0226	0.0163	0.0183	0.0217
1	P2	0.0344	0.0245	0.0397	0.0269	0.0149	0.0341	0.0291
	P3	0.0307	0.1164	0.0334	0.0266	0.0246	0.0401	0.0453
	P4	0.0266	0.0387	0.0314	0.0355	0.0250	0.0348	0.0320
	P0	0.0184	0.0148	0.0148	0.0148	0.0130	0.0127	0.0148
	P1	0.0214	0.0188	0.0417	0.0795	0.0175	0.0229	0.0336
2	P2	0.0546	0.0607	0.0237	0.0350	0.0545	0.0798	0.0514
	P3	0.0350	0.1059	0.0553	0.0583	0.0726	0.0480	0.0620
	P4	0.0209	0.0390	0.0301	0.0703	0.0801	0.0403	0.0468
	P0	0.0250	0.0185	0.0133	0.0303	0.0145	0.0176	0.0198
	P1	0.0470	0.0303	0.0852	0.0385	0.0483	0.0323	0.0469
3	P2	0.0540	0.1020	0.0502	0.0334	0.2141	0.1206	0.0957
	P3	0.0329	0.1496	0.0680	0.1003	0.0864	0.0400	0.0795
	P4	0.0189	0.0404	0.0385	0.0661	0.0393	0.0421	0.0409
	P0	0.0464		0.0245	0.0193		0.0776	0.0419
	P1	0.0377		0.0715	0.0385		0.0319	0.0449
4	P2	0.0647	–	0.0719	0.1522	–	0.1034	0.0981
	P3	0.0506		0.1104	0.1161		0.0472	0.0811
	P4	0.0239		0.0394	0.0414		0.0473	0.0380
	P0	0.0464		0.0637				0.0550
	P1	0.0492		0.0483				0.0488
5	P2	0.0839	–	0.0623	–	–	–	0.0731
	P3	0.0710		0.2130				0.1420
	P4	0.0201		0.0376				0.0289
	P0	0.0116	0.0118	0.0124	0.0141	0.0113	0.0142	0.0126
	P1	0.0215	0.0252	0.0435	0.0516	0.0236	0.0203	0.0309
No classification	P2	0.0457	0.0596	0.0417	0.0390	0.0363	0.0430	0.0444
	P3	0.0361	0.1238	0.0492	0.0530	0.0625	0.0440	0.0615
	P4	0.0240	0.0493	0.0374	0.0613	0.0598	0.0419	0.0456

④ **Prediction of future structural performance of major buildings**

Changes in the expected deterioration level of each member were predicted using the transition probabilities included in Table 2-4-87, and the prediction of the minimum value of the residual vertical load bearing performance ratio R_L for each Level of each building was made.

The allowable value of R_L was defined as 60% by using the standard for major damage of the residual seismic performance ratio R as a reference; Figure 2-4-120 shows the buildings for which R_L reaches 60% early in order of increasing period required for R_L to reach 60%.

As Figure 2-4-120 indicates, repair priority was, in order of priority, Building No.16, Building No.20, Building No.65 (North), Building No.65 (East), Building No.19, Building No.17, Building No.18, Building No.65 (South), Building No.70, and Building No.3.

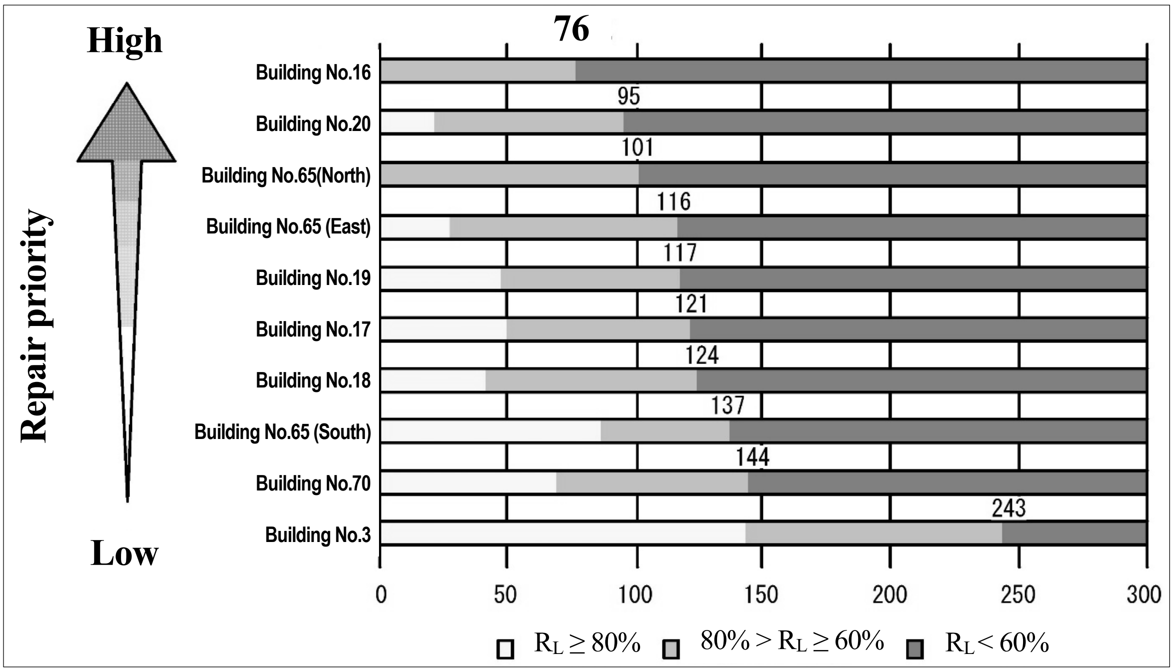

Figure 2-4-120 Determination of repair priority based on the prediction of future R_L

4) Summary

The survey produced the outcomes below.

1. On-site surveys and results of past surveys in Hashima confirmed that the greater annual average incoming salt amount, the greater yearly amount of rain received, and the smaller depth of concrete cover lead to the higher expected deterioration level. However, the depth of concrete cover 80 mm or greater was shown to be hardly affected by rain received.
2. The index of the deterioration environment grade G_E was created from the relationships between the annual average incoming salt amount / yearly amount of rain received / depth of concrete cover, and the expected deterioration level. The proper evaluation of transition probability was made possible by using G_E to classify deterioration environments of members and applying the Markov chain.
3. Repair priority was determined by predicting future structural performance of the buildings through a combination of deterioration predictions based on the Markov chain and the evaluation of R_L, the residual vertical load bearing performance ratio.

Appendix 1